2016

Power Management of Remote Microgrids Considering Battery Lifetime

Santosh Chalise
South Dakota State University

POWER MANAGEMENT OF REMOTE MICROGRIDS

CONSIDERING BATTERY LIFETIME

BY

SANTOSH CHALISE

A dissertation submitted in partial fulfillment of the requirements for the

Doctor of Philosophy

Major in Electrical Engineering

South Dakota State University

2016

POWER MANAGEMENT OF REMOTE MICROGRIDS

CONSIDERING BATTERY LIFETIME

This dissertation is approved as a creditable and independent investigation by a candidate for the Doctor of Philosophy in Electrical Engineering degree and is acceptable for meeting the dissertation requirements for this degree. Acceptance of this does not imply that the conclusions reached by the candidates are necessarily the conclusions of the major department.

Reinaldo Tonkoski, Ph.D Date
Dissertation Advisor

Steven Hietpas, Ph.D Date
Head, Department of Electrical
Engineering & Computer Science

Dean, Graduate School Date

ACKNOWLEDGEMENTS

First and the foremost, I would like to express my gratitude to my thesis advisor, Dr. Reinaldo Tonkoski for his continuous guidance, teaching, and engagement during my PhD study at the South Dakota State University. His useful comments and remarks have not only developed my technical knowledge, but also helped me to grow as an individual and provided an enduring experience. I am very thankful to Dr. David Galipeau for his continuous encouragement, trust, guidance and generosity. I would also like to thank the Department of Electrical Engineering and Computer Science for input and accessibility.

I would like to thank all professors and committee members for encouragement and valuable suggestions. Thank you to my friends – Binod, Yogesh, Prakash, Shekhar, Shaili, Ujjwol, Suman, Hameed, Amir, Ayush for all the experience and work shared and for making the environment cheerful to work.

Last but not least, I would like to thank my loving wife, Kopila Subedi Chalise, my parents, brother and sister for their endless support and love during my study.

TABLE OF CONTENTS

ABBREVIATIONS

PV	photovoltaic
PMS	power management system
BLM	battery lifetime management
SOC	state of charge
NSGI	non-dominated sorting genetic algorithm
RTDS	real-time digital simulator
DG	distributed generation
DSM	demand side management
GA	genetic algorithm
CHP	combined heat and power
PSO	particle swarm optimization
USABC	United States advanced battery consortium
DOD	depth of discharge
DC	direct current
STC	standard irradiance and temperature
AM	air mass
MPPT	maximum power point tracker

RES	renewable energy source
SCADA	supervisory control and data acquisition
MCC	microgrid central controller
LC	local controller
MAS	multi agent system
CERTS	consortium for electric reliability technology solution
PDF	probability distribution function
PI	prediction interval
CI	confidence interval
RMSE	root mean square error
MILP	mixed integer linear programming
QP	quadratic programming
MSE	mean square error
kWh	kilo watt hour
TP	throughput
POC	point of connection

LIST OF FIGURES

LIST OF TABLES

ABSTRACT

POWER MANAGEMENT OF REMOTE MICROGRIDS

CONSIDERING BATTERY LIFETIME

SANTOSH CHALISE

2016

Currently, 20% (1.3 billion) of the world's population still lacks access to electricity and many live in remote areas where connection to the grid is not economical or practical. Remote microgrids could be the solution to the problem because they are designed to provide power for small communities within clearly defined electrical boundaries. Reducing the cost of electricity for remote microgrids can help to increase access to electricity for populations in remote areas and developing countries. The integration of renewable energy and batteries in diesel based microgrids has shown to be effective in reducing fuel consumption. However, the operational cost remains high due to the low lifetime of batteries, which are heavily used to improve the system's efficiency. In microgrid operation, a battery can act as a source to augment the generator or a load to ensure full load operation. In addition, a battery increases the utilization of PV by storing extra energy. However, the battery has a limited energy throughput. Therefore, it is required to provide a balance between fuel consumption and battery lifetime throughput in order to lower the cost of operation.

This work presents a two-layer power management system for remote microgrids. The first layer is day ahead scheduling, where power set points of dispatchable resources were calculated. The second layer is real-time dispatch, where schedule set points from

the first layer are accepted and resources are dispatched accordingly. A novel scheduling algorithm is proposed for a dispatch layer, which considers the battery lifetime in optimization and is expected to reduce the operational cost of the microgrid. This method is based on a goal programming approach which has the fuel and the battery wear cost as two objectives to achieve. The effectiveness of this method was evaluated through a simulation study of a PV-diesel hybrid microgrid using deterministic and stochastic approach of optimization.

CHAPTER 1: INTRODUCTION

1.1. Background

Microgrids are a small scale power supply network designed to provide power for small communities within clearly defined electrical boundaries [1]. To be called microgrid, the network must have its own sources, storages, load, monitoring, and control techniques to keep the system running with or without a grid support [2]. Based on the availability of a grid, microgrids are divided into two types: Grid connected and remote. Grid connected microgrids mostly operates in the presence of the grid but can be disconnected and work by itself during a grid failure or emergency. Nevertheless, remote microgrids always operate by themselves and has no access to grid. One major distinction between these microgrids is the design approach. In case of a remote microgrid, the generation sources must have the capacity to serve the entire load along with a required reserve capacity for contingency management [3], which is not necessarily required for the grid connected system. According to the recent Navigant research study, remote microgrids are the example of an isolated system applicable for village electrification, commodity extraction, physical islands (remote telecommunication) and remote military [4]. This dissertation focuses on the microgrid used for the remote village electrification purpose.

Currently, 20% (1.3 billion) of the world's population still lacks access to electricity and many live in remote areas where connection to the grid is not economical or practical [5]. Those areas lack access to modern energy services, which is a serious hindrance to economic and social development. One of the aims of the United Nations

Secretary General's Sustainable Energy for All (SE4ALL) initiative is to help achieve the goal of universal access to modern energy services by 2030 [6]. This effort in village electrification increases the remote microgrid market in current years. According to a Navigant Research, the global remote microgrid market will expand from 349 megawatts of generation capacity in 2011 to more than 1.1 gigawatts by 2017, with the majority of this growth expected in the developing world [7]. A large portion will also take place in the rapidly developing, and often remote, the island nations of the world. These nations are inherently deprived of many resources, sometimes importing 100% of the fuel needed to meet energy demands [8].

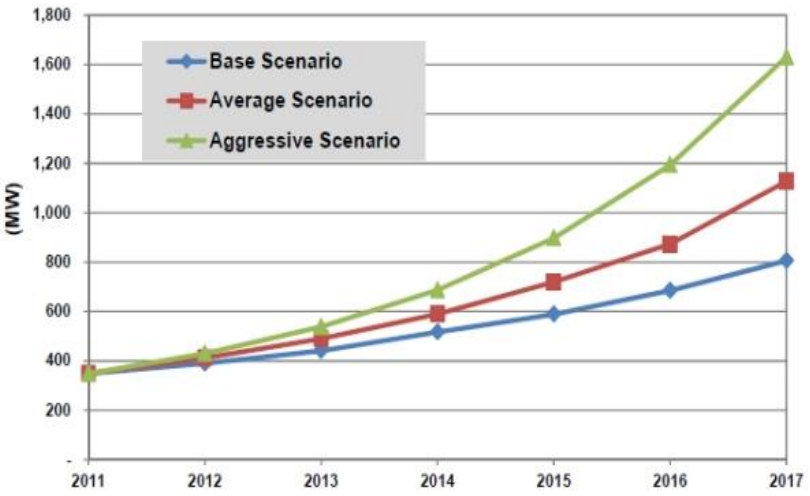

Fig. 1.1. Total remote microgrid capacity [7].

There are many potential locations for remote microgrid across the world in both developed and underdeveloped countries. In developed countries like the USA, this type of microgrids is mostly found in Alaska and Hawaii. In Canada, there are about 292 remote communities. In underdeveloped countries like Nepal, India, and Bangladesh, most remote part of the country can be considered as the potential location.

The ideal remote community power system is a hybrid that combines one or more renewable energy technologies (RETs) and a fossil-fueled system as shown in Fig. 1.2. Diesel generators are the primary source of energy in those remote areas due to lower initial investment, readily available and easy transportability to the remote areas [9]. However, due to high fuel procurement, transportation, and storage expenses, the true energy cost can be as high as $2.5/kWh [9, 10]. Although isolated from urban areas, renewable energy resources such as solar and the wind can be integrated with the microgrid's diesel generators to reduce overall fuel consumption. This is because the key driver for this type of microgrid is to displace diesel fuel with available renewable sources [4]. Today, photovoltaic (PV) technology is widely used in microgrids and the trend is continuously increasing. This is mostly because of the declining cost of electricity generated from solar $1/watts and still declining. With technology to compensate the PV output variability, it will be the primary source of electricity. In 2010, almost 40 MW of off-grid PV capacity was added in the US through systems that use PV arrays as a single generator or with a genset or small wind turbine in hybrid systems, reaching a total installed capacity of 440 MW of off-grid PV systems [11]. In principle, the integration of renewables into a genset-based system is relatively simple. These integrated systems operate as passive generation units, with no participation in the control strategy of the microgrid [3, 12].

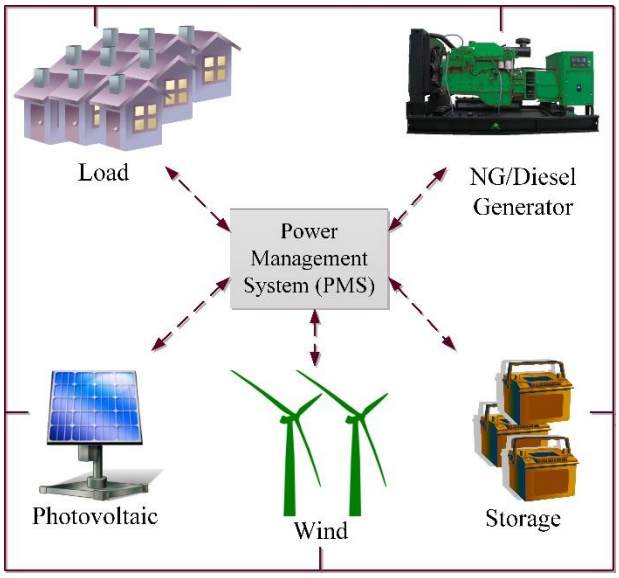

Fig. 1.2. Typical remote microgrid with renewable energy sources, storage, load and natural gas (NG)/diesel generator.

Remote microgrids have loads with high peak to average ratios [13] and generators are typically sized to meet the peak load requirements. Diesel generators have characteristics that the efficiency decreased when loading decreases. Thus, the generator often operates at low loading with resulting poor fuel efficiency [14]. In addition, frequent low-load operation below recommended by the manufacturer (usually 30%) causes wet stacking, carbon buildup, fuel dilution of lube oil, water contamination of lube oil, and damaging detonation [15, 16]. The addition of PV to the microgrid further reduces the load on the generator and causes even poorer fuel efficiency. Further, the PV resource does not correlate with load demand and the full potential of PV cannot be achieved. The traditional approach to maintain minimum loading of a generator is either dump load or PV power curtailment [17]. In either case, there is a loss of energy. Therefore, to overcome the aforementioned issues with the introduction of PV in the diesel microgrid, a storage system can be used [9].

Various storage technologies such as lead-acid batteries, Nickel-cadmium batteries, lithium-ion batteries, supercapacitors, flywheels are applicable for the remote microgrids [18]. In addition, new technologies such as fuel cells and hybrid energy storage techniques (e.g., battery and capacitor) [19] are making their way to the microgrids. Although the lithium-ion battery technology has many advantages over lead acid such as higher voltage, greater energy density, reduced weight, faster recharge time, more discharge cycles and deeper discharge tolerance [20], lead acid is mostly used in case of remote microgrid because of low capital cost. The cost of Li-ion battery is about 5 times of the lead acid battery. Another advantage of using a lead acid battery is its maturity [21]. Manufacturers have a long history of manufacturing these types of batteries and change is reluctantly accepted [22].

Energy storage systems have been added to microgrids to enable dispatch of the generators to meet load requirements [9]. The battery can act as a source to augment the generator or a load to ensure full load operation of the generator. In addition, a battery increases the utilization of PV by storing extra energy. However, the battery represents a significant cost component of the microgrid and requires proper disposal or recycling. Further, the battery has a limited energy throughput [23, 24] and maximum calendar lifetime which is also called float life. Float life is typically 10 years for a lead-acid battery [25]. For the full value of the battery to be realized, the maximum energy throughput must be consumed before the float life has been met.

There is a compromise between battery life and fuel consumption in microgrid operation. For example, generator fuel consumption can be minimized by heavy use of the battery which drastically decreases the battery lifetime. Since the battery has a high

initial cost and difficult transportation to remote areas, frequent replacement is impractical. On the other hand, if battery use is constrained to extend lifetime, generator efficiency decreases which increase fuel consumption. Thus, fuel reduction and battery lifetime improvements are two conflicting objectives of a microgrid power management system (PMS) as demonstrated in Fig. 1.3.

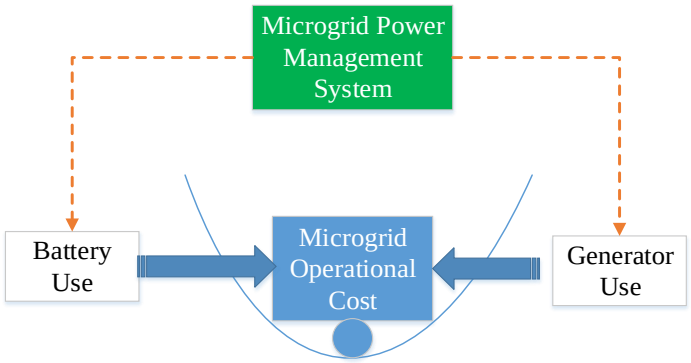

Fig. 1.3. Balance between battery and generator use cost.

Traditionally, the lower fuel consumption was achieved by running the generators in a high efficiency region at maximum load; using the battery as needed [15]. However, the battery was quickly consumed. While the system could be redesigned with a larger capacity battery, this would require a higher initial investment and may not reduce the operational costs. The battery lifetime management (BLM) strategy in the PMS algorithm helps to prolong the battery life. This paper tests the hypothesis that the use of BLM strategy not only extends the battery lifetime but also decreases the microgrid operational cost. Now, the PMS has two distinct objectives to achieve: minimize fuel consumption (obj_1) and minimize battery throughput (obj_2) to extend the battery lifetime. To achieve both of the objectives simultaneously, which also considers the float life of the battery, a novel PMS algorithm is required. Detail of the method is presented in Chapter 3.

1.2. Previous work

This section makes a review of the literature on remote microgrid systems, which is mostly used for village electrification purpose using various sources making them hybrid small-scale power supply system. The first part provides the detail of two remote microgrid operation strategies, namely: i) simple traditional (rule-based), and ii) complex (consist of schedule and dispatch algorithms), used for power management. These strategies focus on the reduction of the diesel fuel consumption, which is the primary cost of a remote microgrid. Advantages and disadvantage of each of those strategies along with how battery is utilized in the operation are provided. In addition, the importance of considering battery lifetime in the microgrid is presented. The second part of this section introduces the battery lifetime and how it is measured.

1.2.1. Remote microgrid operation

1.2.1.1. Traditional methods

Traditional methods of power management are motivated by the idea of reducing diesel consumption while satisfying the customer load. It is not necessarily required that the hybrid system must have storage to compensate for the fluctuations caused due to the stochastic nature of PV output. For such hybrid systems without storage, the diesel generator compensates intermittency. In one of the currently running examples of such systems, Nemiah valley microgrid [9], generator follows the net-load (load minus PV) demand of the system. The problem with such system is reduced loading of the generator, which causes less efficient operation and increased fuel consumption per kWh of energy [14]. There is no linear relationship between energy supplied by the PV and fuel displacement. In case of a Nehemiah Valley system, PV system supply about 14% of the

yearly energy needs of microgrid resulted in an only 5% reduction in the fuel saving. The similar study shows only 3% reduction in the fuel saving [26]. Such batteryless system requires a dump load or PV power curtailment methods to satisfy the minimum loading suggested by the manufacturer. This reduced the maximum benefit from the installed photovoltaic system.

Similar study without storage in isolated microgrid was conducted by Beyer et. al. in 2002 [27]. This study presents the results of simulation calculations and the analysis of the performance of a pilot project in the Brazilian Amazon. Fuel saving about 250 – 300 kg per kW of PV installed can be expected, but the restrictions are: PV rating close to the average daytime load and diesel generator should size reasonably in relation to the load.

Studies suggest that, in case of the batteryless or with the battery system, generator cycling can be used to match the appropriate generator size to load [9, 28, 29]. Generators are individually switched ON or OFF according to the load requirements and PV resources available. This ensures the operation of the generator(s) close to their maximum efficiency regions, improving fuel utilization, and decreasing energy costs. However, in order to maintain the generators operating near their maximum efficiency zone, curtailment of PV power output may be required or the use of the dump load to absorb excess PV generation.

Some other key notable examples of currently running microgrid without storage are provided in the study [30]. Studies suggest that without storage, there is a limitation on renewable sources that can be connected and required dump load or active power

curtailment techniques for voltage and frequency balance. Without the storage, advantages of PV integration cannot be fully realized.

The most common approach to control microgrid with storage (typically a battery) is a “rule-based” or “set-points” [15, 31, 32]. In this method, the ON/OFF control of generators, battery charger operation, dump load, and curtailment of power all based on battery state of charge (SOC). Four mostly used set-points are maximum SOC, minimum SOC, SOC when generator stops, and SOC when generator starts. When generator starts, it keeps supplying the load and charge the battery until the SOC reach to a generator stop set point. This generator stops set-point is lower than the maximum SOC of battery to provide sufficient room to store excess energy generated by PV. Otherwise, energy generated by PV goes wastage. After generator stops, battery acts as a master unit to form a grid [30]. Generator again starts when SOC goes below the generator start set-point. This generator start set-point is slightly higher than the minimum SOC. This type of battery charging is also called cycle charging [25]. When to curtail non-critical load (if available) and turn on dump load are based on the predefined rules or set points. Therefore, finding the best set points is key to improve performance [15].

A study [32] presents an optimal set point results from their Dongfushan Island microgrid, China. The optimization problem was solved using the non-dominated sorting genetic algorithm (NSGA-II). The authors found that the 61% SOC as a generator stops set- point in case abundant renewable resources and of 90% in case of short of renewable resources. This shows that the higher availability/penetration of renewable lower down the generator stop set-point. Similarly, in the study [33] conducted in South Dakota State

University microgrid research lab, 17% reduction in cost of energy was reported with 50% and 80% as generator start and stop points respectively.

Some other examples of running microgrids including famous microgrid system such as Kythnos, SSM mini-grid on Kapas Island, Malaysia with their detailed operation strategies are presented in [30]. Example of kythnos microgrid presents the operation of single phase isolated microgrid electrifying 12 houses in a small valley in Kythnos situated in the middle of the Aegean Sea. It consists of three sunny-island battery inverters, each with a maximum capacity of 3.6 kW in a master-slave configuration. Microgrid consist of 10 kW of Photovoltaics system, battery nominal capacity of 53 kWh with f-P and V-Q droop control schemes, and diesel genset of 5 kVA output. Generator start SOC is not mentioned in the study, but mentioned that the generator starts at times when the battery needs to be charged, the grid frequency is lowered. Similarly, in Kapas Island, Malaysia, the generator starts when the battery SOC less than 30% and stops when greater than 80%. The overall objective of these microgrids control strategies is to minimize the use of diesel fuel and diversify the resources.

These set-point methods are simple and easy to implement. In addition, this technique does not require the PV forecasting techniques to operate. However, one key drawback is frequent charging and discharging of a battery, which reduces the lifetime drastically. In addition, since no forecasting is implemented, renewable energy is curtailed. One simple example is if there will be the sun next hour, no need to charge battery now. If battery fully charged now, renewable needs to be curtailed next hour. Therefore, forecasting is implemented in optimization in order to fully utilize the effectiveness of renewable. The system is optimized in two different time steps. First is

scheduling and the second is dispatching. Forecasting method can help to reduce the stress on the battery for its longer life and smaller size. It will decrease the unnecessary stress from the battery.

1.2.1.2. Schedule and dispatch methods

This method is commonly used in the system capable of forecasting the load and variable sources [3]. In this double layer strategy, the schedule layer selects the resources (also called unit commitment in big electric grids) in day ahead timescale using the forecasted value of PV and load and dispatch layer performs economic dispatch in real-time. A day ahead scheduling is to obtain economic and environment friendly operation [34] whereas real-time dispatching is for reliability and power quality.

Proper scheduling of microgrid components is the key to achieve the goal of reducing fuel consumption. Since PV power output is variable in nature, forecasting helps to reduce the uncertainty while solving the problem and it also helps to maximize the use of renewable power sources. Several studies are presented in the literature on the topic of microgrid scheduling and dispatch.

In the study [35], a two-stage power management system using multi-agent system was proposed. Day ahead schedule set points are obtained in hourly basis and real-time set-points were in every 5 min basis. A real-time digital simulator (RTDS) was used to model the microgrid in real-time. The study presents the results in both grid connected and isolated mode of operation. In real-time operation, demand side management was also applied which curtails load to decrease the power consumption by controllable loads whenever required. The authors present the result of 5% reduction in operational cost by load shifting and stable microgrid operation. However, no further

study was performed to improve the battery lifetime and battery wear cost is not included in the optimization.

A study [36], showed the schedule and dispatch approach for microgrid energy management to method to provide smooth dispatch and minimize error between schedule and dispatch layer. Presented results are for both grid connected and isolated microgrids. Similarly, in [37], triple layer control (schedule, dispatch, and interaction with other microgrids) with decomposition approach in the dispatch layer increased speed was presented. A similarly, in [38], a novel energy management system, rolling horizon strategy using consumer based demand side management (DSM) scheme increased dispatch efficiency with 1-hour refresh rate of sliding window for microgrid schedule and dispatch was presented. Although most of these methods present novel algorithms for schedule and dispatching of microgrid, none of them presents analysis regarding battery use and lifetime in both schedule and dispatch algorithm.

Battery wear cost is the significant cost in case of remote microgrid operation and without battery wear cost; it is not possible to obtain the true operational cost. Few studies have considered both fuel and battery lifetime objectives during problem formulation and optimization. Studies [24, 39, 40] have used battery wear cost in an optimization model but no effort has been made to further decrease the operational cost. It is not studied that whether or not simply adding battery wear cost increases the fuel consumption and operational cost. In addition, effect of varying SOC on battery lifetime has not been studied.

Few studies have considered both fuel and battery lifetime objectives during problem formulation and optimization. A recent study presented a multi-objective optimization formulation using Genetic Algorithm (GA) to minimize power generation cost and to maximize the useful life of lead–acid batteries [32]. A weighted sum method was used to combine two objectives into a single optimization objective. However, both objectives were assumed equally important and given equal weight. Furthermore, the lifetime assumption was only applicable to the specific battery under consideration. Similar study presented in [41] presents the results of scheduling considering the battery life. Multi-objective optimization was used but with equal weightage (0.5 for each) similar to the previous study. Results show the slight increment in fuel consumption when the battery lifetime model was included. However, sensitivity analysis of weights was not performed. In addition, effect of an SOC on battery throughput was not considered.

Above methods of scheduling are based on the deterministic approach. One major drawback of such deterministic method is an assumption of perfect forecasting of solar irradiance [35]. Any variability caused by the PV is compensated by providing sufficient spinning reserve in microgrid operation. Power quality and availability are maintained mainly by operating with large reserves in gensets, leading to low energy conversion efficiency. In order to overcome the drawbacks of deterministic approach, a stochastic method of optimization can be used. In this method, a variability of PV is explicitly incorporated in the optimization [42] (see Section 2.1).

In study [34] scheduling of building microgrid components which include PV system, battery, combined heat and power (CHP) unit, and electrical loads were

performed using CPLEX solver. This paper presents both deterministic and stochastic approach of the optimization. Scenarios tree were developed in order to address the variability in PV and load requirement. Optimization was performed for only grid-connected system and no attempts were made for the isolated microgrid optimization. Researchers did not provide forecasting method. Further, the error distribution of load and forecasted PV system were assumed as a percentage of the mean (forecasted) value. Battery optimization was not considered not either attempts were made to increase battery life.

In the study [39], energy scheduling in microgrid is presented using both stochastic and deterministic optimization methods. Expected operational cost results were compared to demonstrate the superiority of stochastic method over deterministic. This study does not present the multi-objective optimization but battery degradation (wear) cost was considered in the objective function. The limitation of this study is lack of battery lifetime improvement studies and more importantly, effect of battery SOC during the operation is not considered. The maximum SOC for a day was 35%. In this low SOC, wear cost should be very high, which is not considered. Therefore, presented results cannot be justified.

Similarly, a study [43] presents stochastic and deterministic results in isolated microgrid using particle swarm optimization (PSO) method. The microgrid model consists of PV generation (30 kW), wind generation (20 kW), diesel generator (30 kW) and battery (300 kWh). It was presented in the study that with stochastic optimization, use of battery is slightly reduced but studies regarding lifetime improvement were not provided. In fact, the wear cost of battery was not considered in the objective function.

1.2.2. Battery lifetime

According to the United States Advanced Battery Consortium (USABC), battery life is a time by which the battery capacity reduces to 80% of its rated value [44]. Various approaches were presented in [23, 45, 46] for the prediction of lead acid battery lifetime. One study suggested that a lead-acid battery with Q Ah capacity provides approximately 390×Q effective Ah throughput during its service life [24]. The limitation of this approximation is that it is useful only for the specific lead-acid battery under consideration. However, this study uses the data provided by the battery manufacturer so the method is applicable to other types of batteries. Similarly in [45], three different approaches: i) Physico-chemical ageing model, ii) Weighted Ah ageing model, and iii) Event-oriented ageing model, were compared based on their complexity, precision and calculation speed. Among the aforementioned methods, the weighted Ah ageing model predicted the most accurate result compared to others [46]. This model is based on the fact that a battery can provide a fixed amount of lifetime throughput (Ah or kWh) in its useful life. When the cumulative sum of throughput provided by a battery is equal to the lifetime value, the battery's capacity is considered to be reduced to 80% [23].

The lifetime information in the battery datasheet is for the standard laboratory test conditions such as rated DOD, fixed discharge rate and temperature. However, the real-time operation of the battery with stochastic PV sources is much different from the standard, therefore, prediction of the battery lifetime is a complex task.

1.3. Summary of previous work

In summary, it was found on literature that the most of the studies were mostly focused on the grid connected microgrid but few for the completely isolated remote

microgrids. In addition, none of the literature has presented the optimal weights based on the battery lifetime and operational cost. In addition, studies do not consider the effect of battery SOC during the selection of the weights. Thus, a proper power management scheme providing effective means to address microgrid functionalities is necessary.

1.4. Motivation

Need a remote microgrid power management system that can reduce the operational cost while extending battery lifetime.

1.5. Objectives

The research objective of this project is to develop a novel PMS for PV-diesel hybrid microgrids that will coordinate distributed energy resources, diesel generators and loads in order to minimize operational costs of the microgrid. The tasks identified to accomplish the objective were

Task 1: Develop remote microgrid benchmark and optimization framework to prolong battery life and minimize fuel consumption.

Task 2: Develop a two-layer novel power management system algorithm and implement new irradiance forecast method based on Markov witching method.

Task 3: Validate developed PMS in remote microgrid test cases using deterministic and stochastic approaches.

1.6. Contributions

The original contributions of the dissertations are:

- Proposed a novel PMS algorithm considering battery lifetime and float life of the battery.
- Provides comprehensive analysis of battery lifetime using Ah-weightage method and implemented in the proposed PMS.
- The effectiveness of the proposed method was validated using a currently working remote microgrid as a test case.
- Provides a detailed method to validate the use of PV power forecasting by Markov switching model using real-time analysis of the remote microgrid.

1.7. Dissertation outline

The structure of this dissertation follows:

Chapter 2 discusses the various known theories related to microgrid operation and control. This includes mathematical modeling of the microgrid components, various PMS control architecture, optimization methods and solar irradiance forecasting method.

Chapter 3 presents the remote microgrid optimization framework. This includes a development of microgrid benchmark and the detailed process how the optimal operation is achieved. Furthermore, developments of various test cases are discussed.

Chapter 4 discusses the simulation results obtained during the study using a PMS proposed in this dissertation. Daily and yearly simulation results are discussed to validate the effectiveness of the proposed method.

Chapter 5 presents the summary and key finding of the research. A brief description of future work that can be performed based on this research and limitation of the study are presented at the end of the chapter.

CHAPTER 2: THEORY

This chapter discusses the various know theories related to microgrid operation and control upon which this dissertation is based on. Section 2.1 describes the mathematical modeling of the typical remote microgrid components and their operational characteristics. These typical components include mainly diesel generators, batteries, and PV systems. Section 2.2 describes the various power management strategies for microgrids with high penetration of renewable. This includes a single and multi-master operation of remote microgrid and PMS control architecture such as central, distributed, and hybrid. Section 2.3 describes the scheduling and optimization approaches followed by a solar irradiance forecasting method in Section 2.4 and methods to compensate the variability in PV output in Section 2.5.

2.1. Remote microgrid components

A typical remote microgrid consists of a diesel generator, battery, and renewable energy sources (PV is considered in this study) as shown in Fig. 1.2.

2.1.1. Diesel generator

Diesel generators are primarily used electric power source in remote microgrids. These diesel generators possess a unique operational characteristic of the relationship between loading and efficiency. Operation at low load results in lower fuel efficiency [16, 47] and maximum efficiency can be obtained only when operates near the full load capacity. A Kohler 30 kW diesel generator efficiency curve is shown in Fig. 2.1. The amount of fuel consumption in an hour by the diesel generator is based on the power output, which can be approximated using the quadratic relation as given in Eq. 2.1 [48].

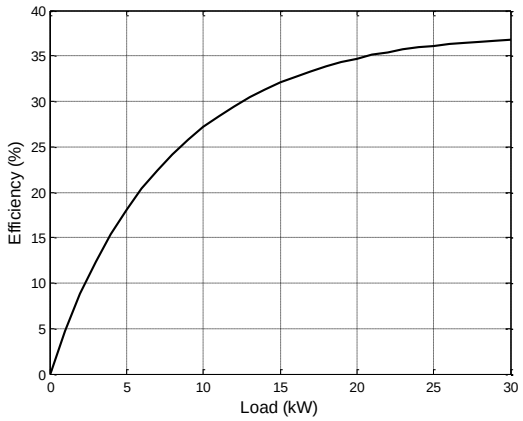

Fig. 2.1. Generator loading vs. efficiency.

$$Fuel\_Consumption(\text{vol/ hr}) = \left(a \times P^2 + b \times P + c\right) \tag{2.1}$$

where *a*, *b* and *c* are the fuel curve coefficients, *P* is the generator power output. The operation of the generator typically specified by the minimum required power output (P_{min}) to prevent the carbon buildup and to improve the life of the generator as given in Eq. 2.2.

$$P_{\min} \le P_t \le P_{\max} \tag{2.2}$$

where P_t is the power output of the generator at any time *t*, which is always in between the minimum and maximum power output limit.

For any power system network, the generated power must match the demand and voltage must be within the specified limits. In order to provide this match, the rotating diesel generator can operate in isochronous or droop mode. The isochronous mode has a fixed steady state frequency and applicable in an isolated system when a single generator is running. Governor of the generator is responsible for changing the power output to meet the demand and automatic voltage regulator is responsible for the voltage control. When generation is less than load, the frequency drops. The governor detects this drop in

frequency and the control system increases the opening of the fuel valve to increase the power output of the generator. The governor attempts to maintain the same frequency regardless of the load it is supplying up to the full load capabilities of the generator set as shown in Fig. 2.2. In addition, operating most generators below 30% of rated capacity can lead to reduced life or engine failure due to liner glazing [49] and wet stacking [40, 50] so dump loads are often employed to ensure minimum loading [11].

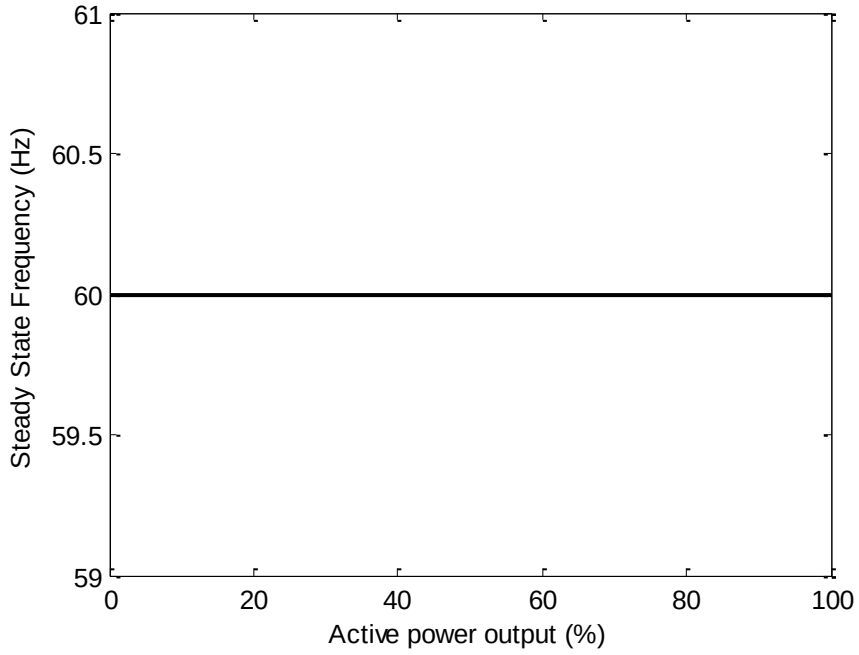

Fig. 2.2. Isochronous mode of operation.

Droop mode is applicable when two or more generators are running in parallel and need to share the load. Typically, in such a case, one generator (bigger) operates in an isochronous mode and another (smaller) in droop mode. If both generators operate in isochronous mode, there will be conflict to control the system frequency.

In droop mode, active power output from the generator changes as the frequency deviates as shown in Fig. 2.3 with droop slope [30], [51]. In another word, speed decreases by a fixed percentage from no-load to full load and provides a stable working point for each load in case of parallel operation [52]. A typical droop slope setting is between 2 to 4% (usually 4%), which means a power output changes by 100% (no-load to full-load) with 4% change in frequency [53]. Power output at certain frequency can be changed by shifting up or down the droop curve or by setting no-load frequency.

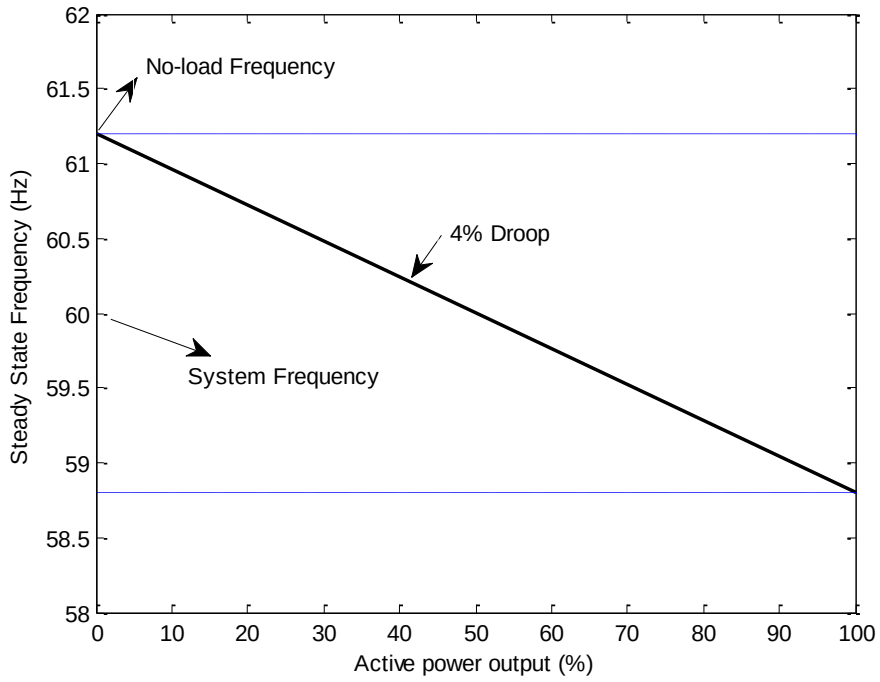

Fig. 2.3. Frequency droop control technique.

2.1.2. Battery

Batteries are the key component of the remote microgrid, which helps to improve the microgrid system performance by increasing the renewable energy utilization and improving the generator efficiency [41]. Its dynamics can be represented by state of

charge (SOC) parameter. SOC provides the information regarding how much energy is stored in the battery and can be expressed as Eq. 2.3 and 2.4 [34].

During charging event, next hour state of charge (Eq. 2.3), *SOC(t+1)*, depends upon the current *SOC(t)*, current charging power ($P_{b,t}$), time interval between two consecutive measurement (Δt), battery capacity ($BattCap_{kWh}$), and charging efficiency (η_{crg}).

$$SOC\left(t+1\right) = SOC\left(t\right) + \frac{\eta_{crg} \times p_{b,t} \times \Delta t}{BattCap_{kWh}} \tag{2.3}$$

Similarly, during discharging event next hour SOC (Eq. 2.4) depends upon current discharging power ($P_{b,t}$) and discharge efficiency (η_{dcrg}). Other parameters are same as defined for Eq. 2.3.

$$SOC\left(t+1\right) = SOC\left(t\right) + \frac{p_{b,t} \times \Delta t}{\eta_{dcrg} \times BattCap_{kWh}} \tag{2.4}$$

In order to protect from deep discharge, SOC operating range is defined between the maximum and the minimum values.

$$SOC_{\min} \le SOC_t \le SOC_{\max} \quad \forall t \in T \tag{2.5}$$

Similarly, the maximum charge and discharge rate of a battery are also defined in the allowable range.

$$P_{b,mcrg} > P_{b,t} > P_{b,mdcrg} \quad \forall t \in T \tag{2.6}$$

2.1.3. Photovoltaic (PV) system

A photovoltaic system is a type of distributed generation where solar panels are used to convert solar radiation into direct current (DC) electricity. Since the characteristic

IV (current-voltage) curve of the panel is not linear, the power produced from the panel depends upon the operating voltage and maximum power (P_{mpp}) occurs at the knee of the I-V curve as shown in Fig. 2.4. The voltage where maximum power is obtained is called the maximum power voltage (V_{mpp}), and the current at this voltage is called the maximum power current (I_{mpp}). The power P_{mpp} is simply the product of V_{mpp} and I_{mpp} (P = VI). V_{oc} is a maximum voltage available from the panel, which occurs at the zero current condition (i.e., no load) and I_{sc} is a current through the solar panel when the solar cell is short circuited (i.e., zero voltage).

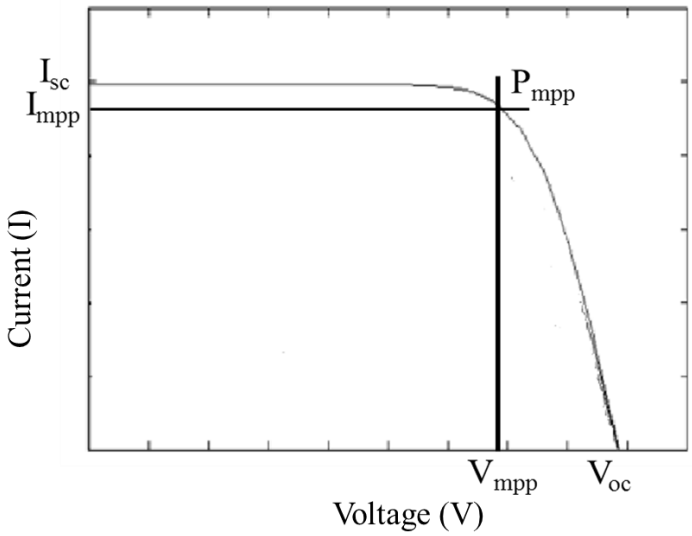

Fig. 2.4. I-V characteristic of PV panel.

The electrical characteristics of PV modules (V_{oc}, I_{sc}, V_{mpp}, I_{mpp}, P_{mpp}) are rated at standard irradiance and temperature (STC) conditions. The standard conditions are the AM1.5 spectrum, 1000 W/m^2 and 25 °C, but in practice, a PV panel does not operate under these conditions most of the time. The short circuit current is proportional to the irradiance as shown in Fig. 2.5 and has a small temperature coefficient. The open circuit

voltage has a negative temperature coefficient and depends logarithmically on the irradiance. Therefore, the open circuit voltage, short circuit current and maximum power point change with a change in irradiance or temperature. Typically, a PV system utilizes a maximum power point tracker (MPPT), an electronic device to continuously track the maximum power point on the I-V curve regardless of environmental conditions and solar irradiance [54]. For the sake of simplicity, effect of temperature neglected and PV power output depends primarily on solar irradiance (G_t). Therefore, the maximum power output from the PV system of nominal capacity (PV_{nom}) is given in Eq. 2.7 as presented in [25]. f_{PV} represents the photovoltaic derating factor.

$$P_{PV,t} = f_{PV} PV_{nom} \frac{G_t}{G_{STC}} \tag{2.7}$$

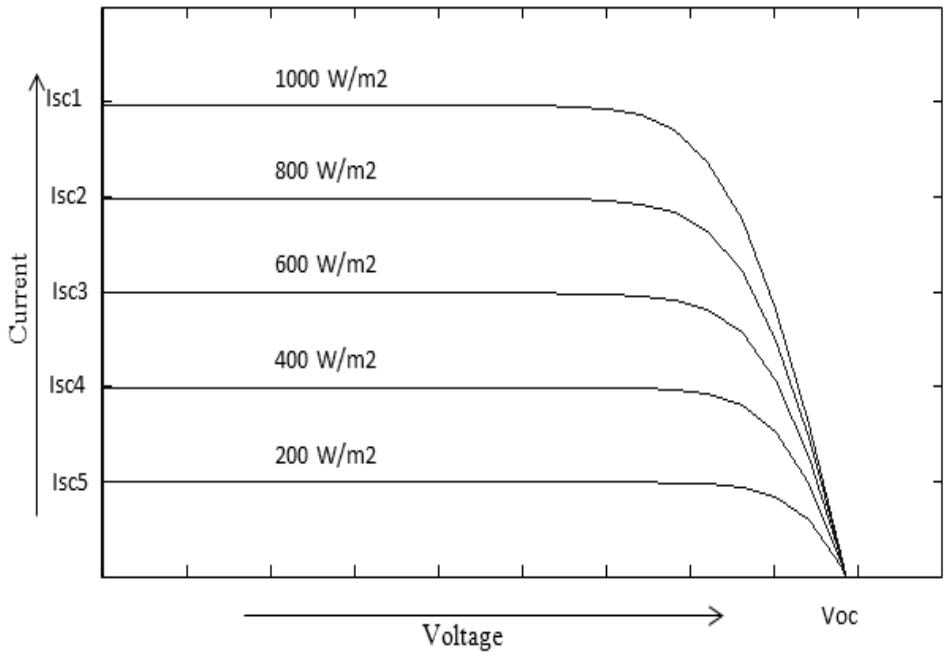

Fig. 2.5. I-V curve for a typical PV panel at different irradiance levels [55].

2.2. Microgrid operation and control

2.2.1. Microgrid operation

Microgrid operation can be classified based on the architecture and how frequency and voltage are maintained [56, 57]. Based on the number of master units available in the remote microgrids, operation can be classified in to the single and multi-master operation.

2.2.1.1. Single master operation

Single master operation is characterized by one power generation unit (P_{G1}) at a time which is responsible for maintaining the frequency and voltage. Since remote microgrid can consist of diesel generators and sometime battery backup with inverter, grid forming unit (master) can be either of them. For low penetration of renewable energy sources, typically a rotating generator operates as a master unit [30], but for high penetration with long-term storage, battery inverter can operate as master unit and allows the rotating generator to be switched OFF. Further, the presence of storage reduces the need for dump loads [58]. The excess available power is used to charge the batteries, which keeps the rotating generator operating at rated load (high efficiency). When the battery is fully charged, the generator is turned OFF and the battery system becomes the master. This method is suited for applications where the load profile is not well known.

2.2.1.2. Multi master operation

In a multi master system, the rotating machine and the electronically interfaced units share the task of maintaining the frequency and voltage through power sharing methods such as droop control [59]. As numerous DG units contribute to maintain system stability, coordinating the control of the units becomes challenging. This technique is

usually applied in a microgrid with high penetration of RES combined with long-term storage.

2.2.2. Microgrid control

A PMS provides microgrid control necessary for the efficient operation and optimum utilization of the RES. The PMS coordinates with microgrid resources and provides an effective means to meet load requirements. The management of non-dispatchable RES (e.g. PV, wind) is one of the main challenges in the operation of microgrid [60]. The choice of a control technique depends upon the distance separating the sources and loads, resource characteristics (dispatchable/non-dispatchable), and load requirements. Due to the difference in resources availability and location as well as load requirements, one single control technique is not applicable to all microgrids. Mainly three control techniques are available.

2.2.2.1. Centralized control

The centralized control method utilizes a central controller communicating to microgrid resources. The central controller contains all the relevant information of the microgrid components. This information includes: forecasted values of the non-dispatchable sources, load, operational limits (maximum, minimum and most efficient region) of dispatchable sources, SOC of the battery, and the state of the components (ON or OFF) [60]. Control strategies to obtain optimal operation can be accomplished by supervisory control and data acquisition (SCADA) systems [61, 62]. A fast and reliable communication link is required for real-time operation and optimization of the system. The required communication between MCC and component can be obtained through telephone lines, power line carriers, or a wireless medium. However, it could be

prohibitively expensive if a long distance transmission is needed. This type of control is most suitable for situations where all components are located in one central station.

An advantage of central control is the ability for central monitoring and the availability of a large amount of system data that can be used to optimize microgrid operation. Since, the entire microgrid system depends upon a single controller, the failure of that controller will cause system failure. Other disadvantages include the inability to support plug and play flexibility and the high computational power and memory requirements necessary for manipulating a large number of data points.

A typical architecture for the central control method is shown in Fig. 2.6. Each component accepts the command and performs the operation accordingly. Example commands could include active and reactive power dispatching values and load shedding. Studies [57, 60, 61, 63-65], presents various test cases using this type of control technique.

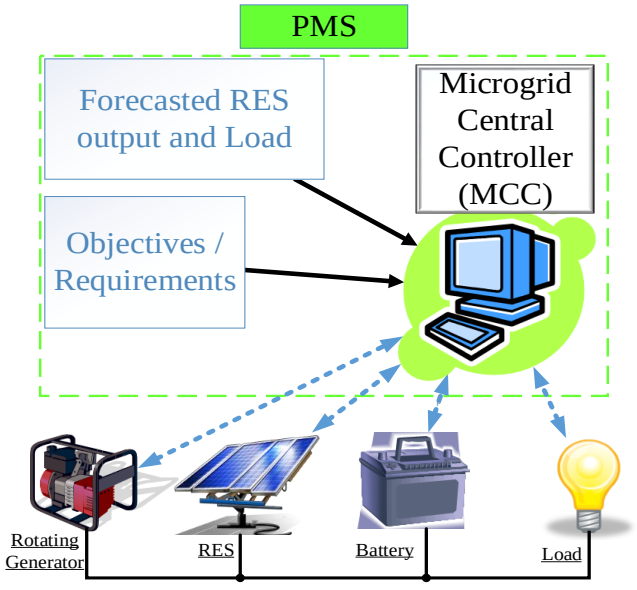

Fig. 2.6. Microgrid central control architecture with various resources including renewable energy sources (RES) [66].

2.2.2.2. Distributed control

In a distributed control, the local controllers (LC) independently manage the microgrids components. Distributed control can be divided into two types depending on whether or not the LCs communicates with each other. First is droop-based communication-less control. In this type of control, local measurement of voltage and frequency, which does not require a communication link as shown in Fig. 2.7 is used for load sharing among the generators [67-69]. Frequency droop is typically used to control the active power and voltage droop to control the reactive power [51]. When there is change in load or generation, frequency changes and master unit (battery or generator) adjust the power accordingly. In this type of control, no regular update on droop setting is provided. This method is useful when the resources are dispersed across the microgrid [70]. Droop control also enables plug and play flexibility to expand the system with additional DGs [71].

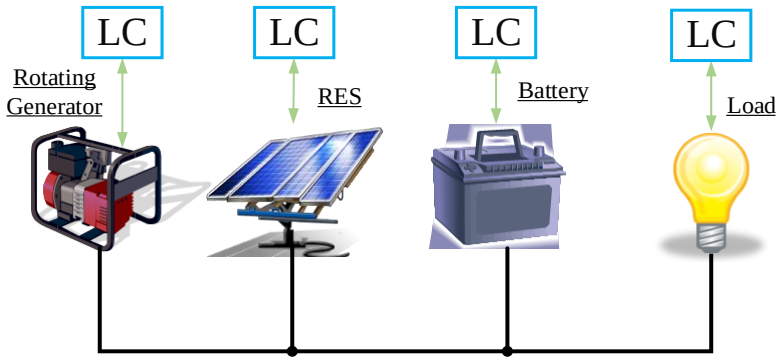

Fig. 2.7. Typical LC-based microgrid.

Second type of distributed control is multi-agent system (MAS). A limitation of communication-less system is the inability to optimize the utilization of microgrid resources. The addition of a communication link between the LCs enables the optimal dispatching of DGs to better utilize RES and reduce fuel consumption [60, 72-74]. A

typical architecture for MAS is shown in Fig. 2.8 where each component is assigned to the respective agent and all agents communicate with each other.

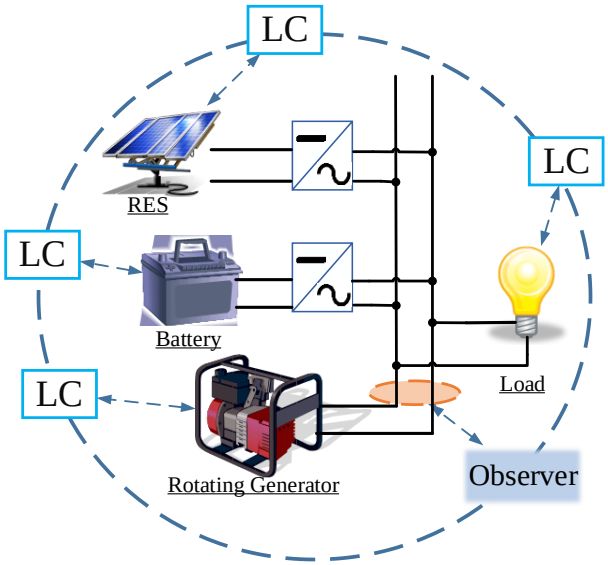

Fig. 2.8. Typical MAS architecture for PV hybrid microgrid.

2.2.2.3. Hybrid control

Hybrid control is a method where a central controller is used to modify droop parameter of LCs via low cost, slow communication link [75]. A typical architecture for the hybrid control method is shown in Fig. 2.9. The central controller sets steady state parameters while the LC provides transient response without relying on communication [59, 71]. An example of a hybrid system is the one used in the Consortium for Electric Reliability Technology Solution (CERTS) microgrid. In another example [76], a method utilizing frequency partition instead of droop control was presented.

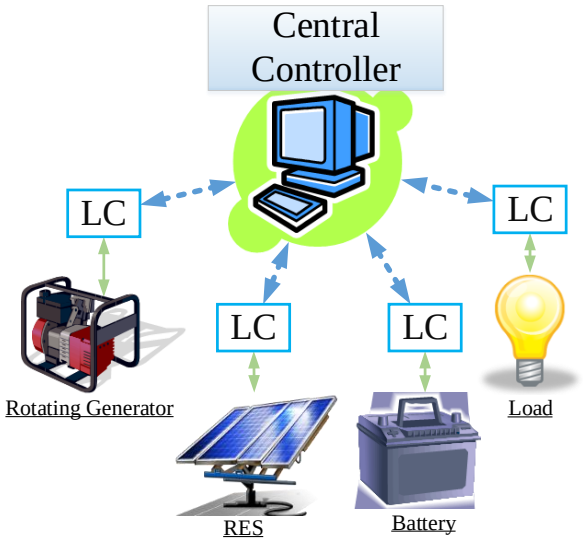

Fig. 2.9. Hybrid control method.

Summary of aforementioned control techniques are presented in Table 2.1 [66].

Table 2.1. Major characteristics of different control techniques

Methods	Control	Pros	Cons	Application
Central PMS	Central	Broad observability, Higher control over resources, Increasing energy efficiency	Fast and reliable, communication channels required, Reduce flexibility, Low PMS system reliability	Single master operation, Co-location of microgrid components, High penetration of non-dispatchable RES
Distributed PMS	LC Based	No communication channel required, Low cost solution, Increasing flexibility, Support Plug and play feature	Low energy efficiency	Multi-master operation, Microgrid components are dispersed throughout the network, When plug and play feature required
	Multi Agent System	High reliability, Increasing energy efficiency	Communication between agents required	Multi-master operation, Microgrid components dispersed throughout the network, High penetration of non-dispatchable RES
Hybrid PMS	Central + LC	Higher system reliability, Increasing energy efficiency	Slow communication channels	Single master or multi-master operation, Microgrid components dispersed throughout the network, High penetration of non-dispatchable RES

2.3. Scheduling and optimization

Scheduling is the process of allocating resources ahead of time to achieve certain required objective. Typically, a day ahead scheduling is performed to achieve economic and environmental benefits and real-time (also called economic dispatch or 15 minutes ahead scheduling [35]) is to achieve the reliability as shown in Fig. 2.10. For scheduling, it is required to have time ahead prediction of the uncertain variable with some degree of confidence such as PV power output and load demand. Scheduling provides the power output set points of each generator for scheduling horizon.

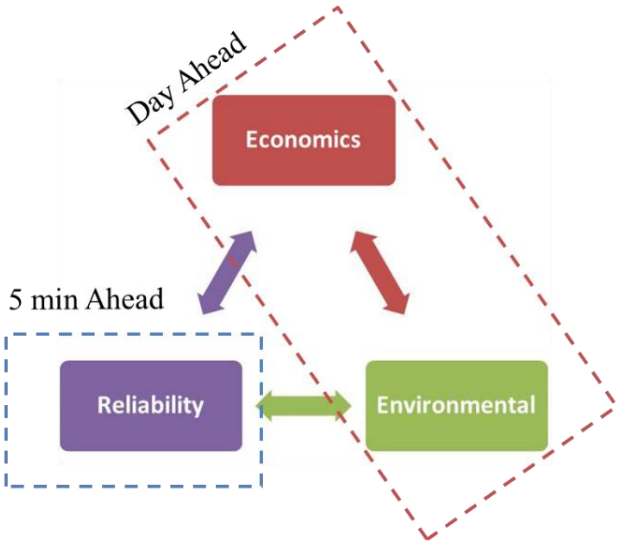

Fig. 2.10. Microgrid optimization timeframe.

The day ahead schedule module gathers the 24-hour load and PV resource forecast as well as information about the system architecture and constraints. In typical microgrids, this information is used to determine the schedule for each generator and storage device which results in the lowest fuel consumption [77]. The schedule is then sent to the real-time dispatching module, which implements the schedule and compensates for any deviations from the forecast to ensure the power balance. The

dispatching module also ensures the effectiveness of the scheduling module by compensating the deviation from the forecasted.

Microgrid scheduling is an optimization problem where the presence of both continuous and discrete decision variables exists. Continuous variables are power output from individual generating resources and discrete variables are ON/OFF status of those generating sources. These problems also have some equality and inequality constraints. In addition, microgrid scheduling has to deal with the inclusion of stochastic variables such as PV power output and load demand. Furthermore, microgrid must be capable of handling the uncertainties. Such an optimal scheduling problem mostly handled using two different approaches described next.

2.3.1. Deterministic approach

In the deterministic approach, it is assumed that the real values of PV power output and loads are equal to their forecasted values. However, PV power and load demand are stochastic in nature and cannot be forecasted accurately. Therefore, the power management system must have a means to address the variability in PV power generation. One way to address variability is by scheduling a spinning reserve for each hour and assuming the PV output equal to the forecasted value [78].

One important aspect of the power system that needs to be considered for reliable power is a short-term power and a long-term energy balance. Long-term energy balance is considered in the planning phase of the microgrid, including, but not limited to, selection of size and type of storage, characteristic of distributed generation units. Short-term power balance requires sufficient spinning reserve during the time of operation, which is critical in case of remote microgrid since it is running without any grid support.

Furthermore, remote microgrids are typically operated with the large penetration of the non-dispatchable energy sources, spinning reserve plays an important role to compensate the uncertainty. In typical remote microgrids, main causes of uncertainty are: i) due to equipment failure, and ii) due to load and renewable uncertainty. The probability of equipment failure is not considered in this study. Therefore, allocation of the proper spinning reserve during the scheduling process is important to provide quick compensation required due to an uncertainty of load and renewable source.

As presented in [78], two main approaches are available in the literature to determine the required spinning reserve capacity, they are deterministic and probabilistic. Deterministic is a traditional approach, where reserve capacity equal to the largest unit running or the certain percentage of the load demand is allocated as spinning reserve. Whereas in probabilistic approach, probability measures were used to determine the spinning reserve such as standard deviation and confidence interval.

2.3.2. Stochastic approach

The deterministic method does not include variability of PV generation in optimization, which might lead to underutilization of the sources and does not realize the scenarios that could happen in real-time. As the exact realization of PV power output was not available at the scheduling stage, the decisions must be flexible enough to cope with uncertainties. Therefore, stochastic optimization approach can be used to further improve the system performance. One method to incorporate the uncertainties is developing a number of scenarios those likely to happen in the future and minimizing the expected value of the objective function over all scenarios, which is the operational cost of a remote microgrid in this dissertation. In another word, instead of minimizing function *f(x)*

for one single scenario, the algorithm will try to minimize E[*f(x)*] over all developed scenarios.

Scenarios are the set of possible future alternatives based on some sort of probability. Development of the realistic scenarios is the critical to capture the variability in the system. Unrealistic scenarios could lead system to the wrong direction and reliability and the benefits of the optimization process can be compromised. In a case of the system where optimization which is performed under the influence of uncertainty of PV system output, probability distribution function of the irradiance forecasting errors plays an important role while developing the scenarios.

2.3.2.1. Scenario generation

For the development of the scenario with the available forecasting error pdf, various methods can be used ranging from statistical methods to the random sampling and the Monte Carlo method. In the literature, a large number of studies talks about the various methods of scenario generation. Four main methods are presented in [79], those are: Sampling, Statistical approaches, Simulation, and Hybrids. Similarly, in the study [80] authors presented the various other scenario generation methods available namely: Bound-based constructions, Monte Carlo sampling, optimal quantization of probability distributions, Quasi-Monte Carlo based discretization methods, probability metric based approximations and EVPI-based sampling and reduction within decomposition schemes.

Since the infinite number of scenarios can be developed using the Monte Carlo with the available continuous PDF, studies limit the number of sampling either by internal sampling or with the procedure, which discretized the continuous PDF to the

small set of discrete outcomes [81]. The previous study also collectively presents the various methods available in the literature to discretize the continuous PDF and keeping the characteristic. The standard approach is “bracket mean” method, where the outcome regions is divided into N equally probable intervals and mean value is selected in each interval with a probability of 1/N. Since this method assumes equal probability for each of the sample points, this certainly underestimates the probability of occurrence near the mean value. For this types of issues, either previous experience [82] or other methods such as presented in the literature review [81] is used. Once the PDF is discretized, scenario tree can be developed based on the discretized samples. Fig. 2.11 shows a simple example of scenario tree with continuous PDF was discretized into the three samples. For the 24-hour period, extremely large number of scenarios (3^{24}) can be developed using this tree, which requires large computational power and might not be feasible sometimes. Therefore, the various scenario reduction techniques are used to develop a manageable number of scenarios [83].

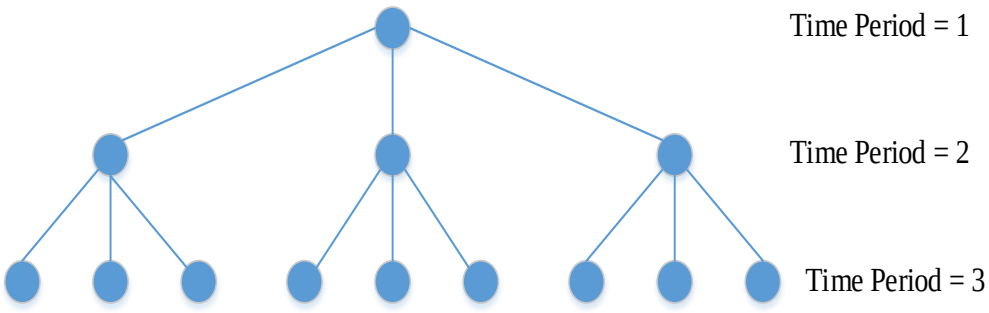

Fig. 2.11. Multi stage scenario tree.

Scenario generation in power system were roughly divide into two categories. Selection of the scenario generation is based on the requirement of their particular study.

i) **Use of continuous PDF:** Although an infinite number of scenarios are required to represent the exact distribution, good estimation can be obtained with a large number of scenarios. These large number scenarios later reduced to a manageable number using a scenario reduction algorithm. In [84], 3000 scenarios are developed using Latin hypercube sampling (LHS) method and assuming a continuous normal distribution for the wind power generation around forecasted value. Later, generated scenarios were reduced to 10, which provides the acceptable result. Similarly, in [34] error probability distribution was used to generate the 100 equally probable scenarios and used in optimization without any reduction. Scenarios were developed assuming a normal distribution and forecasted demand as a mean value. The study assumes that the 100 scenarios will approximate the normal distribution. Scenarios can be generated in the prediction interval (PI) which covers the required percentage (eg. 95%) of the probabilistic confidence interval. Assuming the error distribution follows the normal distribution $N(\mu_{error}, \sigma_{error})$, maximum and minimum fluctuations in certain period of time can be given by:

$$fluctuation = \pm(\mu_{error} + z \times \sigma_{error}) \tag{2.8}$$

where, z-score represents the degree of confidence (1.96 for 95% confidence) and σ is the standard deviation of the forecasting error. Adding and subtracting fluctuation in the forecasted value will provide the 95% confidence range.

ii) **Use of Discrete PDF:** A large number of study talks about this approach. For example, in the study [85], scenarios were developed using forecasted value, forecasted error mean and standard deviation, which covers 90% of the probabilistic confidence interval. The underlying distribution was discretized into the five samples and scenario tree

was developed. After that the scenarios reduction technique is used to limit the number of scenarios.

2.3.2.2. Scenario reduction

It was seen in the previous example that, even with the 3 discrete samples extremely number of scenarios could be developed then realize how many scenarios can be developed using continuous PDF, which is infinite. Therefore, it is extremely important to use scenario reduction during the optimization process. There is a tradeoff between generated scenario numbers and approximately representing the underlying distribution. A higher number of scenarios are required to approximate the distribution, but require high computational power. This provides the importance of the scenario reduction techniques. In addition, not all of them are important because of the probability of occurrence is low and some scenarios are equivalent to another. Therefore, in order to eliminate the low probability scenarios and merge similar ones scenario reduction techniques are important [83]. This method makes the system computationally efficient and viable by selecting only the realistic ones. During the scenario reduction process, the first step is to perform clustering of the scenarios which are close to each other before the application of the scenario reduction algorithm. Some of the well-known methods as mentioned in [83] are fast backward, fast forward/backward and the fast forward method. One example of the fast forward technique is Kantorovich distance scenario reduction method. The following section provides a simplified Kantorovich distance scenario reduction method algorithm. Detailed descriptions of the methods with examples are provided in the studies [86-88].

Kantorovich distance scenario reduction method algorithm

N_s represents the number of scenarios, N_t represents the number of optimization steps (if optimization is for 24 hours then n_t is 24), y_t represents the scenario value at time t, $d_t^{i,j}$ represents the distance between i_{th} and j_{th} scenario at time t, and π_{ns}represents the probability of n[th] scenario.

Step 1: Find the distances between scenarios at time t

$$d_1^{i,j} = \begin{pmatrix} d_1^{1,1} & d_1^{1,2} & d_1^{1,3} & \ldots d_1^{1,N_s} \\ d_1^{2,1} & d_1^{2,2} & d_1^{2,3} & \ldots d_1^{2,N_s} \\ \ldots. & & & \\ d_1^{N_s,1} & d_1^{N_s,2} & d_1^{N_s,3} & \ldots d_1^{N_s,N_s} \end{pmatrix}$$

$$\ldots\ldots\ldots \qquad (2.9)$$

$$d_{N_t}^{i,j} = \begin{pmatrix} d_{N_t}^{1,1} & d_{N_t}^{1,2} & d_{N_t}^{1,3} & \ldots d_{N_t}^{1,N_s} \\ d_{N_t}^{2,1} & d_{N_t}^{2,2} & d_{N_t}^{2,3} & \ldots d_{N_t}^{2,N_s} \\ \ldots. & & & \\ d_{N_t}^{N_s,1} & d_{N_t}^{N_s,2} & d_{N_t}^{N_s,3} & \ldots d_{N_t}^{N_s,N_s} \end{pmatrix}$$

Step 2: Calculate cost function

$$c = \sum_{t=1}^{N_t} d_t^{i,j} = \begin{pmatrix} (d_1^{1,1}+..+d_{N_t}^{1,1})\ (d_1^{1,2}+..+d_{N_t}^{1,2})\ \ldots (d_1^{1,N_s}+d_{N_t}^{1,N_s}) \\ (d_1^{2,1}+..+d_{N_t}^{2,1})\ (d_1^{2,2}+..+d_{N_t}^{2,2})\ \ldots (d_1^{2,N_s}+..+d_{N_t}^{2,N_s}) \\ \ldots. \\ (d_1^{N_s,1}+..+d_{N_t}^{N_s,1})\ (d_1^{N_s,2}+..+d_{N_t}^{N_s,2})\ \ldots (d_1^{N_s,N_s}+..+d_{N_t}^{N_s,N_s}) \end{pmatrix} \qquad (2.10)$$

Step 3: Calculate the Kantorovich distance of scenarios

$$\begin{aligned} Kd_1 &= \pi_1 \times c(1,1) + \pi_2 \times c(1,2) \ldots + \pi_{Ns} \times c(1,N_s) \\ Kd_2 &= \pi_1 \times c(2,1) + \pi_2 \times c(2,2) \ldots + \pi_{Ns} \times c(2,N_s) \\ &\ldots\ldots\ldots \\ Kd_1 &= \pi_1 \times c(N_s,1) + \pi_2 \times c(N_s,2) \ldots + \pi_{Ns} \times c(N_s,N_s) \end{aligned} \qquad (2.11)$$

Step 4: Determine scenario with minimum Kantorovich distance and update the elements of cost function (c) matrix. If Kd_2 is found minimum, the second scenario is the first one to get selected. The cost function elements are updated as:

$$c(i,j) = \min_{i \neq j}(c(i,2), c(i,j)) \tag{2.12}$$

Step 5: Use Step 3 to determine the next scenario to be selected

Step 6: Repeat process until the required number of scenarios are selected

Step 7: Transfer probability of non-selected to selected scenarios. Each non-selected scenario probability will be transferred to the nearest selected scenario based on initial cost function matrix.

2.4. Irradiance forecasting

In order to define the schedule that will lead to optimal performance of a microgrid, an estimate is necessary of how much energy will be consumed by the loads and how much will be available from renewable resources like PV system. Detailed method regarding the solar forecasting is given in the study [89]. This is simple and easily implementable solar forecasting method developed using the Markov Switching Model. It uses available historical data for the region and local measurements. The case for solar irradiance forecasting will be shown as an example of how this method will be applied.

Regional, hourly data from the past three consecutive years is collected from a database like solaranywhere.com. In order to capture the variability, two Fourier basis expansions are fitted. The first expansion accounts for monthly and seasonal irradiance trends. Summer months are expected to have more daily solar irradiance than winter months. The second expansion accounts for daily irradiance trends. Mornings and evenings have less irradiance than middays. Clear sky irradiance, radiation under a cloudless sky as a function of the solar elevation angle, site altitude, aerosol concentration, water vapor, and various atmospheric conditions [90], are calculated for

the area. Linear model, y(t) is fitted to forecast the hourly irradiances using least-squares.

$$y(t) = \beta_1 CSI(t) + \sum_{i=1}^{m_1} \beta_{1i}\phi_{1i}(t) + \sum_{i=1}^{m_2} \beta_{2i}\phi_{2i}(t) + \varepsilon(\mathrm{t}) \quad (2.13)$$

where $CSI(t)$ is the clear sky irradiance value for time t, $\sum_{i=1}^{m_1} \beta_{1i}\phi_{1i}(t)$ is the yearly Fourier component, $\sum_{i=1}^{m_2} \beta_{2i}\phi_{2i}(t)$ is the daily Fourier component, and $\varepsilon(\mathrm{t})$ is a random noise component.

The irradiance available at time point *t* has a latent state variable. This latent variable confounds the linear model and creates large discrepancies between the forecasted and observed irradiance. Therefore, three different irradiance forecast models were developed: high, medium and low energy regimes using the Markov Switching Model. Knowing the standard deviation of the forecasting error, we can generate a variety of scenarios for stochastic optimization. This model can forecast based on the first four hours of data to determine the rest of the day's irradiance and uses publicly available environmental information to train the system. Fig. 2.12 shows the three different energy regimes with forecasted and actual irradiance data for two different days. The first day was predicted as a high-energy day and the second was predicted as a medium energy day. Identifying changes in energy regime are challenging when using this method. In order to address this problem, we are developing an algorithm in the real-time dispatch unit to readjust set points when regime switching is detected. This simple method mostly applies to remote areas where sophisticated forecasting techniques such as those based on a satellite image, numerical weather prediction, and artificial neural networks are unavailable.

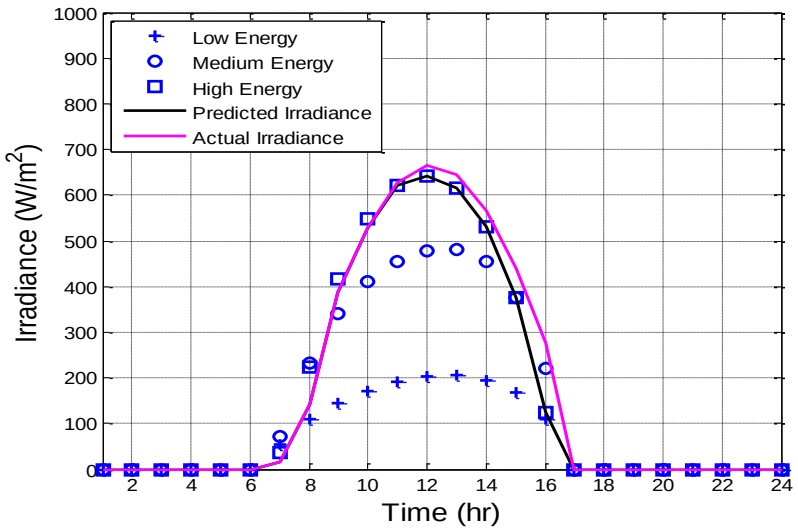

(a)

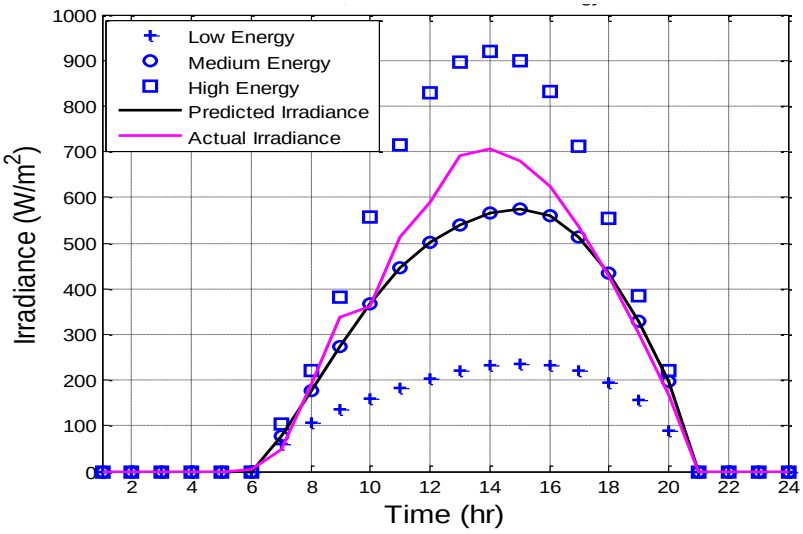

(b)

Fig. 2.12. Solar forecasting using Markov switching model: (a) high energy prediction day and (b) medium energy prediction day.

Error in the forecast can be measured by using a mostly used metric called average root mean square error (RMSE). RMSE was calculated by averaging the errors in

each forecasting period. RMSE gives the measure of the largest deviation, which gives the measure of the largest error.

$$\mathrm{RMSE} = (\frac{1}{\mathrm{M}} \times \sum_{\mathrm{n=1}}^{\mathrm{M}} \mathrm{e_n^2})^{\frac{1}{2}} \tag{2.14}$$

2.5. Real-time power balancing

Because the PV system has a varying power output, a real-time power management (short term power balancing) is required to ensure the reliability and to provide continuous matching of supply and demand system [91]. Such power management is also required to keep the effectiveness of the scheduled layer [35]. Real-time power balancing in large power network and remote microgrid is a different process. In case of a system with large number of generators and transmission lines, automatic generator control changes the power set points of the generators to provide the best economic dispatch. This is because, different generator power output goes through different transmission line and transmission line could be congested. Therefore, typically in each five minutes (in real- time), power set points are adjusted [92]. This is also to maintain the tie line flow. However, in case of the small remote microgrids where only radial system is working and either generator or the battery is running as a master unit, this method is quite hard to implement and sometime does not have any practical meaning. Most generators are running on isochronous mode of operation; PV is not dispatchable and only component to control is battery with the inverter. Use of available reserve is the primary method to keep the reliability in the system. Master unit (generator or battery) compensates the variability with running on isochronous or droop mode of operation. This is not always possible in two situations:

i) When operational constraints do not meet or required power goes outside the master unit's capacity range.

ii) When operation is not economical or disregards the effectiveness of the scheduling unit.

In order to provide the short-term power balancing in microgrid, various load management techniques can be used to bring the forecasted net-load close to the predicted one. Such techniques include:

a) Power curtailment: When PV real-time generation is higher than the scheduled and operational constraints of the units (battery and generator) are violated, power curtailment method is used. PV power output can be curtailed completely [9] or partially [26]. During complete disconnection, PV output is wasted. Another method of power curtailment presented in study [93], where maximum peak power point of the PV is controlled as required.

b) Load management/Demand response: For the real-time operation of the microgrids in isolated mode, load shifting and load curtailment are the essential means to deal with sudden power fluctuations [36]. Typically, microgrids consist of two types of load: critical and non-critical. Non-critical load can be shifted from peak to non-peak hours and can be disconnected if required to maintain the power balance [35]. Similarly, end-users can be encouraged to make short-term reductions in energy demand in response to signal initiated by the microgrid operator, which is called demand response [94].

CHAPTER 3: PROCEDURE

The chapter describes detailed procedures to complete the three tasks defined previously in the Chapter 1. Section 3.1 describes the development of remote microgrid benchmark for the study. The benchmark description includes characteristics and parameters of the resources. For example, efficiency of the generators, load and PV profile, battery and generator cost model. In addition, a procedure to calculate the lifetime throughput and battery throughput cost is described in Section 3.1. Once the benchmark is developed, the implementation of the developed PMS using both deterministic and stochastic approach is described in the Section 3.2. Furthermore, the real-time dispatch, which consist of various real-time power balancing strategies are presented in the Section 3.2.3. Section 3.3 describes the various cases studied to verify the developed algorithm.

3.1. Remote microgrid benchmark

A 75 kW PV-diesel hybrid remote microgrid similar to that described in [9] has been adopted for analysis as shown in Fig. 3.1. This microgrid consists of 30 kW and 75 kW diesel generators running in isochronous mode and a 27 kW PV system. Minimum operation of the generators were limited to 30% of their rated capacity. A 170 kWh lead-acid battery with 80% round-trip efficiency and a maximum 50% DOD was added to improve reliability, fuel efficiency and renewable utilization. The battery was sized to supply an average load for four hours, which is typical in case of remote microgrid systems [33]. The hybrid power management system was used to control the microgrid components. Batteries, generators and load should follow the instructions from the central controller. Low communication bandwidth was sufficient enough for this type of operation and suitable for the remote microgrids. It is assumed that the communication

link exists in the microgrid. Other assumptions for the study are: i) Voltage levels are considered to be the same at different part of the microgrid, ii) Power losses have been ignored in the model, and iii) Reactive power flows are not considered.

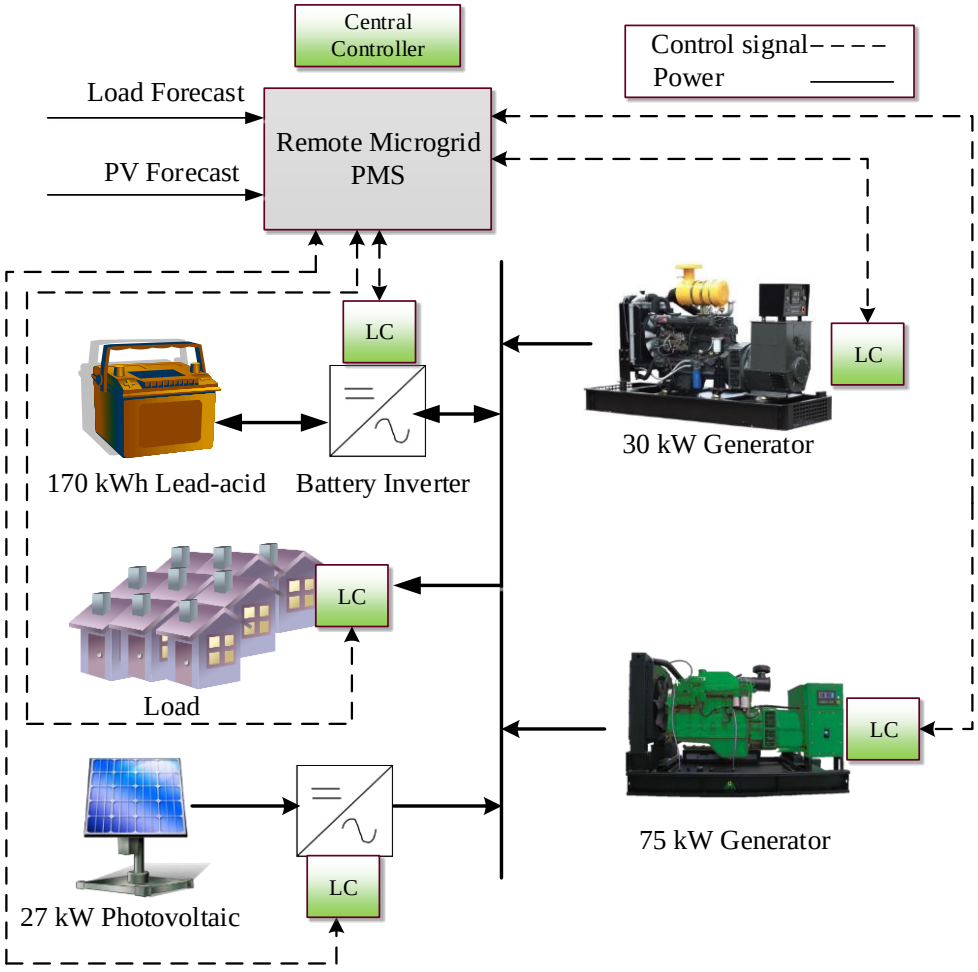

Fig. 3.1. Remote microgrid layout.

Fuel consumption curves for KOHLER 30 kW (model 30REOZJC) and 75 kW (model KT75) diesel generators were developed using product specification sheets provided by the manufacturer as shown in Fig. 3.2. Similarly, the efficiency curve for the selected generators is shown in Fig. 3.3. It was observed that the efficiency of a 30 kW generator was higher during the low load condition.

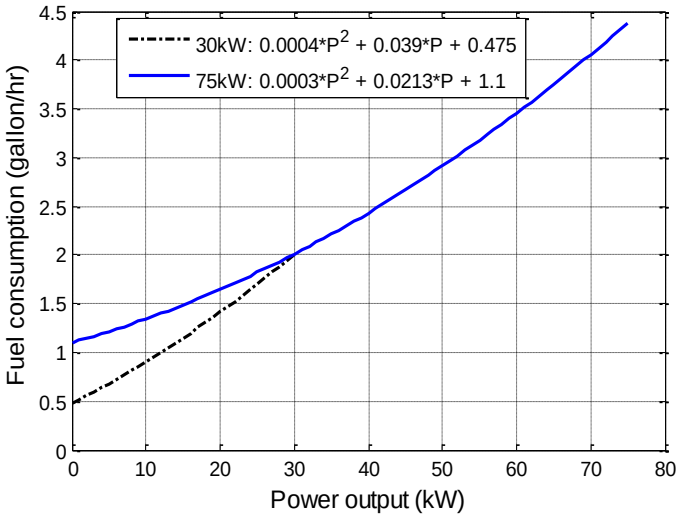

Fig. 3.2. Generator fuel consumption curves.

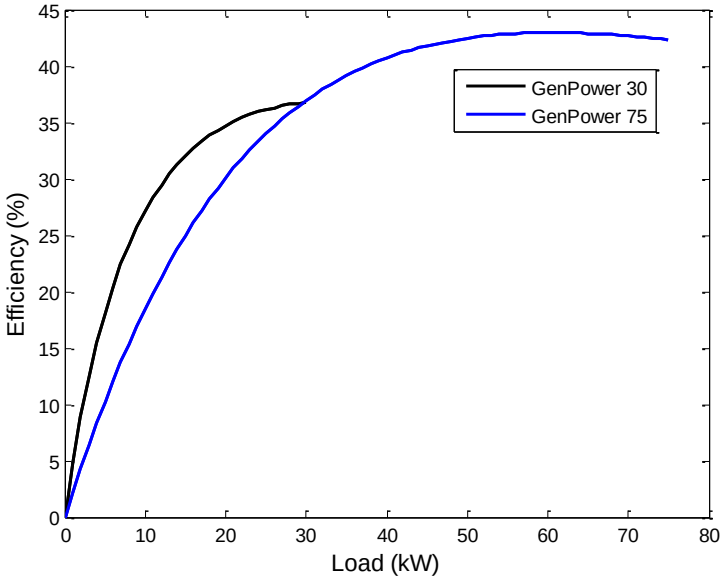

Fig. 3.3. Generator efficiency vs loading.

The annual load profile shown in Fig. 3.4 and PV output shown in Fig. 3.5 used in this study were obtained from a similar remote microgrid currently operating in North America. As shown in Fig. 3.4, the annual peak demand was 64 kW and the average was

25 kW. The peak load was 2.56 times the average load. The total load was divided into critical which includes residential and important commercial loads such as a health clinic and non-critical loads such as water heater and water pumps. In reality, PV is distributed throughout the network but for the simplicity, it is assumed that all PV are connected at the same POC (aggregated as a 27 kW) and experience the same irradiance level. The PV derating factor for the system was 0.77.

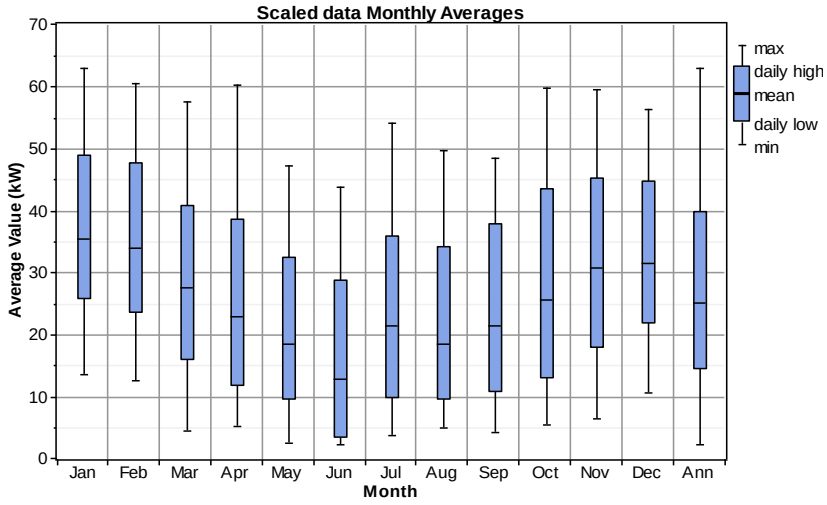

Fig. 3.4. Yearly load demand.

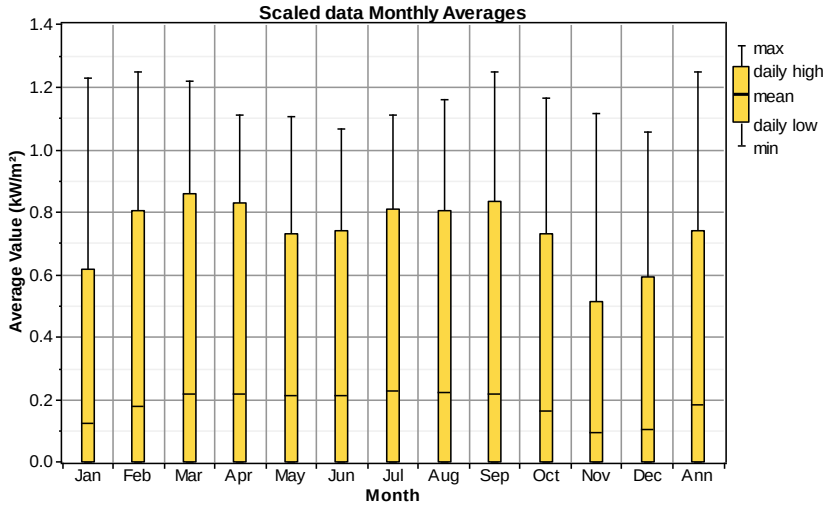

Fig. 3.5. Yearly PV irradiance.

Since generator and battery are the two main components, the cost model for each one of them were developed and presented in the section 3.1.1 and 3.1.2.

3.1.1. Generator cost model

Generator related cost includes fuel cost, generator hourly replacement cost, maintenance cost and emission cost (not included in this study). Fuel consumption can be calculated using the simple quadratic equation. The n^{th} generator's daily fuel cost was estimated by multiplying fuel volume with fuel cost per unit volume as given in Eq. 3.1. The operation of generators was limited to a minimum of 30% of their rated capacity in order to prevent wet stacking, carbon buildup, fuel dilution of lube oil, water contamination of lube oil, and damaging detonation. A 75 kW generator was allowed to operate in the range of 22.5 kW to 75 kW and a 30 kW generator was limited to 9 kW to 30 kW as given in Eq. 3.2.

$$C_n\left(P_n\right) = C_{diesel} \times \sum_{t=1}^{24}\left(a_n \times P_{n,t}^2 + b_n \times P_{n,t} + c_n \times U_{n,t}\right) \tag{3.1}$$

$$U_{n,t} \times P_{n,\min} \le P_{n,t} \le U_{n,t} \times P_{n,\max} \quad \forall t \in T,\ \forall n \in N \tag{3.2}$$

where, $U_{n,t}$ is the generator ON/OFF status at that particular hour.

Generator's lifetime hours was estimated to obtain the hourly replacement cost. Generator lifetime hours depends on various factors such as proper maintenance and frequency of use [95]. From examples of real working microgrids and the manufacturer's documents, 40,000 hours is typically the accepted value for a diesel generator lifetime between two major overhauls or replacements [25, 95, 96]. Using this approximation, the generator's hourly replacement cost ($/hr) was calculated by dividing initial investment of

generator ($) by lifetime hours. It shows that higher generator running hour leads to the higher operation cost. Maintenance cost was assumed constant and equals to $8000.00 per year. Remote microgrid generators are typically small; therefore, startup and shutdown costs were neglected in the study [39]. The generator's minimum up and down time were 1 hour. In the study, total generator use cost is the sum of fuel cost and hourly replacement cost, which is the first objective (Obj_1) that needs to be minimized.

3.1.2. Battery wear cost model

To determine the battery wear cost ($/kWh), it is necessary to approximate the lifetime throughput of the battery. The lifetime throughput can be calculated using information in the battery specification sheet, but this is only applicable to the laboratory standard test conditions such as fixed discharge rate, rated DOD, and temperature. However, the real working condition is completely different from the standard in case of remote microgrids with high penetration of stochastic PV system. Studies [45, 46, 97] presented additional factors upon which the lifetime Ah-throughput varies such as no. of battery life cycle, partial state of charge cycling, incomplete or rare full charging, temperatures, the complex interaction between the various ageing processes, and the operating conditions. Therefore, an amount of throughput in real-time is not equivalent to the same as determined on the standard test conditions (i.e. actual 1 Ah is not equal to 1 Ah at standard test condition). Therefore, throughput continuously needs to be weighted during real-time operation and when the total weighted throughput is equivalent to the throughput calculated from the manufacturer datasheet, the battery is considered to have reached its lifetime. In this study, a weighted Ah method originally presented by Schiffer in [97], was used to calculate actual Ah throughput and battery lifetime.

3.1.2.1. Calculate datasheet lifetime throughput

Usually, a manufacturer specification sheet provides the information required to approximate battery lifetime in the form of battery cycle life vs depth of discharge (DOD). Example of Sun Xtender PVX-2580L is shown in Fig. 3.6 (a) [98]. Here, the DOD of a battery can be expressed in terms of SOC and vice versa (DOD = 1-SOC).

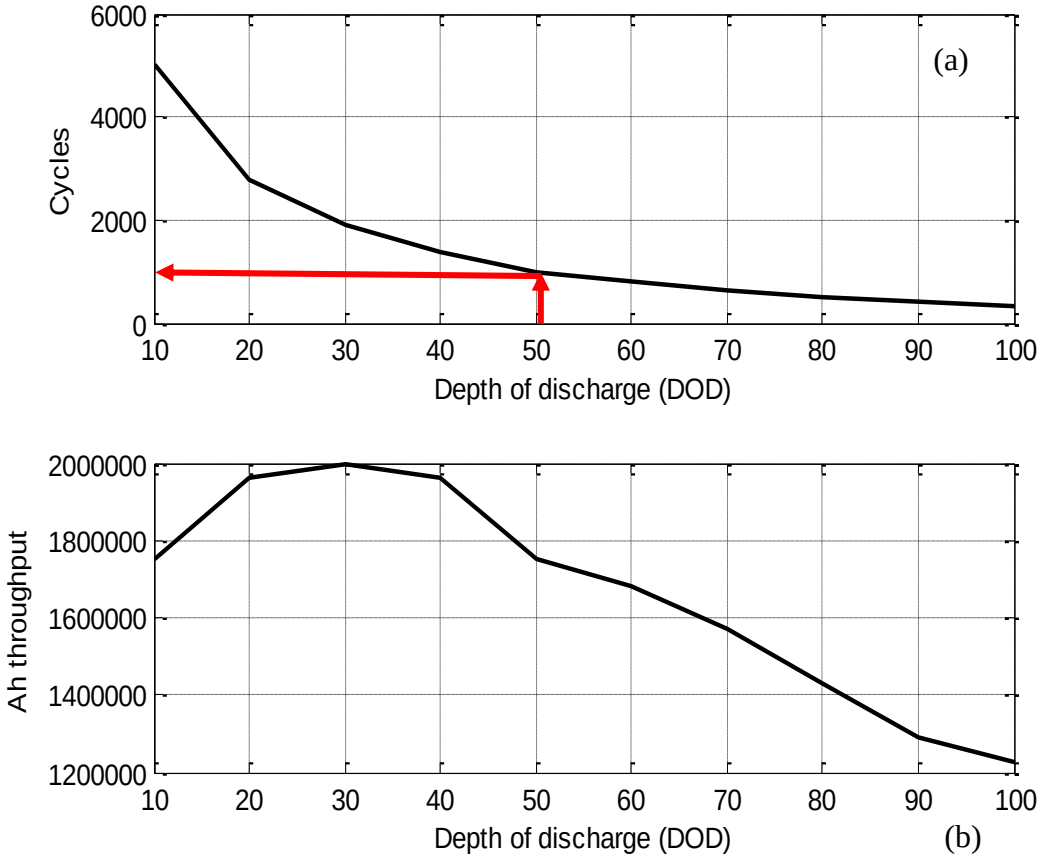

Fig. 3.6. Battery characteristics curves: (a) battery life cycle vs depth of discharge (b) lifetime Ah throughput vs DOD.

The total Ah lifetime of a battery at rated depth of discharge (DOD_R) and Ah capacity ($BattCap_{Ah}$) is given by Eq. 3.3 [23].

$$Ah_{lifetime} = L_{c,DOD} \times DOD_R \times BattCap_{Ah} \quad (3.3)$$

One simple example illustrates the method to calculate lifetime throughput using Eq. 3.3.

Assuming,

Rated battery capacity ($BattCap_{Ah}$) = 258 Ah

Battery rated voltage ($BatteryVolt$) = 12 Volt

Cycle life @0.5 DOD ($L_{c,DOD}$) = 1000

$Ah_{lifetime}$ = 1000 × 0.5 × 258 = 129000 Ah

$kWh_{lifetime}$ = (1000 × 0.5 × 258 × 12)/1000 = 1548 kWh

Since the DOD can vary in between the allowable range (0 to 50% DOD for this study), corresponding life cycle ($L_{C,\,DOD}$) also varies as shown in Fig. 3.6 (b). Here, the life cycle represents the total complete discharge cycle (discharging after complete charging) that the battery can provide in that particular DOD. Therefore, the average total Ah lifetime is calculated by averaging the lifetime throughputs between allowable DODs as shown in Eq. 3.4. Similarly, battery lifetime in terms of average kWh throughput is given in Eq. 3.5.

$$Ah_{lifetime,avg} = Average\left\{ L_{c,DOD} \times DOD \times BattCap_{Ah} \right\}_{DOD=DOD_{\max}}^{DOD_{\min}} \quad (3.4)$$

$$kWh_{lifetime,avg} = \frac{Ah_{lifetime,avg} \times BatteryVolt}{1000} \tag{3.5}$$

Battery wear cost is given by [25]:

$$C_{batt,\,perkWh} = \frac{C_{initial,batt}}{kWh_{lifetime,avg} \times \eta_{dcrg}} \tag{3.6}$$

3.1.2.2. Calculate weighted lifetime throughput

The first step in finding weighted lifetime TP is to calculate battery throughput weighting factor. Actual throughput was multiplied by a weighting factor in each time step to determine the weighted throughput. When weighted throughput equals the throughput calculated in Eq. 3.5, the battery was considered to be dead. The weight factor was calculated using Schiffer's weighted model [97]. This model calculates the capacity loss by corrosion and degradation. However, for simplicity, only the effect of SOC on battery life is considered in this study, which is the most important parameter. The W_{soc} factor (SOC weighting factor) as shown in Eq. 3.7 takes into account the SOC influence [46]. Degradation increases with decreasing SOC of the battery. This process will address impacts due to low SOC and large time gap between two full charges. Both events will increase mechanical stress on the active masses and increase the size of sulfate crystals. It is set to 1 at each full charge and increases with time since the last full recharge (t_0).

$$\begin{aligned} W_{SOC}(t) = 1 + (&C_{SOC,0} + C_{SOC,\min} \times (1 - SOC_{\min}(t)|_{t_0}^{t}) \times \\ &W_I(I, n_b) \times (t - t_0)) \end{aligned} \tag{3.7}$$

In Eq. 3.7, constant slope for SOC factor ($C_{SOC,0}$) and the impact of the minimum SOC ($C_{SOC,min}$) on the SOC factor were adapted from [97]. The current factor $W_I(\mathrm{I}, \mathrm{n}_b)$ describes the influence of the current as given in Eq. 3.8 where, I_{ref} is the 10 hr current ($I_{10}=C_{10}/10$). The number of bad charges (n_b) depends on the maximum SOC obtained

during the charging process. Charging lower than 0.9 SOC will not affect the number of crystals at all and should therefore not be counted as a bad charge. However, charging higher than 0.9 and lower than 1 is considered as a bad charge because the number of crystals decreases but their size increases. So the current factor is also affected by n_b. When fully charged it is zero, but when charged in between 0.9 to 1, it is calculated as in Eq. 3.9.

$$W_I(I, n_b) = \sqrt{\frac{I_{ref}}{I}} \times \sqrt[3]{\exp \frac{n_b(t)}{3.6}} \tag{3.8}$$

$$n_b(t + \Delta t) = n_b(t) + \frac{0.0025 - (0.95 - soc_{\max})^2}{0.0025} \tag{3.9}$$

Once the W_{soc} for each time period calculated, weighted throughput was calculated by multiplying with the discharged battery power ($Pb_{disc,t}$) with W_{soc} factor at every time step. During charging period, $Pb_{disc,t}$ was zero. Since, hourly optimization was considered, Δt represents one-hour period. Total weighted throughput was the sum of the values for scheduling horizon (24 hour in this study) as shown in Eq. 3.10. Daily battery wear cost was calculated using Eq. 3.11.

$$kWh_{24hr} = \sum_{t=1}^{24} Pb_{disc,t} \times W_{SOC}(t) \tag{3.10}$$

$$C_{batt,24\text{hr}} = C_{batt,\,perkWh} \times kWh_{24hr} \tag{3.11}$$

In order to calculate life in years, the total actual weighted kWh was calculated for one year and compared with the total average lifetime kWh from the datasheet calculated in the Eq. 3.5. Total wear cost of the battery for a particular period was calculated by multiplying total weighted actual throughput with the battery wear cost calculated in the Eq. 3.6.

Since, both objectives can be expressed in terms of cost, the PMS will not only extend battery lifetime, but also decrease the microgrid operational cost. A weighted sum method [99, 100] was used where a single objective is developed from a weighted sum of functions representing the two objectives of the problem as given in Eq. 3.12. The goal of this objective is to minimize the cost of operation. These weights determine the priority of each objective. If both weights are equal (0.5), the objectives are equally important. If one is higher than the other is, it indicates that the objective with the higher weight is more important to achieve the overall goal.

$$obj = (W_1 \times obj_1 + W_2 \times obj_2) \tag{3.12}$$

In this study, the average lifetime throughput of the battery was calculated using a DOD range of 0 to 0.5, which is typical for lead acid batteries. In this study, the battery maximum charge and discharge power output was limited to -45 kW and +45 kW, respectively. This range could be different for different types of battery and microgrid configuration. Further, the range is also subjected to the limitation imposed by a battery charger/inverter. The initial investment cost of the battery and the generators (Table 3.1) were determined based on current market price [101]. The average lifetime throughput of the battery was equal to 90,384 kWh. The fuel cost was $9.00/gallon based on a remote community electric utility [102].

Table 3.1. Battery wear cost and generator hourly replacement cost

Component	Initial cost ($)	Wear and hourly replacement cost
Battery	40,000	$0.5/kWh
Generator (30 kW)	14,000	$0.35/Hr
Generator (75 kW)	20,000	$0.5/Hr

3.2. Two layer power management system algorithm

The proposed PMS consists of two distinct modules (day ahead schedule and real-time dispatch) which schedule and control the operation of the generators and battery as shown in Fig. 3.7.

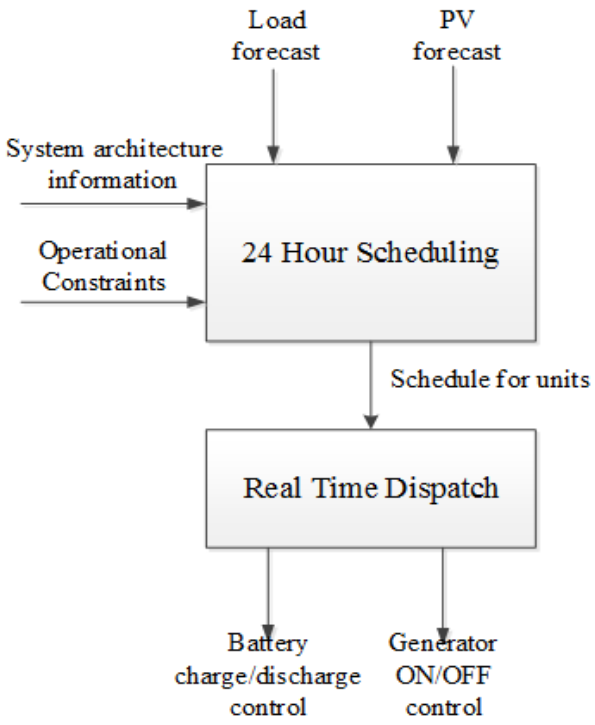

Fig. 3.7. Two distinct modules of remote microgrid PMS.

3.2.1. Day ahead schedule

First task of the PMS is day ahead scheduling. Forecasted value of PV and load along with the information of the system architecture and constraints were provided to the day ahead schedule module. The Markov switching method was used to obtain the forecasted PV power [89]. Microgrid operation was optimized using the IBM ILOG CPLEX v12.6.1 solver. This product is developed by IBM ILOG, which is a high performance solver for Linear Programming (LP), Mixed Integer Programming (MIP)

and Quadratic Programming (QP/QCP/MIQP/MIQCP) problems [103]. A 3.20 GHz processor desktop with 8 GB RAM was used to solve the problem. The computational time for each yearly simulation was about 4 minutes.

Generation set points for the optimal operation of the microgrid were obtained using both deterministic and stochastic optimization approaches. In these approaches, the diesel generators and the battery both can be the master unit of the microgrid. For our study, when battery is acting as a master unit, it is operated similar to a synchronous generator with active power vs frequency and reactive power vs voltage droop characteristic. For remote microgrid, frequency control is more important. Table 3.2 shows the master unit of the microgrid in various scheduled condition.

Table 3.2. Master unit selection

Resources Scheduled	Master Unit
A single diesel generator	Diesel generator (isochronous mode)
Multiple diesel generators	Largest diesel generator
PV + Battery	Battery inverter
PV + Generator	Diesel generator in isochronous mode
Battery	Battery inverter

3.2.1.1. Deterministic approach

While using deterministic approach, a spinning reserve equal to 20% of the forecasted load was used based on a study [78] to compensate the variability in PV power output and load. The deterministic objective function is:

$$obj = \min \left\{ W_1 \times \left(\sum_{n=1}^{N} C_n(P_n) + \sum_{t=1}^{24} \sum_{n=1}^{N} U_{n,t} \times C_{n,\mathrm{hrc}} \right) + W_2 \times C_{batt,24hr} \right\} \tag{3.13}$$

In addition, operational constraints are:

i) Power balance

$$\sum_{i=1}^{N} P_{n,t} - p_{b,t} = \left(P_{L,t} - P_{pv,t} \right) \quad \forall t \in T \tag{3.14}$$

ii) Battery State of charge

$$SOC_{\min} \le SOC_t \le SOC_{\max} \quad \forall t \in T \tag{3.15}$$

iii) Maximum charge and discharge rate of a battery are limited to:

$$P_{b,mcrg} > P_{b,t} > P_{b,mdcrg} \quad \forall t \in T \tag{3.16}$$

iv) Generator power output limit

$$P_{n,\min} \le P_{n,t} \le P_{n,\max} \quad \forall t \in T, \ \forall n \in N \tag{3.17}$$

v) Reserve requirement

$$((SOC_t - SOC_{min}) \times BattCap_{kWh} \times \eta_{dcrg} / \Delta t) + \sum_{i=1}^{N} P_{n,max} \times U_{n,t} \ge (Reserve_t + P_{L,t}) \quad \forall t \in T \tag{3.18}$$

where,

t	Time index, t = {1, 2, ..T}
n	Generator index, n = {1, 2, ..N}
$U_{n,t}$	Generator ON/OFF control at t (1=ON, 0=OFF)

$P_{n,t}$	Power output of n^{th} generator at t (kW)
$C_n(P_{n,t})$	n^{th} generator cost at t ($/hr)
$P_{n,min}$	Min. power output of n^{th} generator (kW)
$P_{n,max}$	Max. power output of n^{th} generator (kW)
$C_{n,hrc}$	n^{th} generator hourly replacement cost ($/hr)
$P_{PV,t}$	Photovoltaic power output at t (kW)
$P_{b,t}$	Battery input/output power at t (positive for charging and negative for discharging)
$P_{b,mcrg}$	Battery maximum charge rate (kW)
$P_{b,mdcrg}$	Battery maximum discharge rate (kW)
SOC_{min}	Minimum battery state of charge
SOC_{max}	Maximum battery state of charge
SOC_t	Battery state of charge at t
η_{crg}	Battery charging efficiency
η_{dcrg}	Battery discharging efficiency
C_{batt}	Battery wear cost ($/kWh)
$P_{L,t}$	Load demand at t (kW)
$Reserve_t$	Required spinning reserve at t

3.2.1.2. Stochastic approach

In this approach, instead of spinning reserve allocation, multiple scenarios with respective probabilities were generated, which explicitly considers the effect of uncertainty [42]. Uncertainties are incorporated with the objective function that better helps to realize and optimize the variability. This approach will consider a large number

of possible power output scenarios of variable sources that likely to happen in the future and provides an average best result over all scenarios [34]. Realistic scenarios were developed using probability density function (pdf) of the renewable output forecasting errors, which was derived from the historical data of the renewable power generation. Quality of forecasting method reduces the error. Since the forecasting error is random in nature and there are large amount of random data for the yearly analysis, its distribution can be assumed normally distributed.

Scenario generation process starts with finding the distribution of the forecast error and its parameters (standard deviation and mean). Monte Carlo sampling method considering the forecasted error distribution was used to develop the required number of scenarios. The detailed scenario generation procedure is as follows:

Step 1: Obtained forecasted and actual PV power and calculate forecast error distribution. Assuming PV forecasting error follows normal distribution, standard deviation (σ) and mean (μ) were calculated. For normally distributed error, the standard deviation of the error can be approximated by the square root of the MSE.

Mean square error (MSE) of the forecasted PV

$$MSE = \sum \frac{(|\ Actual - Forecast\ |)^2}{N} \tag{3.19}$$

Step 2: Prediction interval (PI) of the forecasted value at each time step was determined using Z score, forecasted value and MSE. The Z score represents the degree of confidence (1.96 for 95% confidence). This range between lower and upper value provides the information that forecasted value will be in this range 95% of the time.

$$Lower = F(t) - z \times \sqrt{MSE} \tag{3.20}$$

$$Upper = F(t) + z \times \sqrt{MSE} \tag{3.21}$$

Step 3: Monte Carlo simulation method was used to generate 1000 numbers of scenarios for a day. Each scenario is independent and has an equal probability of 0.1. While using lower and upper bound, it was noticed that the upper limit sometime exceeds the PV system rating. In such case, the upper limit was set to the maximum PV rating. Similarly, if lower limit goes below, it was set to zero. In order to reduce the computational power required to solve 1000 scenarios, fast forward method using Kantorovich distance scenario reduction was used. The output of this method was 10 most probable scenarios with their respective scenarios.

For the stochastic optimization, two-stage decision framework will be used [39, 42]. It is also called two stage recourse models. In first stage, generator ON/OFF decision is made before the realization of the uncertainty in a PV system. These are called first-state decision variables [104]. In second stage power output of generator and battery will be decided. These are the recourse decisions made after the realization of the uncertainty. In such multi-framework optimization, decisions made in first stage will be same for all developed scenarios.

The stochastic objective function is

$$obj = \min \left\{ \sum\nolimits_{s=1}^{S} \Pi_S \left\{ W_1 \times \left(\sum_{t=1}^{T} \sum_{n=1}^{N} C_n(P_{n,t}^s) + \sum_{t=1}^{T} \sum_{n=1}^{N} U_{n,t} \times C_{n,hrc} \right) + W_2 \times C_{batt,24hr}^s \right\} \right\} \tag{3.22}$$

where, Π_S is the probability of the individual scenarios respectively, $P_{n,t}^{s}$ is the power output of the n^{th} generator at time t in scenario *s*, $C_{batt,24hr}^{s}$ is the battery wear cost of scenario *s*. Other variables are same as explained in the deterministic section. Operational constraints are same as deterministic and reserve requirement constraint (Eq. 3.18) was not used for the stochastic optimization method.

3.2.2. Determining weights W_1 and W_2

The best set of weights W_1 and W_2, which determines the proper use of generator and battery was determined by yearly analysis using deterministic approach. The annual hourly average load and the PV power output, shown in Fig. 3.4 and 3.5 respectively, were applied to the test microgrid. The initial SOC for the first day of the year was assumed to be 0.8 (80%). For every other day, the initial SOC was equal to the final SOC from the previous day. The total battery lifetime throughput was allocated equally for a 10-year float life which was equal to 9038 kWh/year. If the yearly throughput was found to be less than the allocated, the battery was not fully utilized and a float life cost equal to the difference between allocated and utilized throughput multiplied by the battery wear cost was calculated.

It is an iterative simulation process where the initial set of weights $W_1 = 1$ and $W_2 = 0$. This is the case when the battery wear cost was not considered in the objective function. In this case, yearly operational cost was determined and set of weight changes to $W_1 = 0.9$ and $W_2 = 0.1$. This is the case when battery wear cost was considered with low weightage. Yearly operational cost was calculated and weight changes to $W_1 = 0.8$ and $W_2 = 0.2$. In a similar fashion value of W_1 and W_2 varied and operational cost calculated. It is important to note $W_1 + W_2 = 1$. Comparing the operational costs obtained

from different sets of weights, set with lowest operation cost was selected.

3.2.3. Real-time dispatch

A real-time dispatch module is a collective form of all local controllers available in microgrid, which accepts set-points from scheduled unit. Once, real-time module obtains set-points, it implements them and support required deviation from set- points to ensure all constraints were satisfied during the operation of microgrid. Since real-time dispatch is based on locally available information, it is a primary control of microgrid operation and secondary control is a schedule module.

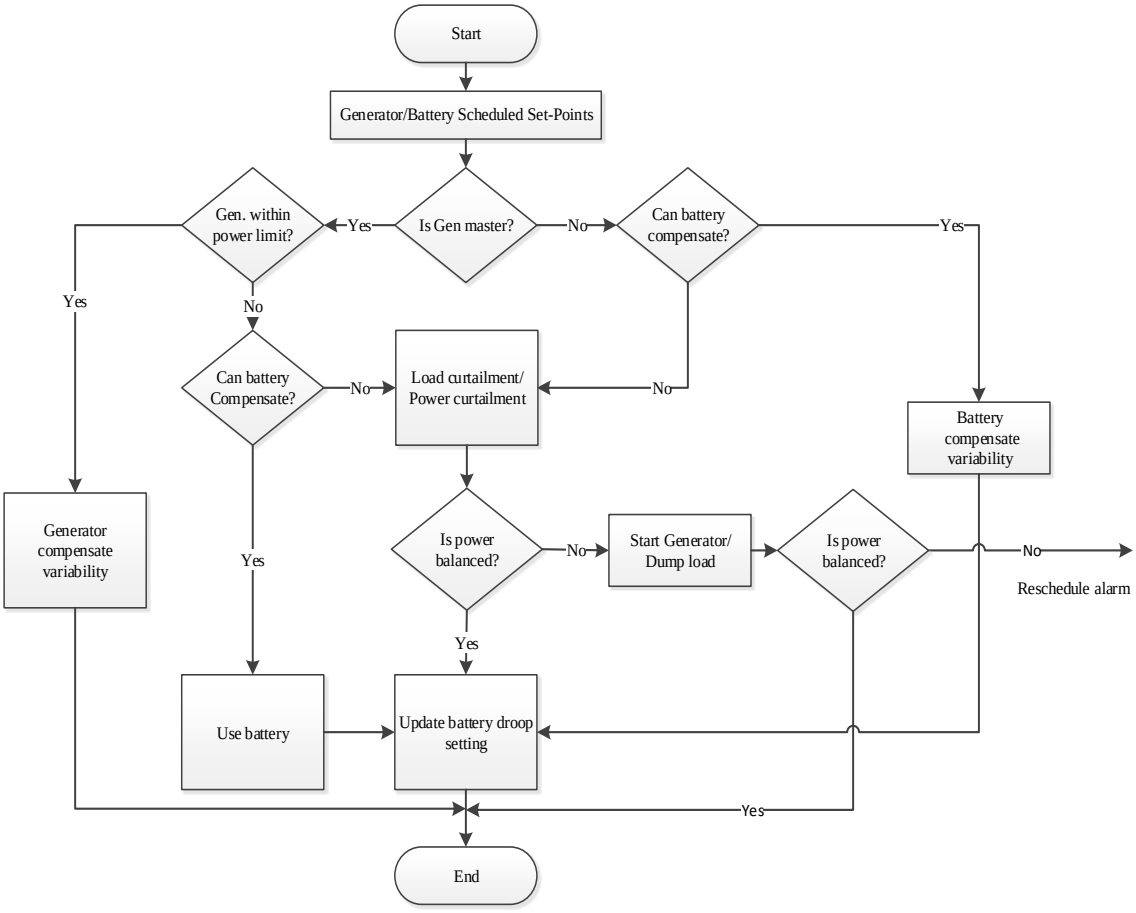

Fig. 3.8. Real-time microgrid operation algorithm.

In this study, since generators are running in isochronous mode, primary control is governors in the diesel generators and droop control in the battery inverter. In order to keep the effectiveness of the scheduled layer, when net-load deviates and allocated reserve cannot compensate the change, the dispatch module performs a corrective action as shown in Fig. 3.8. This corrective action includes PV power and load curtailment, dump load, and rescheduling (if required). Real-time module behaves differently in the following cases.

A) Less PV power

If generator is acting as a master unit, it will compensate the variability until its maximum operational limit reached. If generator is not sufficient then battery provides the power within its limit. If still not sufficient, non-critical load will be curtailed. It is assumed that at any hour there is at least 25% non-critical load available. Similarly, in case when battery is acting as a master unit, non-critical load will be curtailed if battery cannot compensate the variability. If still not sufficient, one of the generator starts based on the load requirement.

B) Excess PV power

If generator is acting as a master unit, it will compensate the variability until its minimum operational limit. If net-load goes less than the minimum limit, battery store the power within its capacity. If still not sufficient, dump load (10 x 1 kW) will be used to maintain the generator loading. Here, dump load is different from the non-critical. When battery acting as a master unit and cannot store the excess PV power, then dump load will be used to keep the power balance.

3.2.4. Coordination between day-ahead schedule and real-time dispatch

The required coordination between a day ahead schedule and real-time dispatch module is provided using hybrid PMS control structure. In this structure, a low bandwidth communication link was used to update the droop parameter of the battery inverter when required [66]. The complete coordination between these two layers is as follows:

1. Solve objective function and determine day ahead generator and battery operating set-points based on: i) day ahead hourly forecasted load ($P_{L,t}$), ii) PV ($P_{PV,t}$) output, iii) microgrid system architecture information, and iv) constraints.
2. Set-points are provided to the real-time dispatch module using a low bandwidth communication channel.
3. Dispatch module controls the sources using pre-determined set points obtained from the day ahead module.
4. The dispatch module follows the dispatch algorithm as described in Section 3.2.3.
5. If the operation is not acceptable, (described in section 3.2.3) a reschedule alarm will be sent.
6. New optimal set-points are calculated and provided to local controller and operation resumes starting the next hour.

3.3. Solar forecast validation

The required solar forecast for the study was obtained from the study [89], which uses Markov based switching model. The effectiveness of the PV forecast method used in this dissertation was validated using yearly and daily analysis. This validation is to determine whether the forecast method available is sufficient for use or required to have a better method for more accurate forecasting.

First step in this validation is to calculate the forecasting error for each of the 8760 hours in a year. The error was calculated by subtracting actual PV power (P_A) with forecasted value (P_F) as given in Eq. 3.23. Once the difference is calculated, forecasted power with reduced error (P_{FR}) was calculated for each interval of time using the Eq. 3.24, where E_R is the percentage of error reduction.

$$\Delta P = P_F - P_A \tag{3.23}$$

$$P_{FR} = P_A + \Delta P \times (1 - E_R) \tag{3.24}$$

In this error reduction method, forecast error reduction was conducted proportionally in the step of 20% (i.e. E_R = 0.2, 0.4, 0.6, 0.8, 1), making the forecasted result more accurate. When forecasted PV output is equal to the actual value, it is called 100% reduced error.

The second step in the validation process is to perform five yearly simulation studies using the obtained forecasting results obtained. First simulation is using forecasted value; second using 20% reduced forecasted value and so on. Results in each simulation were compared to determine the effectiveness of the available forecasting method.

CHAPTER 4: RESULT AND ANALYSIS

This chapter presents the detailed analysis of the results obtained to achieve the objective of this study. Section 4.1 describes the method to determine the proper objective weights which ensures the minimum operational cost. This includes yearly simulation analysis of a developed microgrid benchmark. Section 4.2 presents the deterministic approach to solve the battery lifetime problem. In this approach, the results with and without battery lifetime management approach were compared and discussed. Section 4.3 presents the stochastic approach to solve the battery lifetime issue. In addition, the comparison between deterministic and stochastic method will be discussed.

4.1. Determination of weights

Weights W_1 and W_2 were determined from yearly analysis and optimized to provide the lowest yearly operational cost which includes fuel cost, generator hourly replacement cost, battery wear cost, and battery float life cost. Battery wear and generator replacement costs were calculated and presented in Table 4.1.

Table 4.1. Battery wear cost and generator hourly replacement cost

Component	Initial cost ($)	Wear and hourly replacement cost
Battery	40,000	$0.5/kWh
Generator (30 kW)	14,000	$0.35/Hr
Generator (75 kW)	20,000	$0.5/Hr

Since reducing fuel consumption is the first priority in case of a remote microgrid, weight W_1 ranged from 1 to 0.5 ($W_1 \geq W_2$) and W_2=1-W_1. These weights determine the use of batteries and generators. For example, when W_1 = 1 and W_2 = 0, large battery

throughput was used, leading to shorter battery lifetime. Similarly, with increased W_2, battery throughput decreases and cost of operation changes as well. However, the effect of W_{soc} was significantly different in these cases as shown in Fig. 4.1. For $W_1 = 1$, although the battery throughput was higher, the effect of W_{soc} was found to be less than all other cases. Since the average W_{soc} was about 1, weighted throughput (64,132 kWh) was not that much different from the actual throughput (58,822 kWh). This is because of the regular charge/discharge cycles that the battery underwent. However, when $W_1 = 0.7$, the effect of W_{soc} was significant and the average value was about 5. This means that the weighted throughput was about 5 times the actual throughput. In such a case, even though the actual battery throughput seems less (6,905 kWh) and longer battery life, effect of W_{soc} increases the weighted throughput to 35,299 kWh and reduces the battery lifetime. This higher W_{soc} was due to the lack of regular charge/discharge cycles obtained from the simulation (only one full charge was observed during a year of simulation). Similarly, when $W_1 = 0.5$, the effect of W_{soc} was significant (average value was 3.61) also due to the lack of regular charge/discharge cycles and large time gap between two full charges. The SOC histogram in Fig. 4.2 shows the reason behind the different value of W_{soc} for different weights. For $W_1 = 1$, it is seen that the batteries were running on comparatively higher SOC. The worst condition was when $W_1 = 0.7$ and $W_2 = 0.3$, where batteries were running at minimum SOC most of the time. Therefore, it is very important to have a regular full charge to improve battery life. In addition, the actual comparison between different sets of W_1 and W_2 can be made only when battery gets regular full charges.

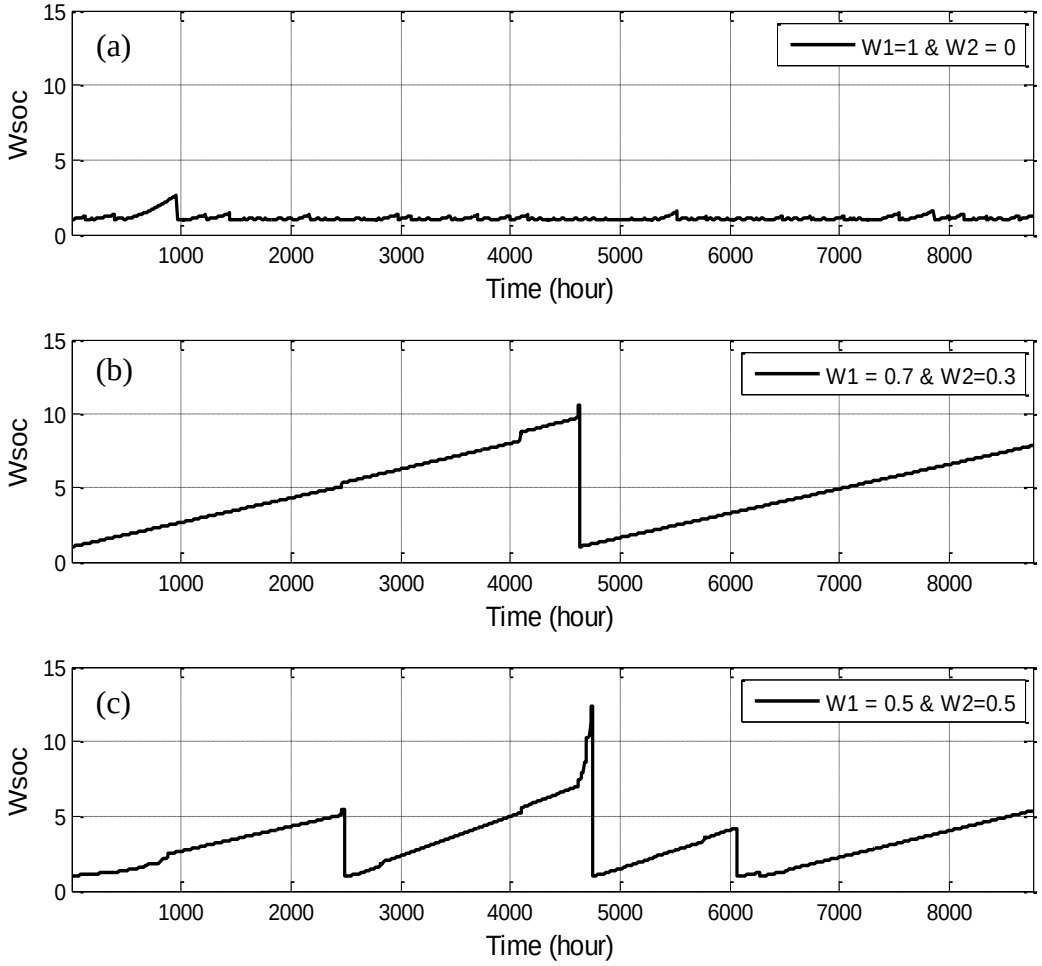

Fig. 4.1. Effect of W_{soc} when cycling is not considered: (a) W_1 = 1, (b) W_1 = 0.7, and (c) W_1 = 0.5.

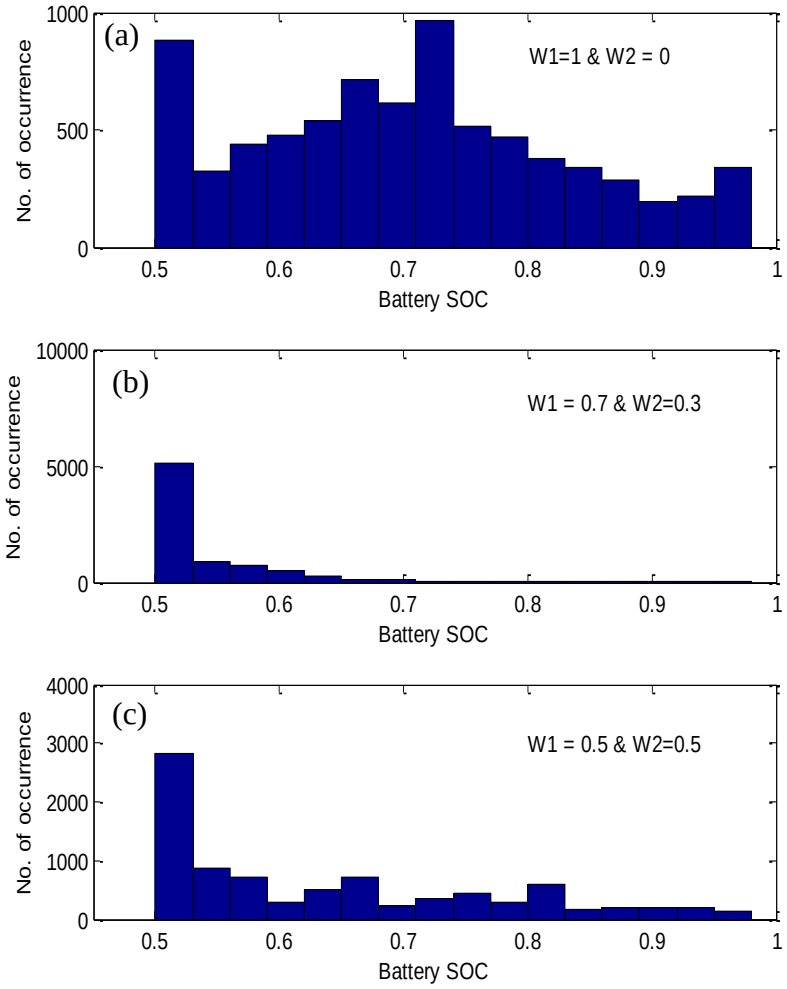

Fig. 4.2. Battery SOC histograms: (a) W_1 = 1, (b) W_1 = 0.7, and (c) W_1 = 0.5.

The best set of weights was determined by considering the battery gets a regular full charge on a weekly basis. It is obtained by running the microgrid system in a cycling charge strategy which fully charges the battery. Once the battery is fully charged, the system will return to normal operation of scheduling and dispatching. While doing so, it was observed that the average value of W_{soc} was found between 1 and 2 as shown in Fig. 4.3.

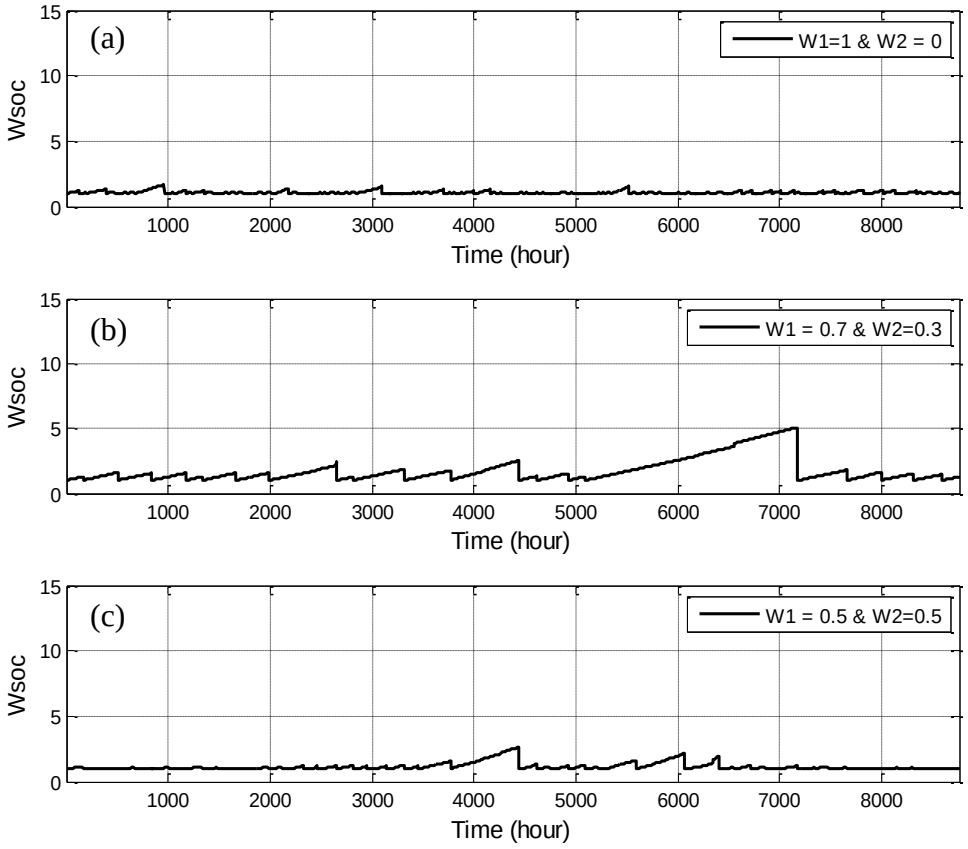

Fig. 4.3. Effect of W_{soc} on throughput with battery cycling approach: (a) W_1 = 1, (b) W_1 = 0.7, and (c) W_1 = 0.5.

When the weekly charging strategy was used, the effect of W_{soc} was greatly reduced. However, it is still a little higher in case of W_1 = 0.7 and W_2 = 0.3. For the sake of simplicity, other factors such as battery self-discharge and losses due to the temperature were not considered during the study. A yearly optimal scheduling analysis was performed for range of weights and the results are presented in Table 4.2. Similarly, graphical representation of the operational cost and battery lifetime is shown in Fig. 4.4.

Table 4.2. Yearly simulation results with 170 kWh battery

W_1 (fuel)	Fuel (gallons)	Weighted Battery Throughput (kWh)	Float Life Cost ($)	Maximum Battery Life (years)	Total Cost of Operation ($)
1	11,978	63,788	0	1.42	141,744
0.9	12,334	39,871	0	2.27	133,658
0.8	12,684	28,522	0	3.17	131,471
0.7	13,089	17,125	0	5.28	129,550
0.6	13,411	11,712	0	7.72	129,782
0.5	13,841	5,265	1,886	10.00	132,380

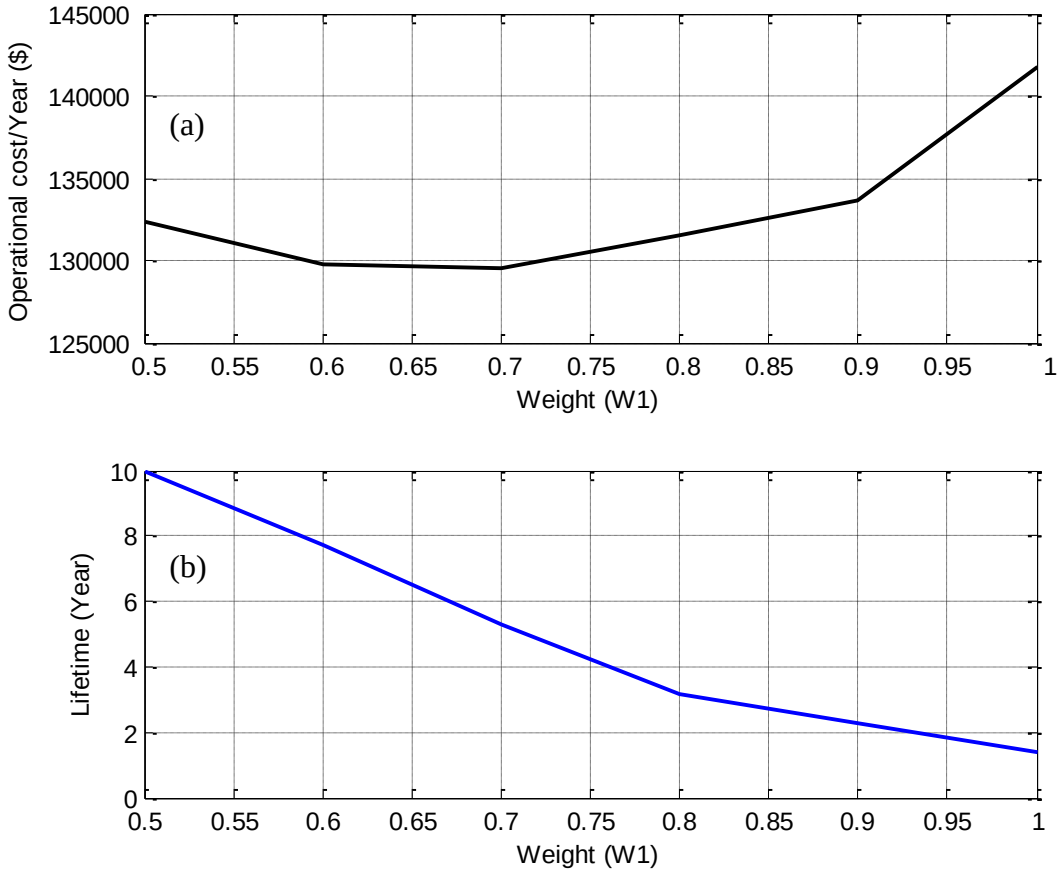

Fig. 4.4. Performance with varying weights: (a) yearly operational cost vs weight (b) total lifetime vs weight.

When W_1 = 1, fuel consumption was the only factor in the optimization process. The generator load histogram (Fig. 4.5) shows that when W_1 = 1, the 75 kW generator operated at full load and maximum efficiency while the lower efficiency 30 kW generator was unused. Since the battery life was not a factor (W_2 = 0) in this case, high throughput resulted in a 1.42 year battery lifetime. Thus, frequent and impractical battery replacement is indicated.

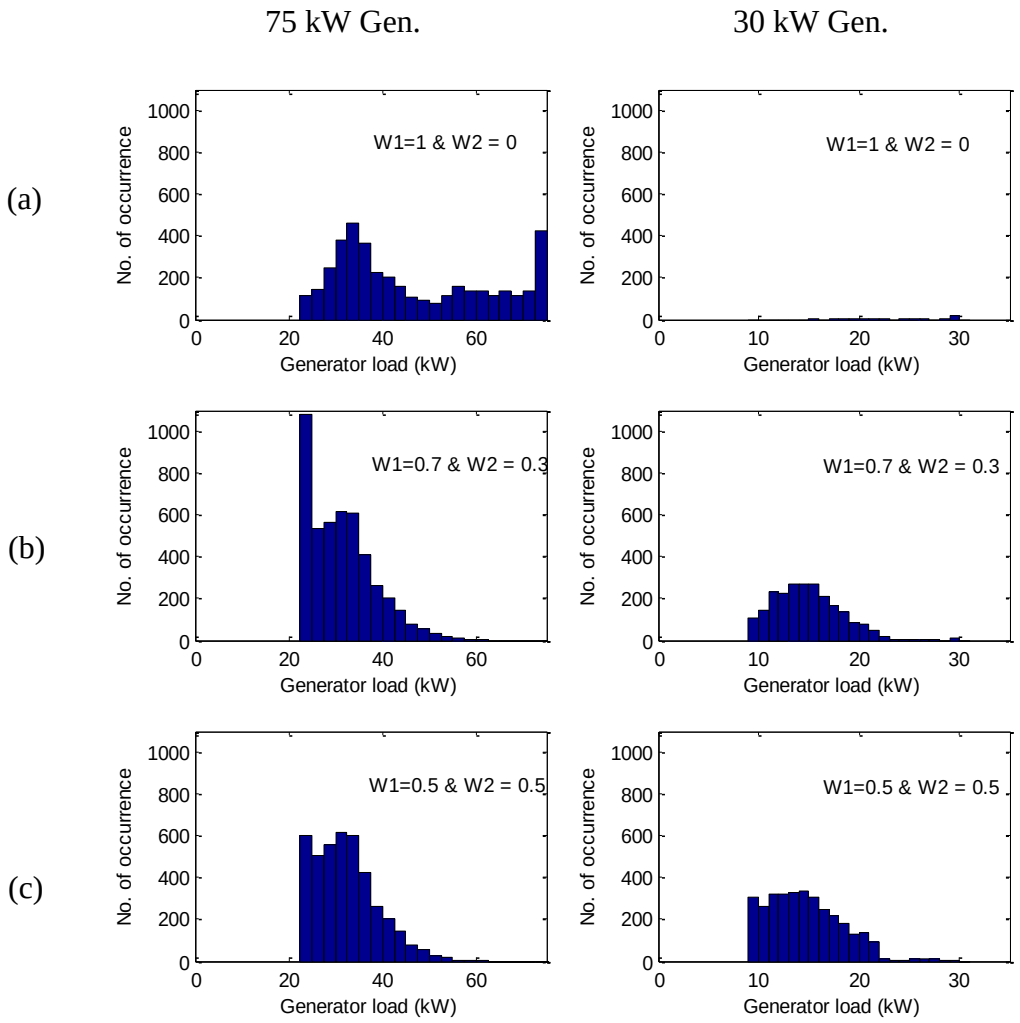

Fig. 4.5. 75 and 30 kW diesel generator loading histograms: (a) W_1 = 1, (b) W_1 = 0.7, and (c) W_1 = 0.5.

As W_1 was decreased (Table 4.2), more consideration was given to battery cost which result in increased fuel consumption but longer battery life due to reduced throughput. In addition, use of the 30 kW generator became cost effective (Fig. 4.5). The lowest operational cost, due to a balance between fuel and battery costs, was with W_1 = 0.7. The battery lifetime was estimated to be 5.28 years and the yearly operational cost

was 9% lower compared to W_1 =1 and W_2 = 0. As W_1 was further decreased, operational costs increased due to greater fuel consumption and lower utilization of the battery within its float life.

The optimal weight W_1 varies slightly as the battery wear cost increases or decreases from the original $0.50/kWh as shown in Fig. 4.6. For lower wear cost, higher W_1 is required to obtain minimum cost of operation. For example, minimum operational cost was found at W_1 = 1 when wear cost was low (0.1$/kWh).

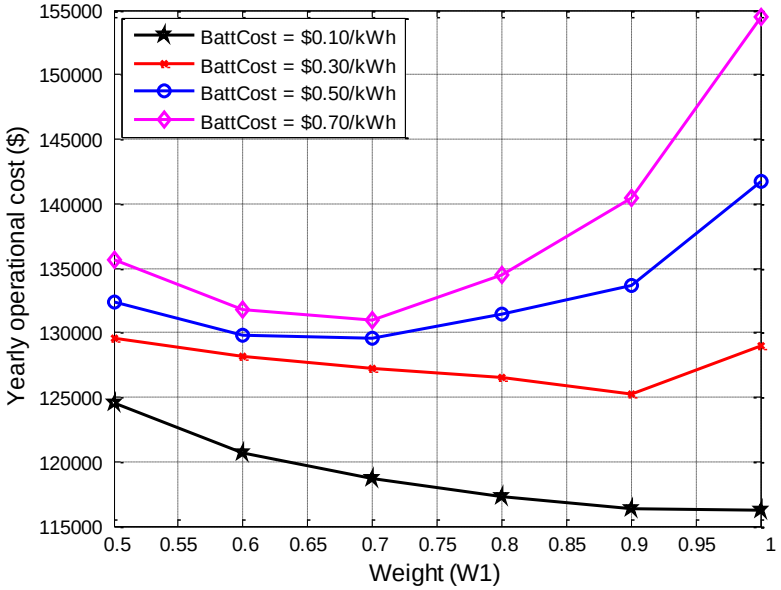

Fig. 4.6. Effect of battery wear cost on operation.

The effect of fuel cost variations was also analyzed for a fixed battery wear cost of $0.50/kWh (Fig. 4.7). For a fuel cost of $12/gallon, the lowest operational cost was found at W_1 = 0.6. However the optimal weight for $3/gallons was W_1 = 0.8. This indicates that when fuel cost is high, the PMS tends to decrease the use of battery. This is because the battery itself is not a source and either generator or PV needs to charge it.

Since the fuel cost is high, the generator is not charging unless the efficiency of the generator can be increased. In addition, capacity of PV is not sufficient to impact on this regard.

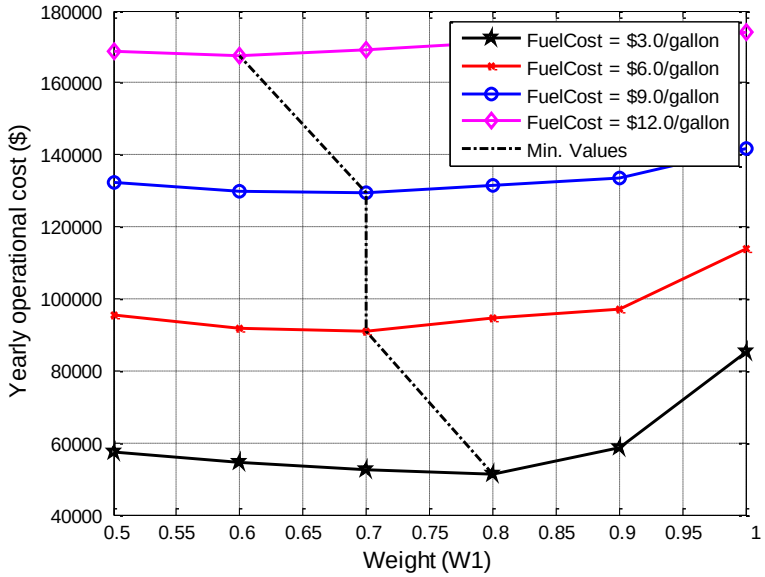

Fig. 4.7. Effect of diesel cost on operational cost.

Results in this Section 4.1 showed that increasing the battery lifetime can reduce the operational cost of the microgrid, even though fuel consumption is increased. The method is not highly sensitive to variations in fuel and battery wear cost. A wide range of weights ($0.65 < W_1 < 0.8$) showed to be effective in reducing the operational. The rest of the study will consider $W_1 = 0.7$ and $W_2 = 0.3$ for the battery lifetime management algorithm.

In order to validate the results in daily analysis, a typical summer day (July 7) with a highly fluctuating load was selected for the simulation. PV and load demand are as shown in Fig. 4.8.

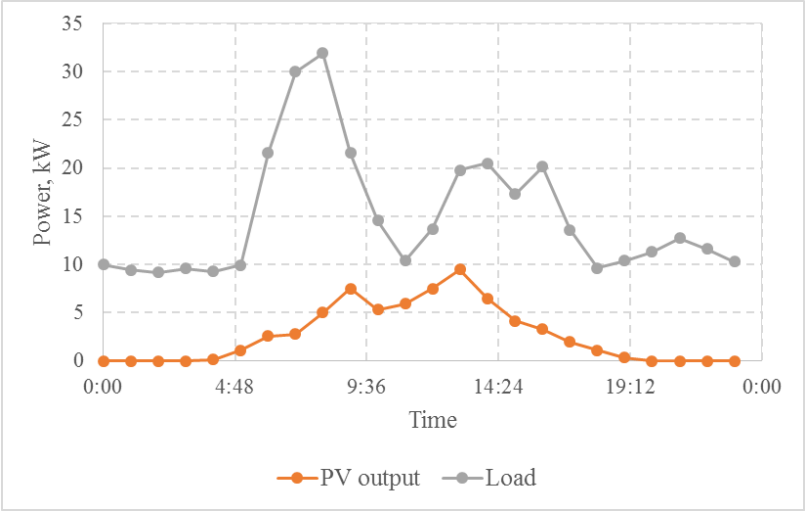

Fig. 4.8. PV output and load demand of July 7 for daily analysis.

The scheduled power outputs (battery and generator set points) using W_1=0.7 are shown in Fig. 4.9. Since the use of the battery was controlled, both generators were scheduled to provide power. The 75 kW generator was turned on when load demand for the first hour and charge the battery. The 30 kW generator was turned on at hours 2, 3, 5, 14, 16, 20, 22 and 24 during low load condition. The battery gets charged when large 75 kW generator was supplying power. At hours 11, 12, 13, 18, and 19 when the load was small, the battery inverter was acting as a master unit and the both generators were turned off. Total battery throughput during this time was 43 kWh and fuel consumption was 25 gallons.

For the sake of comparison, daily analysis without BLM algorithm was also simulated and result is shown in Fig. 4.10. Comparing results shows that running without BLM improves the loading of the generator. A 75 kW generator was running at around 60 kW. The battery was heavily used to improve the efficiency due to which throughput use was drastically increased to 187 kWh and fluctuation in battery SOC was as shown in Fig. 4.11. Total fuel consumption was 21 gallons. The system did not utilize the 30 kW

generator. When the load requirements could be met with the PV and battery, the 75 kW generator was turned off and the battery inverter became the master unit (hours 2, 3, 5, 6, 7, 10, 11, 12, 13, 14, 16, 17, 18, 19, 20, 22, 23 and 24).

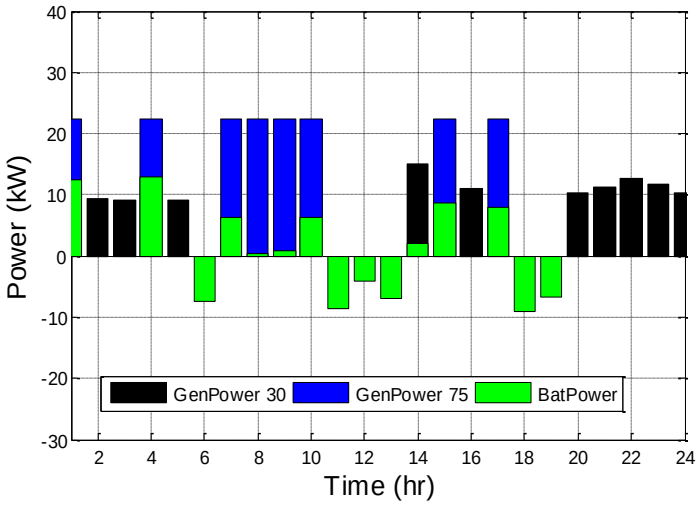

Fig. 4.9. Daily schedule with BLM (W_1=0.7).

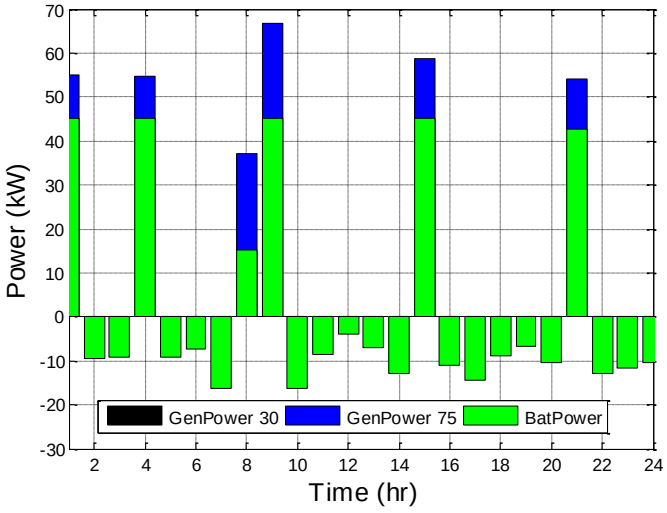

Fig. 4.10. Daily schedule without BLM (W_1=1).

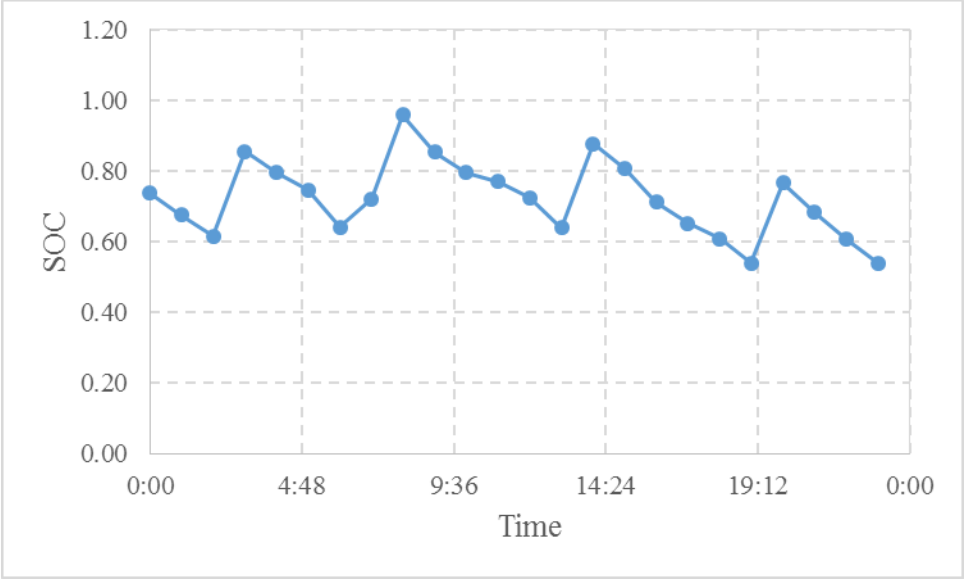

Fig. 4.11. SOC without BLM algorithm.

The comparison of two cases with and without BLM, including fuel consumption, battery throughput and estimated microgrid operation cost is given in Table 4.3. The results show 4 gallons increase in fuel consumption when scheduled with W_1=0.7. However, battery throughput was reduced by 77% which reduced the operational cost by 12% and validates the use of BLM in scheduling.

Table 4.3. Results with and without BLM

Scheduling Cases	Fuel Consumption (gallons)	Battery Throughput (kWh)	Daily Cost of Operation ($)
Without BLM	21	187	280
With BLM	25	43	247

4.2 Real-time operation of microgrid

The test microgrid was analyzed using forecasted and actual power output from Brooking, SD. PV output is forecasted using historical data using Markov switching

model described in Section 2.3. The difference between forecasted result and actual output is shown in Fig. 4.12. RMSE was calculated using only daytime values because at night, all values are zero and 100% correct forecasted results can be obtained which provides a false result. The calculated root mean square error value was 3.62 kW, which approximates the standard deviation of the error.

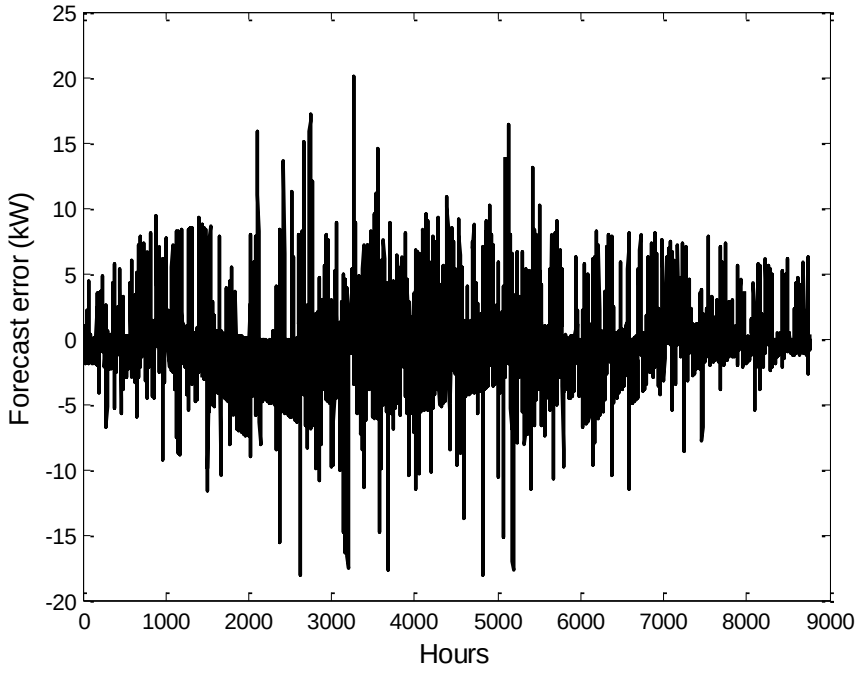

Fig. 4.12. Yearly forecast error.

4.2.1. Daily real-time analysis

The daily real-time analysis includes both deterministic and stochastic approaches. July 7, same day considered in the previous section, is chosen for the analysis. Forecasted PV, actual PV and load demand are shown in Fig. 4.13. For deterministic approach, a spinning reserve equal to 20% of the forecasted load was used

and for stochastic approach, 1000 scenarios with equal probability were generated and reduced to 10.

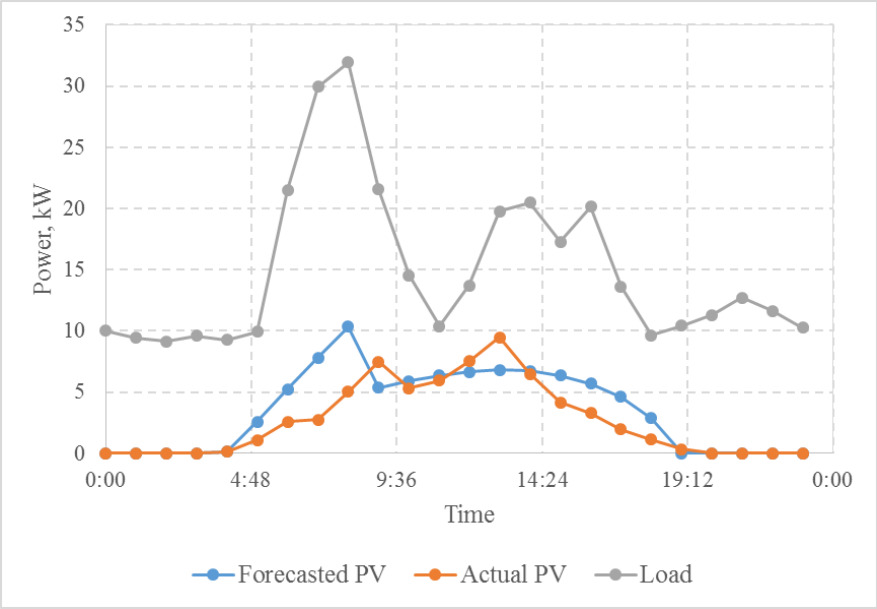

Fig. 4.13. PV output and load demand.

4.2.1.1. Deterministic daily analysis

Table 4.4 presents the detailed analysis result of the deterministic approach with BLM algorithm. The result shows how forecast error affects the actual operation of the microgrid and how much it is different from the scheduled one. Scheduled and actual output power output from generators and battery are presented. The net-load changes in real-time condition because of the stochastic nature of PV output. These variability must be compensated by the running units, according to the real-time dispatch strategy presented in Section 3.44.

Table 4.4. Daily analysis using deterministic approach

Hour	Scheduled set-points				Actual output			
	Net-load	Gen. 1 (kW)	Gen. 2 (kW)	Battery (kW)	Net-load	Gen. 1 (kW)	Gen. 2 (kW)	Battery (kW)
1	10.00	0.00	22.50	12.50	10.00	0.00	22.50	12.50
2	9.41	9.41	0.00	0.00	9.41	9.41	0.00	0.00
3	9.16	9.16	0.00	0.00	9.16	9.16	0.00	0.00
4	9.59	0.00	22.50	12.91	9.59	0.00	22.50	12.91
5	9.13	9.13	0.00	0.00	9.13	9.13	0.00	0.00
6	7.35	0.00	0.00	-7.35	8.85	0.00	0.00	-8.85
7	16.29	0.00	22.50	6.21	18.98	0.00	25.19	6.21
8	22.14	0.00	22.50	0.36	27.22	0.00	27.58	0.36
9	21.61	0.00	22.50	0.89	26.91	0.00	27.80	0.89
10	16.21	0.00	22.50	6.29	14.08	0.00	22.50	8.42
11	8.64	0.00	0.00	-8.64	9.21	0.00	0.00	-9.21
12	4.03	0.00	0.00	-4.03	4.44	0.00	0.00	-4.44
13	7.06	0.00	0.00	-7.06	6.21	0.00	0.00	-6.21
14	12.99	14.94	0.00	1.94	10.32	12.27	0.00	1.94
15	13.79	0.00	22.50	8.71	14.02	0.00	22.73	8.71
16	10.92	10.92	0.00	0.00	13.12	13.12	0.00	0.00
17	14.47	0.00	22.50	8.03	16.89	0.00	24.92	8.03
18	8.99	0.00	0.00	-8.99	11.66	0.00	0.00	-11.66
19	6.76	0.00	0.00	-6.76	8.52	0.00	0.00	-8.52
20	10.42	10.42	0.00	0.00	10.06	10.42	0.00	0.00
21	11.32	11.32	0.00	0.00	11.32	11.32	0.00	0.00
22	12.72	12.72	0.00	0.00	12.72	12.72	0.00	0.00
23	11.62	11.62	0.00	0.00	11.62	11.62	0.00	0.00
24	10.28	10.28	0.00	0.00	10.28	10.28	0.00	0.00

Table 4.4 shows that when the net load is reduced and generator is already running at its minimum limit, the battery consumes more power from generator to maintain its minimum load (10^{th} hour). Most of the hour when generators were running as a master unit, they were able to compensate the PV fluctuation. During times when the battery was acting as a master unit (e.g., hour 6, 11, 12), SOC changes due to the change in power output from the scheduled value.

Actual and scheduled SOC varies as shown in Fig. 4.14. For the simulation, initial battery SOC was 0.5, and scheduled to be 0.53 at the end of the day. However, in actual operation SOC at the end of the day was 0.5. Total fuel consumption, throughput and operational cost changes from the scheduled value. Summary of scheduled and actual operation is presented in the Table 4.5.

Table 4.5. Daily operation summary

Case	Fuel Consumption (gallons)	Battery Throughput (kWh)	Daily Cost of Operation ($)
Scheduled	25	43	247
Actual	23	49	232

As seen in the Table 4.5, actual fuel consumption slightly decreases compared to the scheduled value. This is because of the slight overestimation of PV output for that particular day. When load increases, generator efficiency increases. Although there is a slight increment in battery throughput, total operational cost decreases.

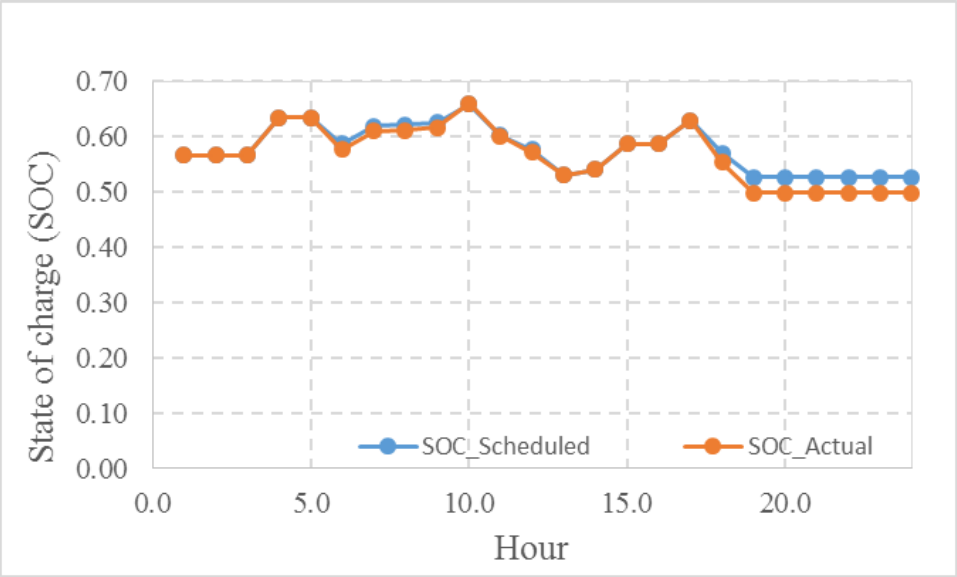

Fig. 4.14. Scheduled and actual SOC variation.

4.2.1.2. Stochastic daily analysis

In order to generate the required number of scenarios, the RMSE of the solar forecast was used to determine the forecasted upper and lower boundary. 95% prediction interval of the forecasted values at each interval is calculated. Total 1000 scenarios with equal probability were generated, which were shown in Fig. 4.15 along with the upper and lower limit. The RMSE was 3.61 kW, error mean was - 0.19 kW, and Z-value was 1.95 (for 95 % prediction interval). The upper and lower limit for each interval were calculated using:

Upper-limit = (forecasted value - 0.19 + 1.95 × 3.61)

Lower-limit = (forecasted value - 0.19 – 1.95 × 3.61)

Initial probability = 1/1000

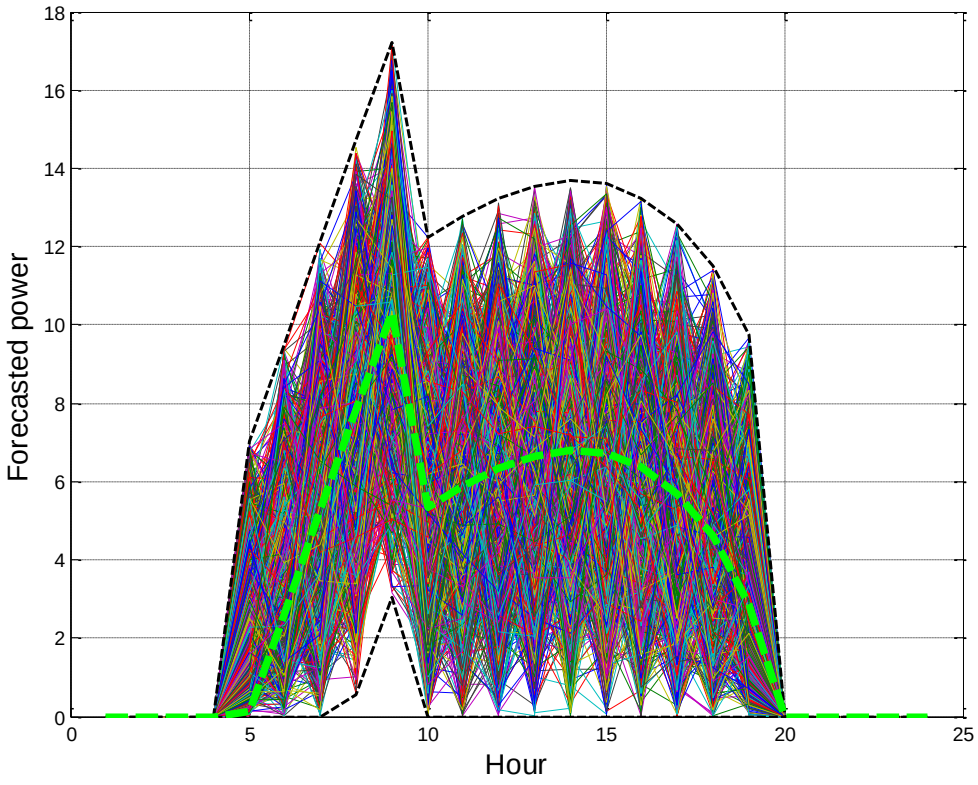

Fig. 4.15. Generated scenarios (1000 scenarios with equal probability) for stochastic optimization.

The generated scenarios were reduced to the final 10 most likely scenarios shown in Fig. 4.16. The probabilities of the remaining scenarios were different from the initial. Final probability values were:

Probability = [0.001 0.042 0.91 0.001 0.001 0.001 0.003 0.003 0.016 0.022]

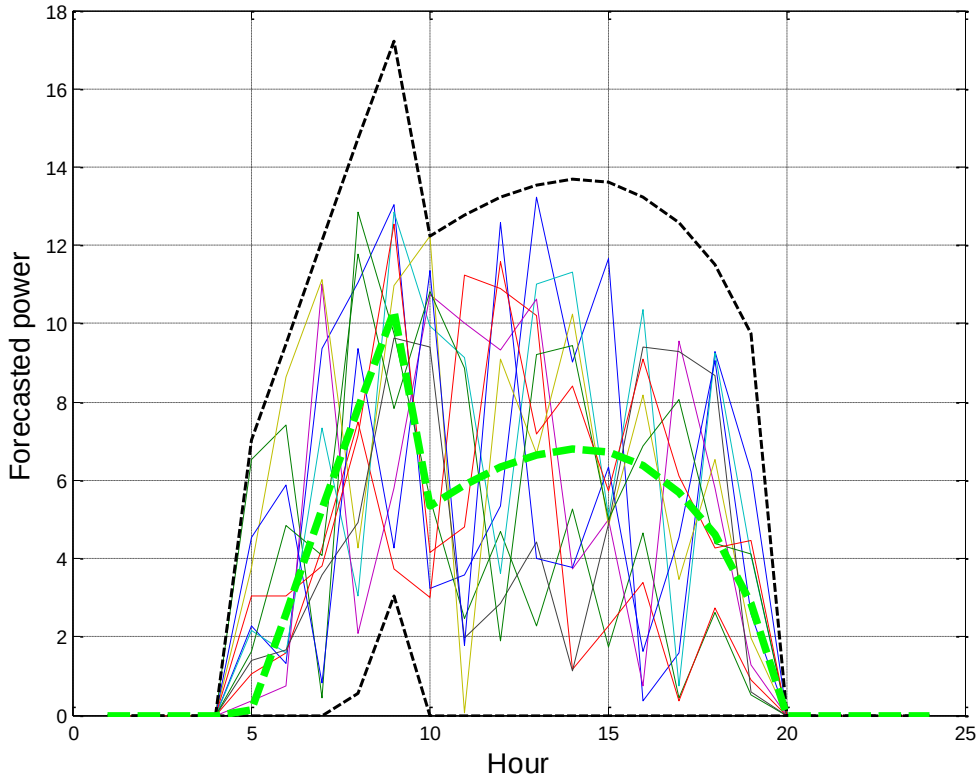

Fig. 4.16. Reduced number of scenarios (10 remaining scenarios).

Table 4.6 presents the detailed analysis result of a stochastic approach with BLM. The result shows how forecast error affects the actual operation and scheduled and actual output power output from the generators and battery.

Table 4.6. Real-time analysis using stochastic approach

Hour	Scheduled set-points			Actual output			
	Gen. 1 (kW)	Gen. 2 (kW)	Battery (kW)	Net-load	Gen. 1 (kW)	Gen. 2 (kW)	Battery (kW)
1	0.00	22.69	12.69	10.00	0.00	22.69	12.69
2	0.00	22.50	13.09	9.41	0.00	22.50	13.09
3	0.00	0.00	-9.16	9.16	0.00	0.00	-9.16
4	0.00	22.50	12.91	9.59	0.00	22.50	12.91
5	0.00	0.00	-6.42	9.13	0.00	0.00	-9.13
6	0.00	0.00	-7.70	8.85	0.00	0.00	-8.85
7	0.00	22.50	5.75	18.98	0.00	24.73	5.75
8	0.00	23.23	0.25	27.22	0.00	27.47	0.25
9	0.00	22.72	2.19	26.91	0.00	29.10	2.19
10	0.00	22.51	7.76	14.08	0.00	22.50	8.42
11	0.00	0.00	-5.49	9.21	0.00	0.00	-9.21
12	0.00	0.00	-4.45	4.44	0.00	0.00	4.44
13	0.00	0.00	-8.79	6.21	0.00	0.00	-6.21
14	13.93	0.00	1.92	10.32	12.24	0.00	1.92
15	0.00	22.50	8.13	14.02	0.00	22.50	8.48
16	11.77	0.00	0.14	13.12	13.26	0.00	0.14
17	0.00	22.50	6.77	16.89	0.00	23.66	6.77
18	0.00	0.00	-8.21	11.66	0.00	0.00	-11.66
19	0.00	0.00	-7.25	8.52	0.00	0.00	-8.52
20	10.41	0.00	0.00	10.06	10.06	0.00	0.00
21	11.32	0.00	0.00	11.32	11.32	0.00	0.00
22	12.72	0.00	0.00	12.72	12.72	0.00	0.00
23	11.62	0.00	0.00	11.62	11.62	0.00	0.00
24	10.28	0.00	0.00	10.28	10.28	0.00	0.00

The real-time operational strategy is similar to the deterministic approach, where, when a net-load reduced and generator is already running at its minimum limit, battery consumes some power to maintain generator minimum load as in the hour 10. Most of the hour when generators were running as a master unit, compensate the PV fluctuation. During times when the battery was acting as a master unit (e.g., hour 11, 12, 13), SOC changes from scheduled due to the change in PV power output.

Actual and scheduled SOC varies as shown in Fig. 4.17. For the simulation, same initial battery SOC was used as in the deterministic case. Total fuel consumption, throughput and operational cost changes from the scheduled value. Summary of scheduled and actual operation is as presented in the Table 4.7. It is seen that battery throughput was higher compared to the deterministic case, but the fuel consumption and total operational cost are less in both scheduled and actual operations.

Table 4.7. Daily operation summary with stochastic approach

Case	Fuel Consumption (gallons)	Battery Throughput (kWh)	Daily Cost of Operation ($)
Scheduled	21	64	222
Actual	22	69	228

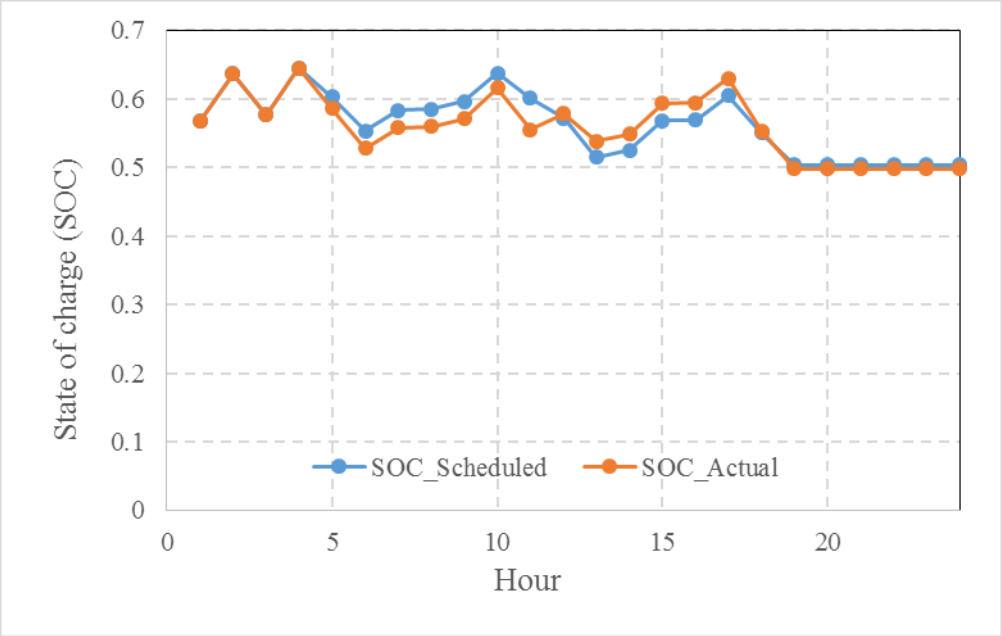

Fig. 4.17. Scheduled and actual SOC variation.

4.2.2. Yearly real-time analysis

The yearly schedule of microgrid is same as described in the Section 4.1. The real-time operation of microgrid is analyzed in this section. It is highly possible that the SOC at the end of the day is different in schedules and actual operation because of the stochastic PV output. Therefore, in order the make the results comparable, SOC at the end of the day is maintained equal to the scheduled one using s generator after PV hours. This makes actual initial SOC of the day is equal to the scheduled one. This ensures that the same scheduled set-points are calculated for that day.

Fig. 4.18 shows actual battery SOC if no any control action is taken during the operation. SOC goes below 0.5 and above 1 for some hours. SOC below 0.5 happened due to the overestimation of the PV power. Because of which, both generators were turned off and the battery did not have sufficient capacity to provide power. This requires

a control action. Action could be either curtailment of the non-critical load or start a generator. Similarly, SOC above the 1.0 (overcharging) was due to the underestimation of the PV output. In such a case, either PV can be curtailed or dump load can be used.

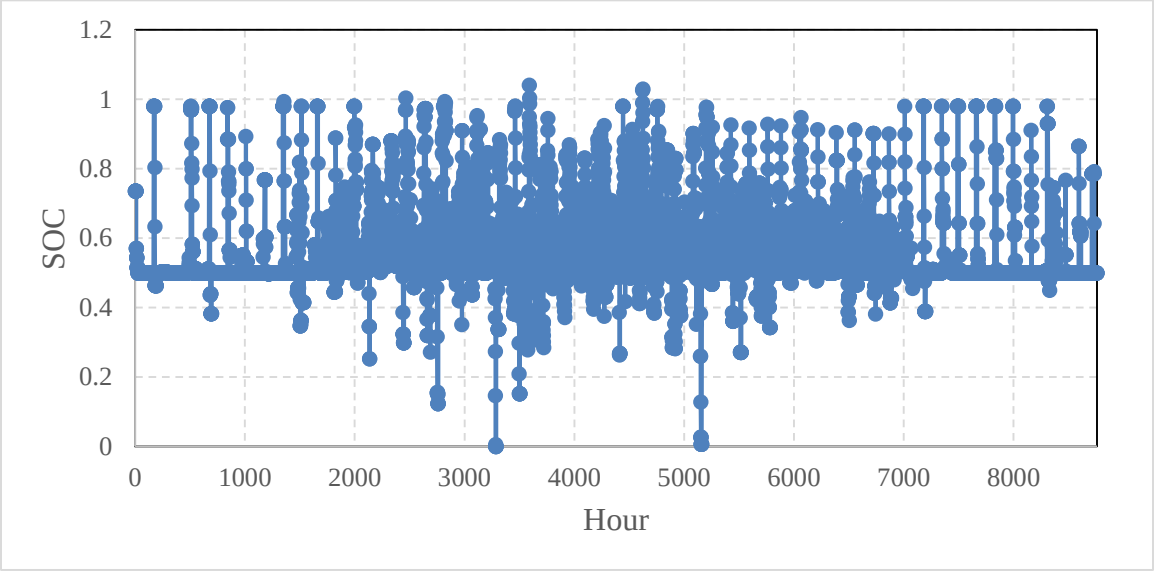

Fig. 4.18. Hourly battery SOC variation for a year.

Since SOC goes beyond the limit in the deterministic case, one of the worst day (September 28) was taken for the analysis with stochastic approach. Initial SOC of the day was 0.503. Forecasted PV power was the same as used in the deterministic case. Generated and reduced scenarios are as shown in Fig. 4.19 and 4.20 respectively.

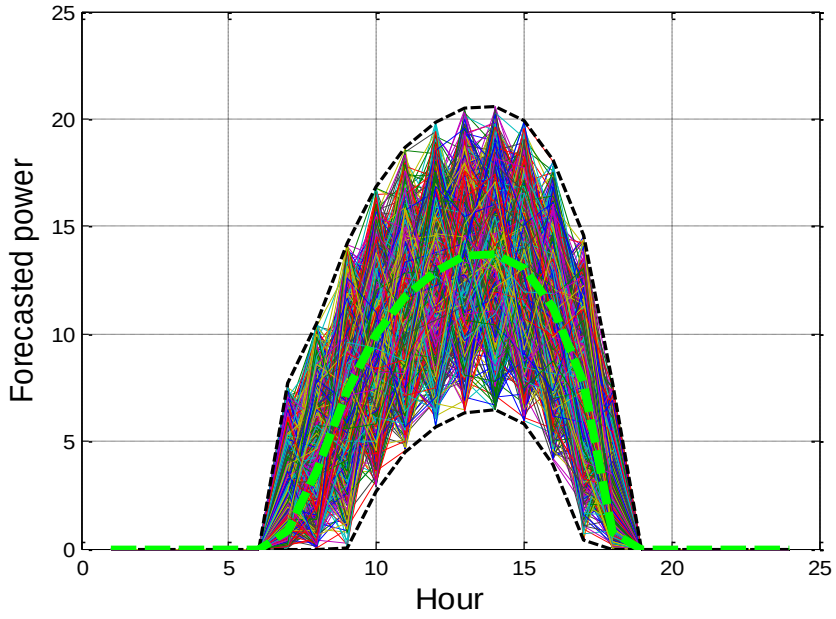

Fig. 4.19. Generated scenarios for stochastic optimization approach.

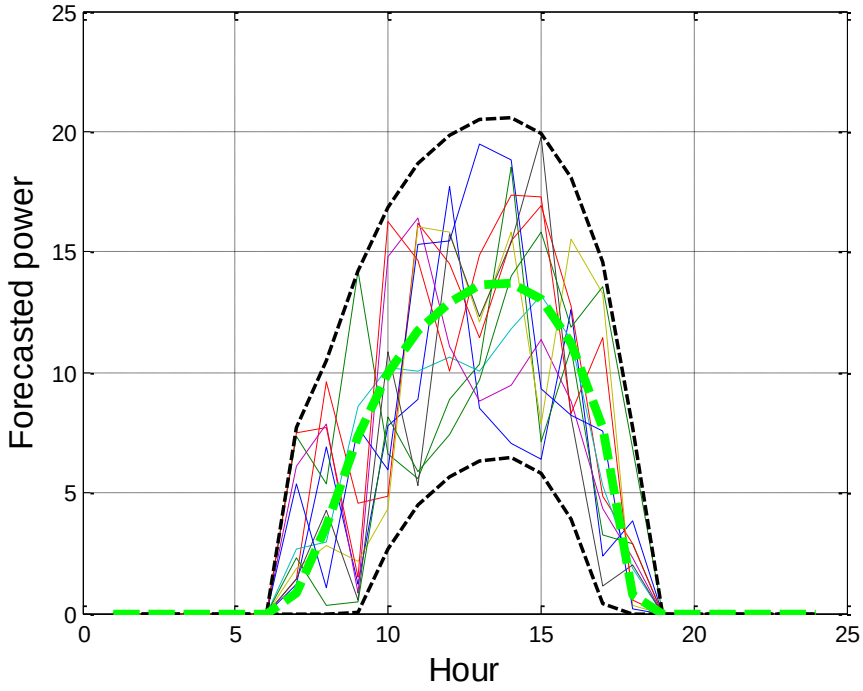

Fig. 4.20. Reduced number of scenarios.

Probability of last 10 scenarios = [0.001 0.001 0.047 0.93 0.002 0.002 0.003 0.004 0.001 0.009]

With the stochastic approach, battery SOC during actual operation was found within the limit, which is shown in Fig. 4.21. This shows that stochastic approach reduces the power mismatch compared to the deterministic approach. This is because the stochastic approach covers large fluctuation using a large number of scenarios. However, the scenarios are developed using 95% of confidence intervals and rest 5% of the time, scenarios does not cover the fluctuation of PV output. An example of such case is shown in Fig. 4.22, where the actual PV output does not fall in the confidence interval. In addition, it is required to optimize a large number of scenarios to reduce the power mismatch, which requires large computational resource.

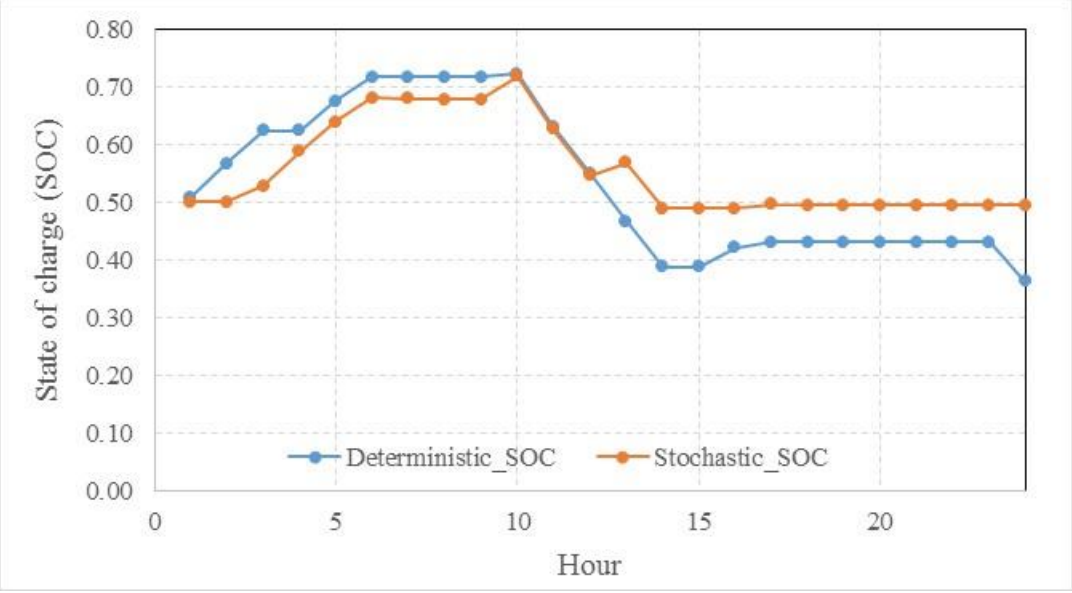

Fig. 4.21. Hourly SOC variation in deterministic and stochastic approaches.

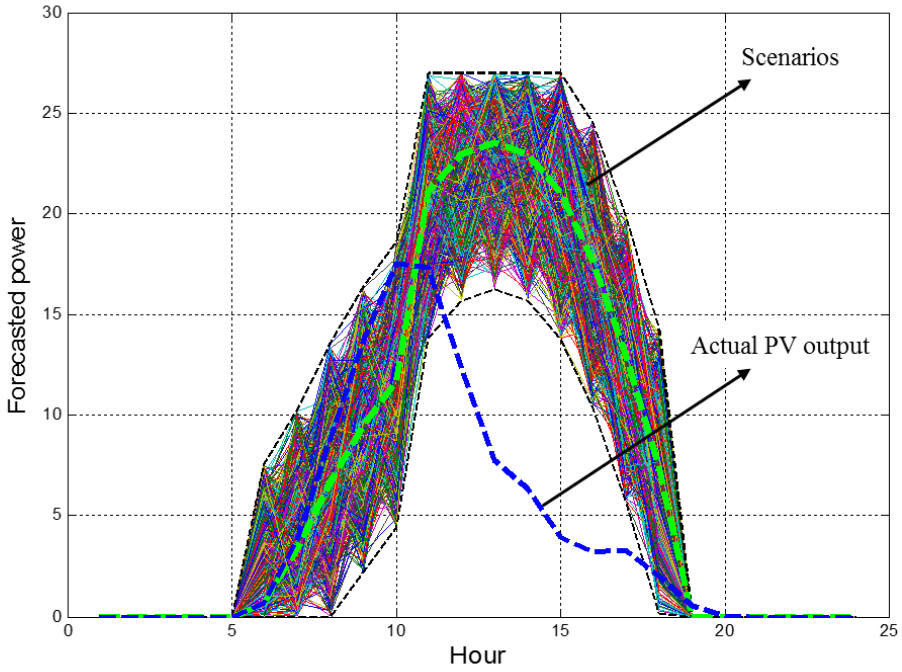

Fig. 4.22. Example of bad forecast day.

4.3. Forecast validation

Yearly and daily validation analysis were performed using the same Microgrid benchmark, actual and forecasted PV power output were used.

4.3.1. Yearly validation analysis

Table 4.8 presents the real-time battery throughput, fuel consumption, and operational cost when forecasted error was reduced by 20%, 40%, 60%, 80% and 100% respectively. These results were obtained by using the weights W_1 = 0.7 and W_2 = 0.3 with deterministic approach.

Table 4.8. Scheduled microgrid operation with a reduced forecast error

Error reduction (%)	Throughput Use (kWh)	Fuel Consumption (Gal)	Operational Cost ($)
0	14,016	12,623	123,815
20	14,016	12,616	123,753
40	13,980	12,607	123,649
60	14,064	12,597	123,595
80	14,322	12,581	123,567
100	14,519	12,570	123,564

Results from Table 4.8 shows that there is a slight reduction in fuel consumption by 55 gallons, but increment by 503 kWh in the throughput when error reduced by 100%. However, the difference in total operational cost is low, which is $251/year. These were the results when battery lifetime management was considered. This is because the average forecasted error is small and generators were able to mitigate the power mismatch issue with small change in their power output from the scheduled set points. For the sake of analysis and to determine whether the reduction in forecast has a large effect on the operational cost without considering battery lifetime, simulation were conducted and the results are as shown in Table 4.9.

Table 4.9. Real-time microgrid operation with reduced forecast error and no battery lifetime management

Error reduction (%)	Throughput Use (kWh)	Fuel Consumption (Gal)	Operational Cost ($)
0	88,354	11,289	148,281
20	88,203	11,292	148,229
40	88,808	11,237	148,037
60	88,038	11,278	148,019
80	84,956	11,439	147,932
100	88,833	11,221	147,907

The results show there is only about $374/year saving when forecasting was 100% accurate. This shows that the current forecasting results have less effect when battery lifetime was not considered in the optimization. This is because the battery was fully utilized to charge from PV and discharge to load.

4.3.2. Daily validation analysis

Forecasted and actual PV outputs of the same day used in previous analysis (July 7) selected for the analysis. For this day, both deterministic and stochastic approaches were used to determine the effect of improved forecast accuracy on microgrid operation.

Fig. 4.23 shows the operational cost, battery throughput and fuel consumption results when forecast accuracy improved from zero to hundred percent. In deterministic case, full improvement in forecast resulted only $7 reduction in the total operational cost of that day. Total operational cost at full improvement in solar forecast was $233. Similarly, battery throughput was increased by 5 kWh, but fuel consumption was reduced

by 1 gallon. The result was slightly better with stochastic approach. Total operational cost at full improvement in solar forecast was $228, which is $5 less than the deterministic approach. Throughput was increased by 16 kWh and fuel consumption was reduced by 2 gallons when forecast improved to 100%.

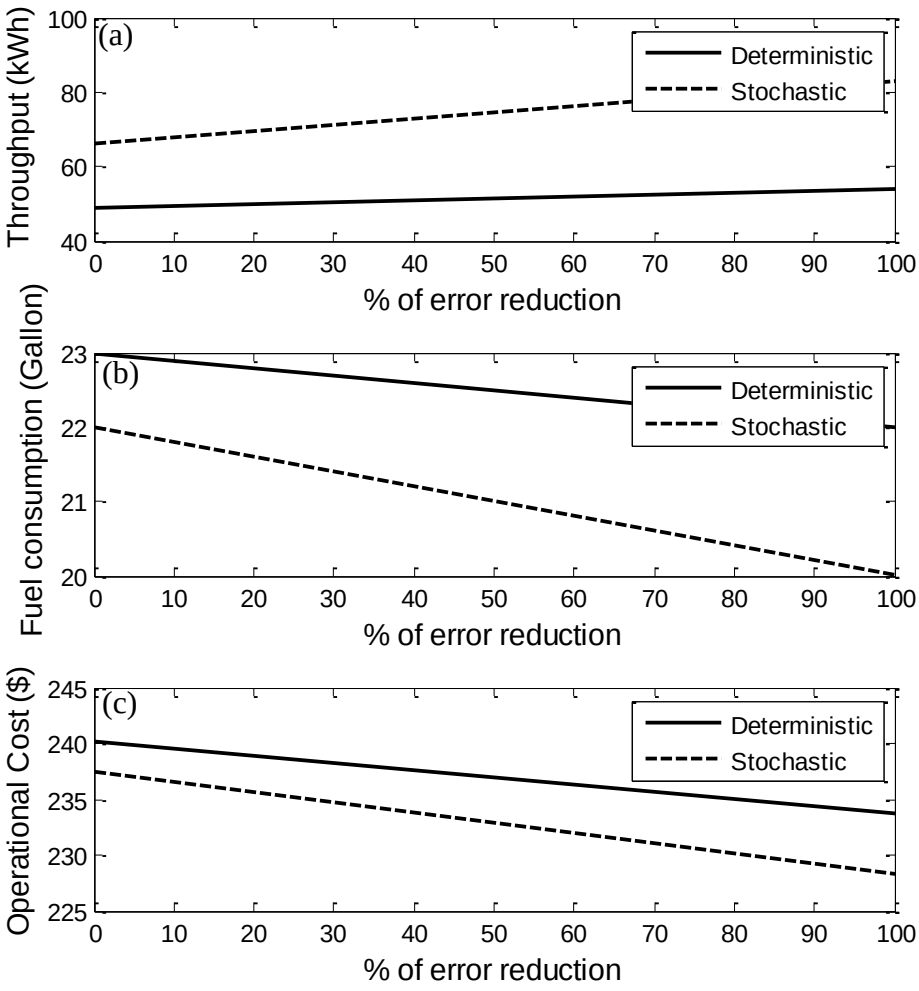

Fig. 4.23. Real-time operation analysis of microgrid on July 7 with % of error reduction: (a) battery throughput, (b) fuel consumption, and (c) operational cost.

One important conclusion drawn from this yearly analysis result is that the reduction in the operational cost of the microgrid decreases with the increase in forecast

accuracy. However, the required forecast accuracy to significantly affect the operational cost depends on the flexibility of the system, which can compensate the forecast error without significant effect in the system. Flexibility of the system depends upon the various other parameters and varies as the parameter changes. Such parameters are size of the PV, average load, resource capacity, and operational constraints.

Therefore, yearly and daily analysis of microgrid validates that the accuracy of PV forecasting would not matter much in case of typical remote microgrid described in this study. For such microgrid, the Markov switching based solar forecast is sufficient operation, which is based on the typical parameters of currently running microgrid.

CHAPTER 5: CONCLUSION AND FUTURE WORK

5.1. Summary

Reducing the cost of electricity for remote microgrids can help to increase access to electricity for populations in remote areas and developing countries. The integration of renewable energy and batteries in diesel based microgrids has shown to be effective in reducing fuel consumption. However, the operational cost remains high due to the low lifetime of batteries, which are heavily used to improve the system's efficiency. In microgrid operation, a battery can act as a source to augment the generator or a load to ensure full load operation. In addition, a battery increases the utilization of PV by storing extra energy. However, the battery represents a significant cost component of the microgrid and contains toxic materials that require proper disposal or recycling. Further, the battery has a limited energy throughput. Therefore, it is required to provide balance between fuel consumption and battery lifetime throughput in order to lower the cost of operation.

This work presents a two-layer power management system for remote microgrids. First layer is day ahead scheduling, where power set points of dispatchable resources were calculated. Second layer is real-time dispatch, where schedule set points from the first layer are accepted and resources are dispatched accordingly. A novel scheduling algorithm is proposed for a dispatch layer, which considers the battery lifetime in optimization and is expected to reduce the operational cost of the microgrid. This method is based on a goal programming approach which has the fuel and the battery wear cost as two objectives to achieve. The effectiveness of this method was evaluated through a simulation study of a PV-diesel hybrid microgrid using deterministic and stochastic

approach of optimization. This test microgrid consists of 30 kW and 75 kW diesel generators, a 27 kW PV system, and 170 kWh lead acid batteries. The microgrid load was mostly residential. The results demonstrate the effectiveness of the proposed approach, where battery lifetime is improved from 1.42 to 5.28 years and the operational cost is reduced by 9%.

5.2. Conclusion

A novel two layer (schedule and dispatch) power management system has been developed which prolongs battery life and reduces the operational cost. The method was based on a goal programming approach that assigns different weights for fuel and battery use cost. Deterministic and stochastic approaches were used to evaluate the effectiveness of the developed method. Results showed that increasing the battery lifetime can reduce the operational cost of the microgrid, even though fuel consumption is increased. The method is not highly sensitive to variations in fuel and battery wear cost. A wide range of weights ($0.6 < W_1 < 0.8$) showed to be effective in reducing the operational cost over relatively wide variations in fuel and battery costs for this case study. In addition, results with a stochastic approach shows the less power mismatch than the deterministic approach and lower operational cost. Although the analysis was limited to lead-acid batteries, the method is expected to be effective with other types of batteries. By using this method, the cost of energy for remote microgrids is expected to be reduced and increase the utilization and effectiveness of renewable sources. In addition, the cost effectiveness of the available solar power forecast model has been validated using the developed microgrid benchmark. Results show that improvement in the forecast towards

the accurate does not have a significant difference in the operational cost for the specific days considered.

5.3. Future work

Future work should include the following:

1. Incorporating a hybrid battery system, which includes a capacitor and battery can be utilized instead of using battery only system.
2. Use of a hybrid approach (deterministic + stochastic) PMS to improve the reliability of the system. This can be an approach with a fixed, optimized reserve requirement with stochastic approach.
3. Study on battery-less microgrid system considering fuel cell, renewable source and super capacitor
    a. PV or wind to generate hydrogen gas
    b. Variability compensated by fuel cells
    c. Uncertainty compensated by super capacitor
4. Detailed study of effect of flexibility of the microgrid system and solar forecast accuracy.

REFERENCES

[1] J. Romankiewicz, M. Qu, C. Marnay, and N. Zhou, "International microgrid assessment: governance, incentives, and experience (IMAGINE)," Lawrence Berkeley National Laboratory, 2014.

[2] L. Tao and C. Schwaegerl, "Advanced architectures and control concepts for more microgrids," EC Project, Tech. Rep. SES6-0198642009, 2009.

[3] F. Katiraei, R. Iravani, N. Hatziargyriou, and A. Dimeas, "Microgrids management," *IEEE Power and Energy Magazine*, vol. 6, pp. 54-65, 2008.

[4] A. Dehamna; and P. Asmus. (2015, July 13). *Energy storage for microgrids*. Available: http://atargroup.com/blog/wp-content/uploads/2014/05/ESMG-14-Navigant-Research.pdf

[5] IEA. (2010 Sept.). *Energy poverty - How to make modern energy access universal?* Available: http://www.se4all.org/sites/default/files/l/2013/09/Special_Excerpt_of_WEO_2010.pdf

[6] REN21, "Renewables 2014 global status report," REN21 Secretariat, Paris, 2014.

[7] Smart Grid Observer. (2012, June 15). *Remote microgrids sector poised for growth*. Available: http://www.smartgridobserver.com/n6-15-12-1.htm

[8] R. Gilchrist. (2014, November 28). *"Islanding" on islands: microgrids set to bring affordable power to remote locations worldwide*. Available: http://cleantechnica.com/2014/11/28/islanding-islands-microgrids-set-bring-affordable-power-remote-locations-worldwide/

[9] S. Pelland, D. Turcotte, G. Colgate, and A. Swingler, "Nemiah valley photovoltaic-diesel mini-grid: system performance and fuel saving based on one year of monitored data," *IEEE Trans. on Sustain. Energy,* vol. 3, pp. 167-175, Jan. 2012.

[10] D. Witmer and S. Watson, "Final report rural energy conference project ", US Department of Energy: Office of Scientific and Technical Information 2008.

[11] K. Bolcar and K. Ardani, "National survey report of PV power applications in the United States 2010," IEA, Washington, 2011.

[12] J. A. P. Lopes, C. L. Moreira, and A. G. Madureira, "Defining control strategies for microgrids islanded operation," *IEEE Trans. on Power Syst.,* vol. 21, pp. 916-924, May 2006.

[13] B. Wichert, "PV-diesel hybrid energy systems for remote area power generation—a review of current practice and future developments," *Renewable and Sustainable Energy Reviews,* vol. 1, pp. 209-228, 1997.

[14] C. Nayar, "Innovative remote microgrid systems," *Int. J. of Environment and Sustain.,* vol. 1, pp. 53-65, Aug. 2012.

[15] M. Ashari and C. V. Nayar, "An optimum dispatch strategy using set points for a photovoltaic (PV)–diesel–battery hybrid power system," *Solar Energy,* vol. 66, pp. 1-9, May 1999.

[16] R. Tonkoski, "Impact of high penetration of photovoltaics on low voltage systems and remedial actions," Ph.D dissertation, Depart. of Elect. & Comput. Eng., Concordia University, Montreal, Quebec, Canada, 2011.

[17] R. Tonkoski, *Impact of high penetration of photovoltaics on low voltage systems*: LAP LAMBERT Academic Publishing, 2014.

[18] B. Espinar and D. Mayer. (2011), The role of energy storage for mini-grid stabilization.

[19] J. I. San Martín, I. Zamora, J. J. San Martín, V. Aperribay, and P. Eguia, "Hybrid fuel cells technologies for electrical microgrids," *Electric Power Systems Research,* vol. 80, pp. 993-1005, Sept. 2010.

[20] E. M. Krieger, J. Cannarella, and C. B. Arnold, "A comparison of lead-acid and lithium-based battery behavior and capacity fade in off-grid renewable charging applications," *Energy,* vol. 60, pp. 492-500, 2013.

[21] H. Chen, T. N. Cong, W. Yang, C. Tan, Y. Li, and Y. Ding, "Progress in electrical energy storage system: A critical review," *Progress in Natural Science,* vol. 19, pp. 291-312, March 2009.

[22] R. Richmond. (2012, June 16). *The use of lithium Ion batteries for off-grid renewable energy applications* Available: http://www.righthandeng.com/rhe_mref_2012_li-ion.pdf

[23] S. Drouilhet and B. L. Johnson, "A battery life prediction method for hybrid power applications," in *AIAA Aerospace Sciences Meeting and Exhibit*, 1997.

[24] D. P. Jenkins, J. Fletcher, and D. Kane, "Lifetime prediction and sizing of lead-acid batteries for microgeneration storage applications," *Renewable Power Generation, IET,* vol. 2, pp. 191-200, 2008.

[25] NREL, "Getting started guide for HOMER legacy (Version 2.68)," National Renewable Energy Laboratory, Golden, CO, Jan. 2011.

[26] R. Tonkoski, L. A. C. Lopes, and D. Turcotte, "Active power curtailment of PV inverters in diesel hybrid mini-grids," in *IEEE Electrical Power & Energy Conference (EPEC)*, Montreal, QC, 2009, pp. 1-6.

[27] H. Beyer, R. Rüther, and S. Oliveira, "Adding PV-generators without storage to medium size stand alone diesel generator sets to support rural electrification in Brazil," in *ISES Solar World Congress, Göteborg*, 2003.

[28] B. Kroposki, K. Burman, J. Keller, A. Kandt, J. Glassmire, and P. Lilienthal, "Integrating high levels of renewables into the lanai electric grid," *Contract*, vol. 303, pp. 275-3000, 2012.

[29] M. D. Bachi, "Economic dispatch and demand side management in diesel hybrid mini-grids," M.S. thesis, Elect. and Comput. Eng., Concordia University, Montreal, Quebec, Canada, 2012.

[30] L. Lopes, F. Katiraei, K. Mauch, M. Vandenbergh, and L. Arribas, "PV hybrid mini-grids: applicable control methods for various situations," *IEA PVPS Task*, vol. 11, 2012.

[31] Y. Bhandari, S. Chalise, J. Sternhagen, and R. Tonkoski, "Reducing fuel consumption in microgrids using PV, batteries, and generator cycling," in *IEEE International Conference on Electro/Information Technology (EIT)*, 2013, pp. 1-4.

[32] Z. Bo, Z. Xuesong, C. Jian, W. Caisheng, and G. Li, "Operation optimization of standalone microgrids considering lifetime characteristics of battery energy storage system," *IEEE Trans. Sustain. Energy*, vol. 4, pp. 934-943, Sept. 2013.

[33] Y. Bhandari, "Fuel reduction in remote microgrids using photovoltaics, battery and multiple generators," M.S. thesis, Elect. Eng. and Comput. Sci., SDSTATE, Brookings, SD, 2013.

[34] G. Xiaohong, X. Zhanbo, and J. Qing-Shan, "Energy-efficient buildings facilitated by microgrid," *IEEE Trans. Smart Grid,* vol. 1, pp. 243-252, Dec. 2010.

[35] T. Logenthiran, D. Srinivasan, A. M. Khambadkone, and A. Htay Nwe, "Multiagent system for real-time operation of a microgrid in real-time digital simulator," *IEEE Trans. on Smart Grid,* vol. 3, pp. 925-933, May 2012.

[36] J. Quanyuan, X. Meidong, and G. Guangchao, "Energy management of microgrid in grid-connected and stand-alone modes," *IEEE Trans. on Power Syst.*, vol. 28, pp. 3380-3389, July 2013.

[37] D. E. Olivares, Can, x, C. A. izares, and M. Kazerani, "A centralized energy management system for isolated microgrids," *IEEE Trans. on Smart Grid* vol. 5, pp. 1864-1875, Jun. 2014.

[38] R. Palma-Behnke, C. Benavides, F. Lanas, B. Severino, L. Reyes, J. Llanos, *et al.*, "A microgrid energy management system based on the rolling horizon strategy," *IEEE Trans. on Smart Grid* vol. 4, pp. 996-1006, May 2013.

[39] W. Su, J. Wang, and J. Roh, "Stochastic energy scheduling in microgrids with intermittent renewable energy resources," *IEEE Trans. Smart Grid,* pp. 1-9, Nov. 2013.

[40] H. J. Khasawneh and M. S. Illindala, "Battery cycle life balancing in a microgrid through flexible distribution of energy and storage resources," *Journal of Power Sources,* vol. 261, pp. 378-388, 2014.

[41] S. Chalise and R. Tonkoski, "Day ahead schedule of remote microgrids with renewable energy sources considering battery lifetime," in *11th IEEE/IAS International Conference on Industry Applications (INDUSCON),* 2014, pp. 1-5.

[42] P. A. Ruiz, C. R. Philbrick, E. Zak, K. W. Cheung, and P. W. Sauer, "Uncertainty management in the unit commitment problem," *IEEE Trans. on Power Syst.,* vol. 24, pp. 642-651, Apr. 2009.

[43] A. Sobu and W. Guohong, "Optimal operation planning method for isolated microgrid considering uncertainties of renewable power generations and load demand," in *IEEE Innovative Smart Grid Technologies - Asia (ISGT Asia),* 2012, pp. 1-6.

[44] M. Dubarry, V. Svoboda, R. Hwu, and B. Y. Liaw, "Capacity and power fading mechanism identification from a commercial cell evaluation," *Journal of Power Sources,* vol. 165, pp. 566-572, March 2007.

[45] D. U. Sauer and H. Wenzl, "Comparison of different approaches for lifetime prediction of electrochemical systems—Using lead-acid batteries as example," *Journal of Power Sources,* vol. 176, pp. 534-546, Feb 2008.

[46] R. Dufo-López, J. M. Lujano-Rojas, and J. L. Bernal-Agustín, "Comparison of different lead–acid battery lifetime prediction models for use in simulation of stand-alone photovoltaic systems," *Applied Energy,* vol. 115, pp. 242-253, Feb. 2014.

[47] Y. V. Makarov, D. Pengwei, M. C. W. Kintner-Meyer, J. Chunlian, and H. F. Illian, "Sizing energy storage to accommodate high penetration of variable energy resources," *IEEE Trans. on Sustain. Energy, ,* vol. 3, pp. 34-40, Jan. 2012.

[48] J. Zhu, "Classic economic dispatch," *Optimization of Power System Operation,* pp. 85-140, 2010.

[49] C. T. Jones, "Diesel plant operations handbook," ed New York: Mc-Graw-Hill, 1991, pp. sec. 3.7, 10.4, 22.12.

[50] (2011, Oct. 6). *NFPA 110: National fire protection agency std. 110, 2010, paragraph 8.4.2 and corresponding entry in Annex A.*

[51] F. Katiraei and M. R. Iravani, "Power management strategies for a microgrid with multiple distributed generation units," *IEEE Trans. on Power Syst.,* vol. 21, pp. 1821-1831, Oct. 2006.

[52] H. Stutvoet. (2014, August 3). *Isochronous vs droop control for generators*. Available: http://www.svri.nl/en/isochronous-vs-droop-control-for-generators/

[53] Stephen J. Chapman, *Electrical machinery fundamentals,* 5th ed.: McGraw Hill, 2012.

[54] R. A. Messenger and J. Ventre, *Photovoltaic systems engineering*: CRC press, 2010.

[55] S. Chalise, "An investigation of the maximum penetration level of a photovoltaic (PV) system into a traditional distribution grid," M.S. thesis, Elect. Eng. & Comput. Sci., NAU, Flagstaff, AZ, 2012.

[56] DOE, "DOE microgrid workshop report," Office of Electricity Delivery and Energy Reliability Smart Grid R&D Program, Aug. 2011.

[57] J. A. Peas Lopes, C. L. Moreira, and A. G. Madureira, "Defining control strategies for microgrids islanded operation," *IEEE Trans. on Power Syst.,* vol. 21, pp. 916-924, May 2006.

[58] F. Baalbergen, P. Bauer, and J. A. Ferreira, "Energy storage and power management for typical 4Q-load," *IEEE Trans. on Ind. Electron.* , vol. 56, pp. 1485-1498, Apr. 2009.

[59] N. Hatziargyriou, H. Asano, R. Iravani, and C. Marnay, "Microgrids," *IEEE Power and Energy Magazine,* vol. 5, pp. 78-94, 2007.

[60] D. E. Olivares, C. A. Canizares, and M. Kazerani, "A centralized optimal energy management system for microgrids," in *IEEE Power and Energy Society General Meeting*, San Diego, CA, 2011, pp. 1-6.

[61] Z. Xiao, T. Li, M. Huang, J. Shi, J. Yang, J. Yu, *et al.*, "Hierarchical MAS based control strategy for microgrid," *Energies,* vol. 3, pp. 1622-1638, Sept. 2010.

[62] Y. Hyun-jae, S. Jong-Wan, S. Myong-Chul, and S. Hee-seok, "Study of data acquisition and communication equipment for microgrid system," in *IEEE 13th International Symposium on Consumer Electronics*, 2009, pp. 671-675.

[63] R. Zamora and A. K. Srivastava, "Controls for microgrids with storage: review, challenges, and research needs," *Renewable and Sustainable Energy Reviews,* vol. 14, pp. 2009-2018, 2010.

[64] A. G. Tsikalakis and N. D. Hatziargyriou, "Centralized control for optimizing microgrids operation," *IEEE Trans. on Energy Convers.,* vol. 23, pp. 241-248, March 2008.

[65] A. Madureira, C. Moreira, and J. A. P. Lopes, "Secondary load-frequency control for microgrids in islanded operation," in *Proc. Int. Conf. Renewable Energy Power Quality*, 2005

[66] S. Chalise, F. B. Dos Reis, J. Sternhagen, and R. Tonkoski, "Power management strategies for microgrids with high penetration of renewables," in *5th International Conference on Power & Energy Systems*, Kathmandu, Nepal, 2013.

[67] K. Jung-Won, C. Hang-Seok, and C. Bo Hyung, "A novel droop method for converter parallel operation," *IEEE Trans. on Power Electron.*, vol. 17, pp. 25-32, Aug. 2002.

[68] K. De Brabandere, B. Bolsens, J. Van den Keybus, A. Woyte, J. Driesen, and R. Belmans, "A voltage and frequency droop control method for parallel inverters," *IEEE Trans. on Power Electron.*, vol. 22, pp. 1107-1115, July 2007.

[69] R. Tonkoski, L. A. C. Lopes, and T. H. M. El-Fouly, "Coordinated active power curtailment of grid connected PV inverters for overvoltage prevention," *IEEE Trans. on Sustain. Energy*, vol. 2, pp. 139-147, March 2011.

[70] L. A. C. Lopes, F. Katiraei, K. Mauch, M. Vandenbergh, and L. Arribas, "PV hybrid mini-grids: applicable control methods for various situations," IEA PVPS Task 11, Subtask 20, Activity 21, Jun. 2012.

[71] R. Lasseter, A. Akhil, C. Marnay, J. Stephens, J. Dagle, R. Guttromson, *et al.*, "Integration of distributed energy resources. The CERTS Microgrid Concept," ed, 2002.

[72] C. M. Colson and M. H. Nehrir, "Algorithms for distributed decision-making for multi-agent microgrid power management," in *IEEE Power and Energy Society General Meeting* San Diego, CA, 2011, pp. 1-8.

[73] C. M. Colson, M. H. Nehrir, and R. W. Gunderson, "Multi-agent microgrid power management," *18th IFAC World Congress,* 2011.

[74] F. Lauri, G. Basso, J. Zhu, R. Roche, V. Hilaire, and A. Koukam, "Managing power flows in microgrids using multi-agent reinforcement learning," *Agent Technologies in Energy Syst. (ATES),* May 2013.

[75] P. Arboleya, C. Gonzalez-Moran, and M. Coto, "A hybrid central-distributed control applied to microgrids with droop characteristic based generators," in *15th International Power Electronics and Motion Control Conference (EPE/PEMC),* Novi Sad, Sept. 2012, pp. LS7a.5-1-LS7a.5-8.

[76] M. Prodanovic and T. C. Green, "High-quality power generation through distributed control of a power park microgrid," *IEEE Trans. on Ind. Electron.,* vol. 53, pp. 1471-1482, Oct. 2006.

[77] J. Driesen and F. Katiraei, "Design for distributed energy resources," *IEEE Power and Energy Magazine,* vol. 6, pp. 30-40, May 2008.

[78] M. Q. Wang and H. Gooi, "Spinning reserve estimation in microgrids," *IEEE Trans. Power Syst.,* vol. 26, pp. 1164-1174, July 2011.

[79] S. Mitra. (2006 July), A white paper on scenario generation for stochastic programming. Available: http://optirisk-systems.com/papers/opt004.pdf

[80] H. Heitsch and W. Römisch, "Scenario tree modeling for multistage stochastic programs," *Mathematical Programming,* vol. 118, pp. 371-406, 2009.

[81] K. Høyland and S. W. Wallace, "Generating scenario trees for multistage decision problems," *Management Science,* vol. 47, pp. 295-307, 2001.

[82] A. Y. Saber and G. K. Venayagamoorthy, "Resource scheduling under uncertainty in a smart grid with renewables and plug-in vehicles," *IEEE Syst. J.*, vol. 6, pp. 103-109, Feb. 2012.

[83] S. Abedi, G. H. Riahy, M. Farhadkhani, and S. H. Hosseinian, *Improved stochastic modeling: an essential tool for power system scheduling in the presence of uncertain renewables*: INTECH Open Access Publisher, 2013.

[84] W. Jianhui, M. Shahidehpour, and L. Zuyi, "Security-constrained unit commitment with volatile wind power generation," *IEEE Trans. on Power Syst.,* vol. 23, pp. 1319-1327, Jul. 2008.

[85] V. S. Pappala, I. Erlich, K. Rohrig, and J. Dobschinski, "A stochastic model for the optimal operation of a wind-thermal power system," *IEEE Trans. on Power Syst.*, vol. 24, pp. 940-950, Apr. 2009.

[86] M. SARFATI, *Modeling the diversification benefit of transmission investments*: LAP Lambert Academic Publishing, 2012.

[87] H. Brand, E. Thorin, and C. Weber, "Scenario reduction algorithm and creation of multi-stage scenario trees," *Optimization of Cogeneration Systems in a Competitive Market Environment*, 2002.

[88] N. Gröwe-Kuska, H. Heitsch, and W. Römisch, "Scenario reduction and scenario tree construction for power management problems," in *IEEE Bologna Power Tech Conference Proceedings*, 2003.

[89] P. Pandey, "Irradiance forecasting using markov switching model for energy management in remote microgrids," M.S. thesis, Elect. Eng. and Comput. Sci. Dept., SDSTATE, Brookings, SD, 2015.

[90] M. J. Reno, C. W. Hansen, and J. S. Stein, "Global horizontal irradiance clear sky models: implementation and analysis," *SAND2012-2389, Sandia National Laboratories, Albuquerque, NM,* 2012.

[91] M. Marzband, A. Sumper, J. L. Domínguez-García, and R. Gumara-Ferret, "Experimental validation of a real-time energy management system for microgrids in islanded mode using a local day-ahead electricity market and MINLP," *Energy Conversion and Manage,* vol. 76, pp. 314-322, Dec. 2013.

[92] B. Wollenberg and A. Wood, "Power generation, operation and control," *John Wiley&Sons, Inc,* pp. 264-327, 1996.

[93] L. D. Watson and J. W. Kimball, "Frequency regulation of a microgrid using solar power," in *26th Annual IEEE Applied Power Electronics Conference and Exposition (APEC)*, 2011, pp. 321-326.

[94] S. A. Pourmousavi and M. H. Nehrir, "Real-time central demand response for primary frequency regulation in microgrids," *IEEE Trans. on Smart Grid,* vol. 3, pp. 1988-1996, Jun. 2012.

[95] T. A. Loehlein, "Maintenance is one key to diesel generator set reliability," ed: Cummins Power Generation, Minneapolis, MN, 2007.

[96] A. Woodruff, *An economic assessment of renewable energy options for rural electrification in Pacific Island countries*: SOMAC, 2007.

[97] J. Schiffer, D. U. Sauer, H. Bindner, T. Cronin, P. Lundsager, and R. Kaiser, "Model prediction for ranking lead-acid batteries according to expected lifetime in renewable energy systems and autonomous power-supply systems," *Journal of Power Sources,* vol. 168, pp. 66-78, 2007.

[98] Sun Xtender. (2014, Nov. 16). *Sun Xtender® PVX-2580L solar battery specifications*. Available: http://www.sunxtender.com/solarbattery.php?id=11

[99] R. T. Marler and J. S. Arora, "Survey of multi-objective optimization methods for engineering," *Structural and multidisciplinary optimization,* vol. 26, pp. 369-395, 2004.

[100] J. P. Ignizio, "A review of goal programming: A tool for multiobjective analysis," *Journal of the Operational Research Society,* pp. 1109-1119, 1978.

[101] BD Batteries. (2014, Aug. 13). *PVX-2580L solar system battery retail small battery order price*. Available: http://www.bdbatteries.com/solarbattery.php?id=11

[102] D. Witmer and S. Watson, "Rural energy conference project," Oil & Natural Gas Technology 2008.

[103] IBM. (2013, Aug. 12). *IBM ILOG CPLEX optimization studio: getting started with CPLEX*. Available: http://www-01.ibm.com/support/knowledgecenter/SSSA5P_12.6.1/ilog.odms.studio.help/pdf/gscplex.pdf

[104] S. Sen and J. L. Higle, "An introductory tutorial on stochastic linear programming models," *Interfaces,* vol. 29, pp. 33-61, 1999.

LIST OF PUBLICATIONS DURING PHD STUDY

Journal

[1] S. Chalise, H. R. Atia, B. Poudel and R. Tonkoski, "Impact of Active Power Curtailment of Wind Turbines Connected to Residential Feeders for Overvoltage Prevention," in *IEEE Trans. on Sustain. Energy*, vol. 7, no. 2, pp. 471-479, April 2016.

[2] **S. Chalise**, J. Sternhagen, R. Tonkoski, "Operation of remote microgrids with renewable energy sources considering battery lifetime," submitted in *Electricity Journal (TEJ), Elsevier*, March 2016.

[3] **S. Chalise**, P. Pandey, R.Tonkoski, "Validation of solar irradiance forecasting by markov switching model using remote microgrid benchmark with stochastic Approach" submitted in *IEEE Trans. on Sustain. Energy*, Feb. 2016.

[4] A. Shakya, P. Pandey, **S. Chalise**, R. Tonkoski, S. Michael, "Solar Irradiance Forecasting in Remote Microgrids using Markov Switching Model" (*under preparation*)

Conference

[5] S.R. Awasthi, **S. Chalise**, R. Tonkoski, "Operation of datacenter as virtual power plant," in *2015 IEEE Energy Conversion Congress and Exposition (ECCE)*, vol., no., pp.3422-3429, 20-24 Sept. 2015

[6] **S. Chalise** et. al, "Data Center Energy Systems: Current Technology and Future Direction", accepted in *2015 IEEE Power & Energy Society General Meeting*, Denver, CO, USA

[7] **S. Chalise**, R. Tonkoski. "Day Ahead Schedule of Remote Microgrids with Renewable Energy Sources Considering Battery Lifetime," *IEEE/IAS International Conference on Industry Applications* 2014, Brazil. (*Best paper award in smart grid track*)

[8] **S. Chalise**, F. B. Dos Reis, J. Sternhagen, R. Tonkoski, "Power Management Strategies for Microgrids with High Penetration of Renewables," in *5th International Conference on Power & Energy Systems*, 2013, Kathmandu, Nepal.

[9] Y. Bhandari, **S. Chalise**, J. Sternhagen, R. Tonkoski. "Reducing Fuel Consumption in Remote Microgrid using Generator Cycling and Battery Systems," in *IEEE EIT 2013 International Conference*, Rapid City, SD, USA.

[10] **S. Chalise**, B. Poudel and R. Tonkoski. "Overvoltages in LV Rural Feeders with High Penetration of Wind Energy," in *2013 IEEE Power & Energy Society General Meeting*, Vancouver, BC, Canada.

[11] L. Bajracharya, S. Awasthi, S. Chalise; T. M. Hansen, R. Tonkoski, "Economic Analysis of a Data Center Virtual Power Plant Participating in Demand Response", accepted in 2016 *IEEE Power & Energy Society General Meeting*.

[12] M. H. Ullah, **S. Chalise**, R. Tonkoski, "Feasibility Study of Energy Storage Technologies for Remote Microgrid's Energy Management Systems", accepted in *23rd International Symposium on Power Electronics, Electrical Drives, Automation and Motion*